University of North Dakota
UND Scholarly Commons

Theses and Dissertations | Theses, Dissertations, and Senior Projects

8-1-1984

Void Fraction During Gas Flow through a Stagnant Liqiud Column in Annular Geometry

Rehana Rahman

Follow this and additional works at: https://commons.und.edu/theses

Recommended Citation
Rahman, Rehana, "Void Fraction During Gas Flow through a Stagnant Liqiud Column in Annular Geometry" (1984). *Theses and Dissertations*. 1128.
https://commons.und.edu/theses/1128

This Thesis is brought to you for free and open access by the Theses, Dissertations, and Senior Projects at UND Scholarly Commons. It has been accepted for inclusion in Theses and Dissertations by an authorized administrator of UND Scholarly Commons. For more information, please contact zeineb.yousif@library.und.edu.

www.manaraa.com

Void Fraction During Gas Flow through a Stagnant Liquid Column in Annular Geometry

by
Rehana Rahman

Bachelor of Science in Chemical Engineering
Bangladesh University of Engineering and Technology, May 1981

A Thesis

Submitted to the Graduate Faculty

of the

University of North Dakota

in partial fulfillment of the requirements

for the degree of

Master of Science

Grand Forks, North Dakota

August
1984

ENG-
T1984
R1991

Void Fraction During Gas Flow through a Stagnant Liquid Column in Annular Geometry

Rehana Rahman

Faculty Advisor: Dr. A. Rashid Hasan

This thesis presents a study of void fraction when gas (air) is bubbled through a stagnant liquid (water) column in annular geometry. The apparatus used resembles an oil-well with a casing (outer tube) of 6.5 inch inside diameter, and it stood eight feet high. Three different sizes of replaceable tubing (inner tube), ranging in outside diameter from 2.38 to 4.49 inches, were used to investigate the effect of annular diameters on void fraction. Superficial gas velocity, which is the single most important variable in determining void fraction, was varied from 0.015 to 0.60 ft/sec. The column temperature did not deviate much from 70^{o} F and the column was open to the atmosphere.

Void fraction data gathered at four different sections (i.e., at different heights) of this column indicated strong influence of liquid height (from gas inlet) on void fraction. A column eighteen feet tall with a 5 inch casing was constructed to gather void fraction data unaffected by liquid height. Experiments conducted with this column (and tubings having 2.785 inches and 3.50 inches outside diameter) did show the absence of entrance effects beyond

601829

nine feet from the gas inlet. These void fraction (E_g) data were correlated with superficial gas velocity(u_g) by a modified Zuber and Hench equation:

$$E_g = u_g/(Au_g+B)$$

The parameter A was found to increase slightly and linearly with the inner tube diameter. The parameter B includes the single bubble rise velocity. The single bubble rise velocity was found to follow the Edger correlation, increasing slightly with the equivalent diameter (casing inside diameter minus tubing outside diameter) of the channel.

Visual observation indicated the existence of slug flow whenever void fraction exceeded a value of 0.25 in all channels. These void fraction data were correlated by an equation suggested by Wallis (and similar in form to the Zuber-Hench Equation). The value of the parameter A was again found to increase slightly with the equivalent diameter of the channel. However, the dependence of void fraction on annular diameter, for both bubbly and slug flow, was found to be relatively small.

This thesis submitted by Rehana Rahman in partial fulfillment of the requirements for the Degree of Master of Science from the University of North Dakota is hereby approved by the Faculty Advisory Committee under whom the work has been done.

_____

_____

_____

This thesis meets the standards for appearance and conforms to the style and format requirements of the Graduate School of the University of North Dakota, and is hereby approved.

_____

Title Void Fraction During Gas Flow through a Stagnant Liquid Column in Annular Geometry

Department Chemical Engineering

Degree Master of Science

In presenting this thesis in partial fulfillment of the requirements for a graduate degree from the University of North Dakota, I agree that the Library of this University shall make it freely available for inspection. I further agree that permission for extensive copying for scholarly purposes may be granted by the professor who supervised my thesis work or, in his absence, by the Chairman of the Department or the Dean of the Graduate School. It is understood that any copying or publication or other use of this thesis or part thereof for financial gain shall not be allowed without my written permission. It is also understood that due recognition shall be given to me and to the University of North Dakota in any scholarly use which may be made of any material in my thesis.

Signature _____

Date _____

CONTENTS

LIST OF FIGURES

LIST OF TABLES

ACKNOWLEDGEMENT

I would like to express my sincere gratitude to Dr. A.R. Hasan for his much appreciated help and encouragement throughout the duration of this project. I would like to thank Dr. David J. Uherka and Dr. Thomas C. Owens for being on my graduate committee and for reviewing the thesis.

Special thanks must go to Dr. Owens for his effort in arranging financial aid to enable me to pursue my graduate studies.

Appreciation is extended to Joe Miller for his technical assistance. In the midst of difficulties and research hardships, his initiative and cheerfulness were a source of courage.

I wish to acknowledge my dearest Barabhaia whose sweet memories have always inspired me to choose the right path in every aspect of my life.

A loving acknowledgement goes to my husband Mustafiz without whose support I may not have made it.

ABSTRACT

This thesis presents a study of void fraction when gas (air) is bubbled through a stagnant liquid (water) column in annular geometry. The apparatus used resembles an oil-well with a casing (outer tube) of 6.5 inch inside diameter, and it stood eight feet high. Three different sizes of replaceable tubing (inner tube), ranging in outside diameter from 2.38 to 4.49 inches, were used to investigate the effect of annular diameters on void fraction. Superficial gas velocity, which is the single most important variable in determining void fraction, was varied from 0.015 to 0.60 ft/sec. The column temperature did not deviate much from 70° F and the column was open to the atmosphere.

Void fraction data gathered at four different sections (i.e., at different heights) of this column indicated strong influence of liquid height (from gas inlet) on void fraction. A column eighteen feet tall with a 5 inch casing was constructed to gather void fraction data unaffected by liquid height. Experiments conducted with this column (and tubings having 2.785 inches and 3.50 inches outside diameter) did show the absence of entrance effects beyond nine feet from the gas inlet. These void fraction (E_g) data were

correlated with superficial gas velocity(u_g) by a modified Zuber and Hench equation:

$$E_g = u_g/(Au_g+B)$$

The parameter A was found to increase slightly and linearly with the inner tube diameter. The parameter B includes the single bubble rise velocity. The single bubble rise velocity was found to follow the Edger correlation, increasing slightly with the equivalent diameter (casing inside diameter minus tubing outside diameter) of the channel.

Visual observation indicated the existence of slug flow whenever void fraction exceeded a value of 0.25 in all channels. These void fraction data were correlated by an equation suggested by Wallis (and similar in form to the Zuber-Hench Equation). The value of the parameter A was again found to increase slightly with the equivalent diameter of the channel. However, the dependence of void fraction on annular diameter, for both bubbly and slug flow, was found to be relatively small.

Chapter I

INTRODUCTION

For the last forty years, interest in multi-phase gas-liquid flows has grown continuously, reflecting the importance of these flows in many industrial and commercial applications. Over half of all chemical engineering is concerned with multi-phase flows. Steel making, paper manufacturing, and food processing are comprised of critical steps which depend on the proper functioning of multi-phase flow devices. Two-phase flow is the simplest case of multi-phase flow.

Mass transfer operations with or without chemical reaction require gas-liquid contactors involving two-phase flows. For successful design of these processes, operating and maximum superficial gas velocities, volume fraction of the gas-phase, size of the gas bubbles, and mass transfer coefficient are important. The fraction of volume occupied by the gas, called void fraction, is one of the most important design parameters because it is indicative of, the residence time of the gas and effective interfacial area. Void fraction along with the mass transfer coefficient estimates mass transfer rate per unit volume.

Knowledge of both flowing and static bottom-hole pressures have been used to improve oil production practices since 1925. In oil-wells, gas is produced through the outer tube (i.e., annulus) containing a stagnant liquid column. The flow of gas through a stagnant or almost stagnant liquid column has been treated as a special case of two-phase flow with zero liquid flow rate. The bottom-hole pressure is the pressure at the holes around the bottom of the outer tube, called the casing. In some oil-wells the bottom-hole pressure is measured directly; in others it is measured indirctly. The direct method involves running a pressure bomb down the annulus on a wire line provided the annulus is sufficiently large. The pressure bomb can not be run on a wire line through the tubing because a down-hole pump is present. Sometimes a special offset flange is used at the surface so that the tubing is not centered in the casing, thus facilitating the procedure. However, even in wells where this method is possible there is the additional problem of the bomb being wrapped around the tubing. Pressure sensors, permanently mounted below the down-hole pump, provide accurate and readily obtainable pressure readings. They cannot be routinely used because of their relatively high cost.

The indirect method of calculating bottom-hole pressure involves adding the surface pressure to the pressure exerted by the gas and the liquid column in the casing. Many pumping wells use the indirect method of calculating bottom-hole

pressure. The height of the fluid column is determined by the reflection of an acoustic wave. If the velocity of the wave is known, then the depth of the fluid level can be calculated. The pressure exerted by the gas-liquid column is lower than the pressure exerted by a totally liquid column because of the lower specific gravity of the gas. This means that the gas void fraction in the liquid column must be determined to obtain the actual pressure exerted by the gas-liquid column. To account for the presence of a gas-liquid mixture in the annulus, several correlations have been suggested in the petroleum engineering literature (1,2,3)[1]. Such correlations use a correction factor for the pressure gradient of the gas-liquid mixture as a function of the casing-head gas flow rate and the cross-sectional area of the annulus.

Research in two areas - mass transfer in gas liquid systems and two-phase flow- has produced a wealth of information for predicting void fraction in stagnant liquid columns. However, no work has yet been published on the effect of annulus diameters on void fraction. Correlations available in petroleum, two-phase flow literature for circular channels (2, 4, 5), and in the area of mass transfer involving two-phases (6, 7, 8, 9,) may not apply to annular geometry.

Numbers in parenthesis that are underlined refer to references cited at the end of this report.

A number of variables have been found to affect the void fraction. Among these are gas flow-rate, liquid properties (mainly density, viscosity and surface tension), and possibly orifice diameter through which gas is injected into the column as well as the column diameter.

This study investigates the effects of annulus diameter and gas flow rate on void fraction. The study is comprised of four parts:

1. Exploring the relevant literature and establishing correlation for void fraction based on theoretical considerations.
2. Design, fabrication and operation of a stagnant liquid column system with annular geometry to gather void fraction and single bubble rise velocity data.
3. Determination of the entrance effect on void fraction. Void fraction has been found to be affected by the height through which voidage measurement is averaged as well as on the method of gas injection and the purity of the liquid (5).
4. Establishing values of the parameters in the proposed correlation from the experimental data.

The data from this investigation will have applications in calculating bottom-hole pressure and hence oil-well pump efficiency and productivity index. The general area of two-phase flow will also benefit from this study.

Chapter II

LITERATURE SURVEY

When gas flows through a liquid column in a conduit, the two phases may distribute in a wide variety of patterns. Each type of flow is the result of various hydrodynamic conditions and should be treated in a different manner. Annular flow, in which the gas phase flows through the core of the channel while most of the liquid flows along the wall forming an annulus, exists only at very high gas flow rates. The flow patterns encountered in bubble and spray columns are mostly bubbly flow and slug flow (10). In bubbly flow, as the name implies, the gas phase flows as discrete bubbles through the continuous liquid phase. At higher gas flow rates however, the bubbles coalesce and may eventually fill up the entire flow cross section. The liquid slugs, flowing in between these larger bubbles, give the name of the flow pattern, slug flow. The practical range of flow patterns encountered in pumping oil through an annulus is mostly bubbly flow and, occasionally, slug flow. Theoretical and experimental models for void fraction in bubbly flow and slug flow are reveiwed here.

In order to understand the theoretical models, it is necessary first to define some of the terms. The models have

been developed principally by Zuber (11), Wallis (4) and Ishii (12) for the general system where both the liquid and the gas phases are flowing. They have pointed out the importance of the relative velocity between the phases, v_{gf}, rather than the absolute velocities, v_g (for gas) and v_f (for liquid). By definition

$$v_{gf} = v_g - v_f = u_g/E_g - u_f/(1-E_g) \tag{1}$$

or

$$v_{gf}E_g(1-E_g) = u_g(1-E_g) - u_fE_g \tag{2}$$

where void fraction, E_g, is the fraction of the total volume occupied by the gas. The superficial velocities, u_g and u_f, are obtained by dividing the volumetric flow rates of each phase by the cross-sectional area. Drift flux, j_{gf}, represents the volumetric flux of a component relative to a surface moving at the average velocity u (total volumetric flow rates of gas and liquid divided by the cross-sectional flow area),

$$\begin{aligned} j_{gf} &= E_g(v_g - u) \\ &= u_g - E_g u \end{aligned} \tag{3}$$

$$\begin{aligned} j_{gf} &= u_g - E_g(u_f + u_g) \\ &= u_g(1-E_g) - u_fE_g \end{aligned} \tag{4}$$

Combining Equations(2) and (4), the drift flux may be defined as

$$j_{gf} = v_{gf}E_g(1-E_g) \tag{5}$$

The above definition is true at any local point in the flow. The velocity of each phase, however, could vary with radial positions in a pipe or annulus, i.e., the velocity profile is in general not flat. Under such circumstances, Equation (3) can be rewritten by taking an average of the physical properties

$$\bar{u}_g = \overline{(E_g u)} + \bar{j}_{gf}$$

Therefore

$$\bar{u}_g/\bar{E}_g = \overline{(E_g u)}/\bar{E}_g + \bar{j}_{gf}/\bar{E}_g$$

and since $\bar{v}_g = \overline{(u_g/E_g)}$ and $\bar{u}_g = u_g$

$$\bar{v}_g = \frac{\overline{E_g u}}{\bar{E}_g \bar{u}} \bar{u} + \frac{\bar{j}_{gf}}{\bar{E}_g} = C_o \bar{u} + \frac{\bar{j}_{gf}}{\bar{E}_g} \qquad (6)$$

where $C_o = \overline{E_g u}/(\bar{E}_g \bar{u})$, the ratio of the average of the product of E_g and u to the product of the averages of E_g and u. C_o may or may not be equal to unity, depending on the velocity distribution across the channel. For turbulent flow when the velocity profile is flat, analyzing the time-averaged equations of motion (Navier Stokes equations) it can be shown that C_o is unity (13). However, when gas bubbles through a liquid column the velocity distribution is such that C_o will never be unity.

Having introduced the variables, the ideal bubbly flow pattern and equations representing void fraction in such

flows are first examined. Modifications required for the actual flow situations are then considered. Finally, the high gas flow situations, when slug flows are likely to exist, are reviewed.

2.1 IDEAL BUBBLY FLOW

Ideal bubbly flow occurs when the gas bubbles are not affected by each other and their concentration remains constant across the channel. The gas is in the form of small discrete bubbles dispersed uniformly in the liquid and unable to agglomerate with each other. Wallis (4) suggested the following empirical equation for the bubble drift flux

$$j_{gf} = v_t(1-E_g)^n E_g \qquad (7)$$

where v_t is the terminal rise velocity which can be defined as the velocity of a single bubble of gas through an infinite medium. The exponent n depends on the bubble size and the flow regime and can be determined experimentally.

For a bubble rising in an infinite stagnant liquid the buoyancy forces are balanced by the drag forces. Wallis (5) obtained a theoretical expression for the terminal rise velocity

$$v_t = C((gs(d_f-d_g))^{1/4}(d_f)^{-1/2} \qquad (8)$$

where s is the surface tension of liquid, d_f and d_g are densities of liquid and gas, respectively, and the coefficient C is, in general, a function of system properties. However, C is approximately constant for most practical purposes when the liquid viscosity is low. Peebles and Garber (14) extensively studied terminal rise velocity of a single bubble. For most practical cases when the bubble Reynolds number is greater than 1000, they suggest a value of 1.18 for the constant term C in Equation (8) which then gives

$$v_t = 1.18((gs(d_f-d_g))^{1/4}(d_f)^{-1/2} \qquad (9)$$

Harmathy (15) proposed the same equation with a value of 1.53 for the constant C

$$v_t = 1.53(gs(d_f-d_g))^{1/4}(d_f)^{-1/2} \qquad (10)$$

Because equation (10) has been used by various researchers (11) to analyze their data, it will be used in all subsequent analyses.

If n=2 as suggested by Wallis (5), is used along with equation (10) for v_t, Equation (7) becomes

$$j_{gf} = 1.53E_g(1-E_g)^2((sg(d_f-d_g))^{1/4}\ (d_f)^{-1/2} \qquad (11)$$

For a stationary liquid column, $u=u_g$, Equation (4) gives

$$j_{gf} = u_g(1-E_g) \qquad (12)$$

Combining Equations (11) and (12)gives

$$u_g = 1.53E_g(1-E_g)((sg(d_f-d_g))^{1/4}\ (d_f)^{-1/2} \qquad (13)$$

Noting that for most cases $d_f \rangle\rangle\ d_g$

$$u_g = 1.53E_g(1-E_g)(sg/d_f)^{1/4} \qquad (14)$$

Equation (13) relates the void fraction to the superficial gas velocity for ideal bubbly flow for a stationary liquid column. Equation (14) is the simplification that results when $d_f \rangle\rangle\ d_g$ Predictions from these two equations are in good agreement with the data of Shulman and Molstad (16) for air-water flow.

There are disagreements over the value of n to be used in Equation (7). Gaylor et al. (17) found a value of n=2 only for very low bubble Reynolds number, R_{eb} (usually less than 2). This is not surprising since ideal bubbly flow is likely to occur for only smaller bubble diameter, d_b. Miles et al. (18), working with stable foams, observed n to vary between 1.6 to 1.9. Lockett and Kirkpatric (6) found similiar variation in n (between 1.8 and 2.4) even though they took special care to maintain ideal bubbly flow. Zuber and Hench (19) presented theoretical analysis and experimental data indicating that n=1.5 for R_{eb} greater than 1000. Wallis (5) obtained significantly different values of n for air bubbling through pure and impure distilled water, tap water and soap solutions. Wallis (5) also noted similar variation in

the values of n with the distance travelled by the bubbles from the point of injection. Lockett and Kirpatric (6) got different values of n depending on the way bubbles were introduced into the column.

A number of correlations were established by various authors in the area of mass transfer involving two-phase flows. The general form of these correlations for E_g as a function of u_g is

$$\frac{E_g}{(1-E_g)^p} = Cu_g \qquad (15)$$

Mersmann (10) proposed the following semi-theoretical relationship (assuming $d_f \gg d_g$) for bubble and spray columns

$$\frac{E_g}{(1-E_g)^4} = 0.46u_g \left(\frac{d_f}{sg}\right)^{1/4} \left(\frac{d_f s^3}{m_f^4 g}\right)^{1/24} \left(\frac{d_f}{d_g}\right)^{5/72} \qquad (16)$$

where m_f is the viscosity of the liquid. Akita and Yoshida (7) analyzed the experimental data for nonelectrolytic solutions by dimensional analysis and suggested

$$\frac{E_g}{(1-E_g)^4} = 0.66 \frac{u_g}{(gD)^{1/2}} \left(\frac{D^2 d_f g}{s}\right)^{1/8} \left(\frac{D^3 d_f g}{m_f}\right)^{1/12} \qquad (17)$$

Several investigators proposed correlations with p=0. For example, Hikita and Kikukawa (20) reported

$$E_g = 1.66(u_g)^{0.47}(s_w/s_f)^{2/3}\ (m_w/m_f)^{0.05} \qquad (18)$$

where the subscript w refers to the property values for water. Hikika et al. (21) suggested a similar equation by applying dimensional analysis

$$E_g = 0.672(u_g m_f/s)^{0.578}(m_f{}^4 g/d_f\ s^3)^{-0.131} (d_g/d_f)^{0.062}(m_g/m_f)^{0.107} \qquad (19)$$

Although the types of correlations mentioned in Equations (16) to (19) use differing values for the exponent p, predictions of these equations do not vary greatly because the applicability of these correlations is limited to a narrow range of void fraction, usually E_g less than 0.1. Fundamental problems with these equations are that they are true only for ideal bubbly flow. In a finite flow channel, such as an oil-well casing, ideal bubbly flow never occurs.

2.2 MODIFICATIONS TO ACCOUNT FOR NON-IDEAL EFFECTS

A certain amount of agglomeration of bubbles occurs in practice in most two-phase systems. A bubbly mixture is essentially unstable against coalescence, since there is always a tendency to reduce the total surface energy. The bubbles may be large with a spherical cap and flat at the tail. Thus, the variation in bubble concentration and velocity necessitates modifying simple bubbly flow theory. Zuber and Hench (19) suggested that the result of the entrainment of bubbles in each others wakes is an increase in the

relative velocity and a decrease in the value of the exponent n in equation (7). They suggested a value of zero for n and to using Equation (10) for v_t. This reduces Equation (11) to the following equation for drift flux (assuming d_f d_g)

$$j_{gf} = 1.53\ E_g(sg/d_f)^{1/4} \qquad (20)$$

Using the expression for j_{gf} in Equation (6)

$$v_g = C_o u + 1.53(sg/d_f)^{1/4} \qquad (21)$$

Henceforth, the bar on top of the variables will be omitted, because all equations apply to nonideal flow. For a stationary liquid column ($u=u_g$) Equation (21) reduces to

$$v_g = u_g/E_g = C_o u + 1.53(sg/d_f)^{1/4}$$

therefore

$$E_g = \frac{u_g}{C_o u_g + 1.53(sg/d_f)^{1/4}}$$

or

$$E_g = \frac{u_g}{C_o u_g + C_1} \qquad (22)$$

where $C_1 = v_t = 1.53(sg/d_f)^{1/4}$. The data of Zuber and Findlay (11), gathered in a circular channel, agrees very well with Equation (22) when $C_o=1.2$. If typical property values for crude oils (s=20 dynes/cm and d_f=1gm/cm^3 at 70° F) are used, C_1 becomes equal to 0.60 ft/sec and Equation (19) becomes the Godbey-Dimon (22) equation for u_g less than 2 ft/sec.

A number of researchers have expressed void fraction data in the form given by Equation (22) with different values for the parameter C_o and property groups (or constants) for the parameter C_1 (8,9,22,23,24,25). Hughmark (23) obtained a relationship similiar to Equation (22) for systems that include air-water, air-kerosene and air-light oil. For typical crude property values the Hughmark correlation is equivalent to Equation (16) with C_1=0.75ft/sec and C_0=2. Mashelkar (24), Haug (8) and Zahradnik (9,25) also used Equation (22), and they obtained essentially similiar values of the parameters: C_1=0.984 ft/sec and C_o=2.0. Kawagoe et al. (26) correlated their data with C_1=1.18 ft/sec and C_o=1.7. Bhaga and Weber (27) used an Equation very similiar to Equation (15) with C_o=1.09 and $C_1=0.91(1-E_g)^2 v_t$. A tabular form of all these correlations for nonideal bubbly flow is shown in Table 1.

All these works, however, were conducted in channels with circular cross-sectional areas. Consequently Equation (22) may not adequately represent void fraction in annular channels. For example, the data gathered by Podio et al. (3) from a constant annular area does not agree with Equation (19).

TABLE 1

Correlations for Void Fraction in Bubbly Flow

Investigator	Void Fraction Correlation u_g in ft/sec	Void Fraction, For Air-Water/Crude at 70° F, E_g	Range of Gas Flow Rates, u_g ft/sec
Godbey and Dimon (22)		$\frac{u_g}{1.2u_g+0.6}$ (Crude Oil)	0-2.0
Hough-mark (23)	$\frac{u_g}{2u_g+1.15X^*}$	$\frac{u_g}{2u_g+1}$ (Water) $\frac{u_g}{2u_g+0.75}$ (Crude Oil)	0.0131-1.476
Mashelkar(24) Haug(8) Zahradnik(9)		$\frac{u_g}{2u_g+0.98}$ (Water)	0.1017-0.906
Kawagoe et al. (25)		$\frac{u_g}{1.7u_g+1.18}$ (Water)	-
Bhaga and Weber (24)	$\frac{u_g}{1.09u_g+0.9Yv_t}$	$\frac{u_g}{1.09u_g+0.55Y^{**}}$ (Water)	0.009-0.077

* $X = \frac{(d_f/d_w)^{1/3}}{(s_f/s_w)^{1/3}}$ ** $Y = (1-E_g)^2$

Subscript w refers to water.

2.3 SLUG FLOW

At higher gas velocities, the agglomerated bubbles become so large that they almost fill the entire available flow cross-section. Bubbles are cylindrical or bullet shaped. The liquid slugs may or may not contain smaller entrained gas bubbles carried in the wake of large bubbles. The liquid slugs in between such bubbles give the name of the flow pattern, the dynamics of which is quite different from bubbly flow. The equations for void fraction derived for bubbly flow are, therefore, not applicable for slug flow. In general, for vertical slug flow, the terminal rise velocity is a function of gravity, forces of inertia, surface tension and viscous forces (28). However, if the dimensionless inverse viscosity

$$N_f = (gD^3(d_f-d_g)d_f)^{1/2}/m_f \qquad (23)$$

is greater than 300 and the Eotvos number

$$E_t = gD^2(d_f-d_g)/s \qquad (24)$$

is greater than 100, the flow is inertia dominant. For example, using typical crude oil property values (with viscosity of 0.0098 gm/cm-sec) and an equivalent diameter of 3.1 inches, N_f and E_t are 70,616 and 3041, respectively. For water (s=72.03 dynes/cm and m_f=0.00984 gm/cm-sec) with the same equivalent diameter, N_f and E_t are 70,616 and 869, respectively. Under such circumstances, Wallis (5) developed

$$v_t = K(gD(d_f-d_g)/d_f)^{1/2}$$
$$= K(gD)^{1/2} \qquad (25)$$

Also for slug flow, the void fraction was given by Wallis (4)

$$E_g = \frac{E_g}{u_g+v_t}$$
$$= \frac{u_g}{u_g+K(gD)^{1/2}} \qquad (26)$$

The constant K, which varied for different geometries and was determined experimentally for various channels, is given by Wallis (29). For circular channels, the value of K was experimentally found to be 0.345 by White and Beardmore (30) and 0.346 by Dumitrescu (31). Nicklin et al. (32) reported K to be 0.35 for circular channels. For very small channels (4.07 square inch cross-section), Birkoff (33) obtained a slightly lower K_1 (i.e., 0.23). Based of theory Davis and Taylor (34) and Dumitrescu (31) arrived at slightly different values of K. Using K=0.345 and an equivalent diameter of 3.1 inches for D, Equation (26) gives

$$E_g = \frac{u_g}{u_g + 1} \qquad (27)$$

Equation (27) was suggested by Godbey and Dimon (22) for estimating E_g when u_g is less than 2 ft/sec.

The applicability of either Equation (26) or Equation (27) to variable bubble concentration is doubtful. For instance, Nicklin et al. (32) pointed out that variable bubble concentration needs to be accounted for by incorporating another parameter in Equation (26) as was done in Equation (22). Griffith (28) showed that for gas slugging through annuli, the outer diameter, instead of the equivalent diameter, should be used in Equation (22). In addition, Griffith (29) found K to depend on the ratio of the inside to the outside diameter of the tubings.

Knowledge of the transition point between bubbly and slug flow is required to determine when Equation (13) or Equation (26) applies. Godbey and Dimon (22) suggested that the transition occurs at a superficial velocity of about 2 ft/sec. Hughmark (23) obtained bubble regimes for superficial gas velocities up to about 1.0 ft/sec in bubble columns. This indicates that transition gas velocity will be higher than 1.0 ft/sec. Christeansen (35) suggested an E_g value of 0.20 for transition in heated vertical channels. Assuming the equation for slug flow (Equation (27)) to be valid at the point of transition, Equation (27) gives a transition velocity of 0.25 ft/sec. However, Griffith and Wallis (36) observed that coalescence rarely occured at E_g less than 0.20. Radovich and Moissis (37) and Griffith and Wallis (36) concluded that, for low liquid flow rates, the transition occured whenever void fraction was greater than 0.3

(i.e., at transition gas velocity greater than 0.43 ft/sec). Taitel and Dukler (38) agreed with this conclusion and presented a theoretical analysis for this flow pattern transition that lead to the following equation for u_g in a stagnant vertical liquid column where d_f d_g

$$u_g = 0.457(gs/d_f)^{1/4} \qquad (28)$$

Taitel et al. (39) in their recent study recommended that the constant 0.457 be replaced by 0.383 in Equation (28). For typical crude oil and water properties, Taitel et al.'s (39) suggestion yields transition gas velocities of about 0.15 ft/sec and 0.20 ft/sec respectively. Thus transition gas velocities ranging from 0.15 (Taitel et al. (39)) to 2.0 ft/sec (Godbey-Dimon (22)) have been suggested by various workers. In addition, all these transition correlations are for circular cross-sectional channel and may not necessarily apply to annular geometry.

Chapter III

PROPOSED CORRELATIONS FOR ESTIMATING VOID FRACTION

3.1 BUBBLY FLOW

The area of flow transition between bubbly and slug regimes can not be analyzed easily because of the complex flow pattern hydrodynamics. Using a flow pattern map, the types of flow regimes can be identified using data such as void fraction, mass flux, density, pressure, viscosity and pipe diameter. However, the available flow pattern maps are not identical, and transition from bubbly to slug flow will not be considered in this study. Based on the preceding discussion and also on Taitel et al.'s (39) analysis, it is assumed that the transition occurs when the void fraction approaches 0.25. Below this value, the void fraction can be estimated using an expression given by

$$E_g = \frac{u_g}{C_o u_g + C_1} \qquad (29)$$

Recent works for circular cross-sectional channels indicate that C_1 is usually greater than v_t. For example, Mashelkar (24), Haug (8) and Zahradnik (9) obtained C_1=0.984 ft/sec with the air-water system for which v_t =0.8 ft/sec. Also,

values of C_o much higher than 1.2 have been reported by many workers. Equation (29) is therefore rewritten as

$$E_g = \frac{u_g}{Au_g + B_o v_t} \qquad (30)$$

For gas bubbling through an annulus, the values of the parameters A and B_o will depend on the inside and outside diameters. The parameter C_o was introduced by Zuber and Hench (19) to account for variable bubble concentration and velocity across the flow channel. The variations in bubble concentration and velocity will be accentuated in an annulus by the presence of an inner tube. Additionally, the inner tube is likely to cause an increase in bubble entrainment. Both of these effects will result in a lowering of gas void fraction with a consequent increase in the value of the parameter A. Assuming the ratio of diameter of the inner tube to the outer tube to be directly proportional to increment in A, the following equation can be written

$$A = A_o + A_1(D_t/D_c) \qquad (31)$$

Equation (31) must be verified by experiment.

The terminal rise velocity, v_t, is also likely to be influenced by the containing walls. Indeed, Edger (40) showed that for fluid bubbles rising in a cylindrical channel, the bubble velocity in a finite medium, v_b, is lower than the

terminal rise velocity, v_t, in an infinite medium and is represented by

$$v_b = v_t/(1+1.6d_b/D) \qquad (32)$$

From theoretical analysis and experimental data, Kutateladze and Styrikovich (41) related the bubble diameter, d_b, to the gas injector orifice radius r_o by

$$d_b = 2r_b = 2(sr_o/g(d_f - d_g))^{1/3} \qquad (33)$$

The bubble diameter, d_b, is thus a weak function of the injector orifice diameter. In this work d_b is assumed to be constant; it was determined by experiment. Replacing D in Equation (32) by equivalent diameter D_e and combining Equations (30), (31) and (32) the following relationship for void fraction is obtained

$$E_g = \frac{u_g}{(A_o+A_1D_t/D_c)u_g + (B_ov_t/(1+B_1/D_e))} \qquad (34)$$

where $D_e=D_c-D_t$ and B_1 is the composite constant $1.6d_b$. If the Harmathy correlation for terminal rise velocity, Equation (10), is used in Equation (34) the following relationship for void fraction is obtained

$$E_g = \frac{u_g}{(A_o+A_1D_t/D_c)u_g +(1.53B_o(sg/d_f)^{1/4}/(1+B_1/D_e))} \qquad (35)$$

Equation (35) is the proposed correlation to estimate gas void fraction in the bubbly flow regime in annular geometry. The four parameters A_o, A_1, B_o and B_1 need to be determined from experimental data.

3.2 SLUG FLOW

A modified form of Equation (26) that accounts for variable bubble concentration and velocity is recommended for estimating void fraction during slug flow. As suggested by Wallis (4), Equation (36) accounts for variable bubble concentration and velocity.

$$E_g = \frac{u_g}{C_o u_g + K_1 v_t} \tag{36}$$

For high velocities Nicklin et al. (32) experimentally determined C_o and K_1 to be 1.2 and 1.0, respectively. Because high velocities are inherent in slug flow, these values for the constants appear reasonable. Thus

$$E_g = \frac{u_g}{1.2u_g + v_t}$$

$$= \frac{u_g}{1.2u_g + K(gD)^{1/2}} \tag{37}$$

Following Griffith's (28) suggestion, the diameter in Equation (37) will be substituted by the outer tube diameter D_c (34). Analysis of Griffith's data further indicates that K could be linearly correlated with D_t/D_c according to

$$K=0.345+0.063(D_t/D_c) \qquad (38)$$

Thus, the proposed equation for estimating void fraction during slug flow takes the following form

$$E_g = \frac{u_g}{1.2u_g + (0.345+0.063D_t/D_c)(gD_c)^{1/2}} \qquad (39)$$

The values of the parameters C_o and K_1 taken as 1.2 and 1, respectively, need to be verified, and the effect of annular geometry on these parameters must be investigated.

Chapter IV

EXPERIMENTAL SETUP AND PROCEDURE

4.1 EXPERIMENTAL SETUP

An experimental rig, consisting of two concentric tubes resembling an oil-well, was built to gather void fraction data. Most of the previous work was carried out in long columns to avoid the entrance effects (5,3). However, an eight foot high column was first built because of its relatively low cost and simple mechanical structure. An illustration of the setup is shown in Figure 1.

The outer tube, resembling a casing, was made of two four-foot plexiglass sections. The two pieces were joined by welding, and special care was taken so that the inner surface remained smooth to avoid any disturbance to bubble flow. Plexiglass was chosen as the material of construction because it is transparent allowing flow visualization. Plexiglass also has excellent machining properties which permit easy mounting of column fixtures such as manometers.

The inner tube was replaceable and was made of a single opaque polyvinyl chloride pipe. The inner tube was empty during experimental runs. The bottom of the tube was

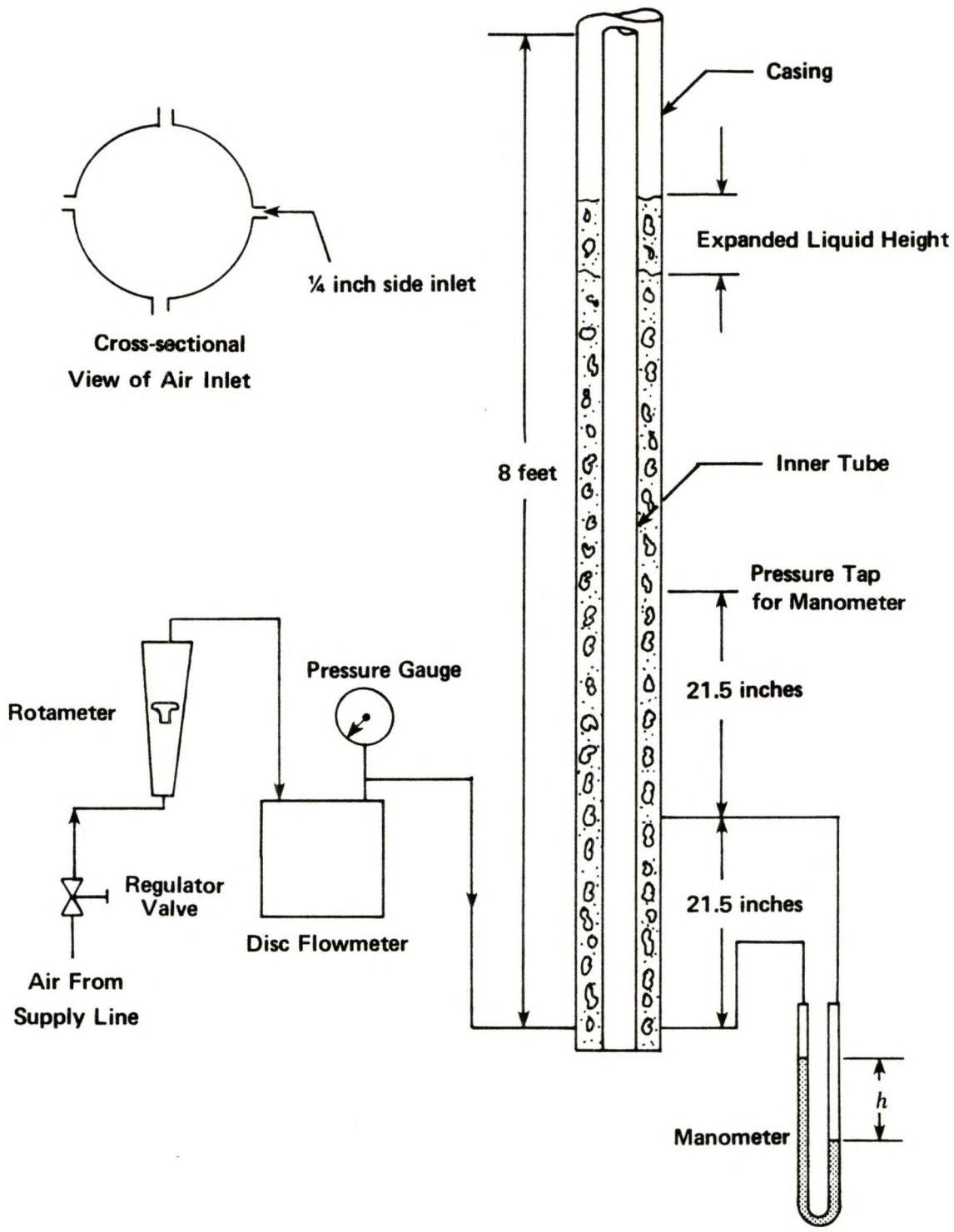

Figure 1: Schematic of Experimental Setup for Measuring Void Fraction

TABLE 2

Dimensions of Casing and Tubes

Casing Diameter (Inside), Inch	Tube Diameter (Outside), Inch	Cross-Sectional Area Ft^2
6.515	None	0.2315
6.515	2.380	0.2006
6.515	3.527	0.1637
6.515	4.490	0.1216

threaded inside and was joined to a two-inch extended pipe (threaded outside) which was placed in the middle at the bottom of the column. Table 2 lists the dimensions of the casing and the tubes.

The top of the casing was fixed with a flange which holds together four support rods. The lower ends of the support rods were bolted to the bottom support of the column. The inner tube was centered by four adjustable screws placed on the top of the flange. The top of the column was thus firmly mounted to fix the vertical position and to prevent vibrations during gas bubbling.

The annulus was filled with tap water to the desired height in the column. The outer surface of the casing was

marked at various heights to facilitate measuring single bubble rise velocities. These markings also helped to record the changing height of the liquid column with gas velocity.

Air was allowed to flow into the bottom of the annulus through four equally spaced inlets placed around the bottom of the casing. Air from the supply line was regulated by a regulator valve. Air from a single line was distributed to a four sided system through a horizontal mild steel pipe placed on the stand of the column. A smoother control of air flow rate at low pressure was obtained by regulating four metering valves used for air-inlets around the bottom of the casing. At pressures greater than 30 psig, the metering valves were kept fully open and only the regulator valve was used to control the flow rate. The pressure at the regulator could hardly reach 75 psig because of lower supply pressure and pressure drop across the line.

The air flow rate was measured upstream of the annulus using a disc flowmeter and a stopwatch that measured to 1/100th of a second. The flow rate indicated by the flowmeter was at a base temperature of 60^{o} F. A pressure gauge (accurate to 1 psi) was located on the downstream side of the flowmeter so that flow rate could be converted to column operating conditions. The column operating temperature was measured by inserting an ordinary mercury thermometer (grad-

uated to 10 F) into the water in the annulus. The average operating temperature was 68° F.

A rotameter was placed between the disc flowmeter and metering valves. The float of the rotameter was made of aluminum, and the rotameter tube was marked from 0 to 100. Although the rotameter was not highly accurate, it was useful in obtaining uniform distribution of experimental data over the whole range of flow rates.

The gas void fraction data were calculated from differential pressure data gathered with manometers between various points in the column (Figure 1). Pressure taps were mounted on column wall at various distances from the gas inlet. The positions of the taps are indicated in Table 4. Manometer tubes having inside diameter of about 9 mm (larger than usual manometer tubes) were used to avoid air bubbles inside the tubes. A mixture of gauge oil and carbon tetra chloride, having specific gravity of about 1.23-1.30, was used as manometer fluid. The specific gravity was measured using a 'Westphal balance' (43). Gauge oil was used because of its red color, good mixing property with carbon tetrachloride and lower specific gravity. Because the maximum pressure difference between various points in the column was 11 inches of water, a fluid of low specific gravity was used to facilitate pressure measurements at low flow rates. Flexible transparent tubes were used to connect the valves at the

open ends of the manometer tubes with the manifolds at the pressure taps in the column. Transparent tubes allowed detection of the presence of any air bubbles. Sufficient flow of water was not available to detach all the air bubbles from the tube wall, because water in the column was stationary. Hence, flexible tubes were used so that bubbles could be detached from the wall by pressing the tubes by hand. Valves were used at the open ends of the manometer tubes, for easy removal of air bubbles from the manometer system. These valves were operated slowly to avoid any sudden change in flow.

The increase in column height for a given gas flow rate, compared to the stagnant liquid height, could also be used to calculate void fraction. The liquid column height, however, was difficult to measure accurately because of frothing and fluctuations for any but the lowest gas flow rates. Thus, this method was only used as a rough check on the data gathered by the differential manometers.

Another experimental setup, very similiar to the previous one, was built because of the limited scope of the previous setup (discussed in the following chapter). The "new" column height uses eighteen feet, and it required welding of more plexiglass sections. The mechanical support system for the new column was complicated becsuse of its height. The pressure taps were 9 to 13 feet from the air-inlets which were at the bottom around the casing.

4.2 EXPERIMENTAL PROCEDURE

Tests using the apparatus described in the previous section were conducted with water and air in the annulus and in the circular channel. The superficial gas velocity was varied from approximately 0.02 to 0.6 feet/sec. Differential pressure measurements taken at four pairs of pressure taps at different heights (Figure 1) allowed observation of the effect of distance from gas entrance on void fraction.

The annulus (or circular channel) was filled with water up to two inches above the top pressure tap. Air was permitted to flow into the water through all of the side-inlets and about thirty minutes was allowed for the flow rate to stabilize. Stability of the flow rate was indicated by stability of the rotameter float. The following data were then recorded:

1. differential heights on the manometers
2. the flow rate of gas (Q) in ft^3/min into the column,
3. the pressure (P) at which gas was measured,
4. the height (H_f) of the gas-liquid mixture in the annulus (or circular channel), and
5. the temperature (T) of the gas-liquid mixture.

Step 4 was followed only for the first few experimental runs to check the voidage data obtained by differential pressure measurements.

Financial resources initially limited us to gathering data from a eight foot high column. Literature review indicated that entrance effects will be significant in such a short column. It was, therefore, decided to gather data at four different heights from the gas inlet. If entrance effects were detected, extrapolation would be possible to estimate results from a infinitely tall column.

At the end of the first five experimental runs, 200 ml of water was collected to measure the surface tension of water using the 'drop weight method' (43). The surface tension of several samples (taken at different times) averaged 72.03 dynes/cm, which was equal to that of distilled water. The surface tension was 72.03 dynes/cm for this study. The flow pattern was observed during all experimental runs to find out the transition point from bubbly to slug flow.

Single bubble rise velocity data for circular and annular geometry were gathered by measuring the time required for a single bubble to travel various heights (4-7 feet). Very low air flow rate was maintained through one side-inlet to keep track of a single bubble.

Chapter V

RESULTS AND DISCUSSION

5.1 EXPERIMENTAL RESULTS USING DATA GATHERED FROM EIGHT FEET HIGH COLUMN

Experimental data are presented, correlated and discussed in this chapter. First the bubble rise velocity data and results are discussed. Then the void fraction data are used to show the entrance effect. Finally, the data unaffected by the entrance effect are analyzed to establish a correlation for void fraction.

5.1.1 Bubble rise velocity

Bubble rise velocities were calculated from the slopes of the plots of distance travelled by a single bubble versus time required by the bubble to travel that distance. Figures 2, 3, 4 and 5 show distance (H) traveled versus time (t) required by the bubble to travel distance H for channels with no inner tube, 2.38 inch inner tube, 3.527 inch inner tube and 4.49 inch inner tube, respectively. The data are also presented in Table 12 in Appendix F. The values of the bubble rise velocities, v_b for various channels are tabulated in Table 3.

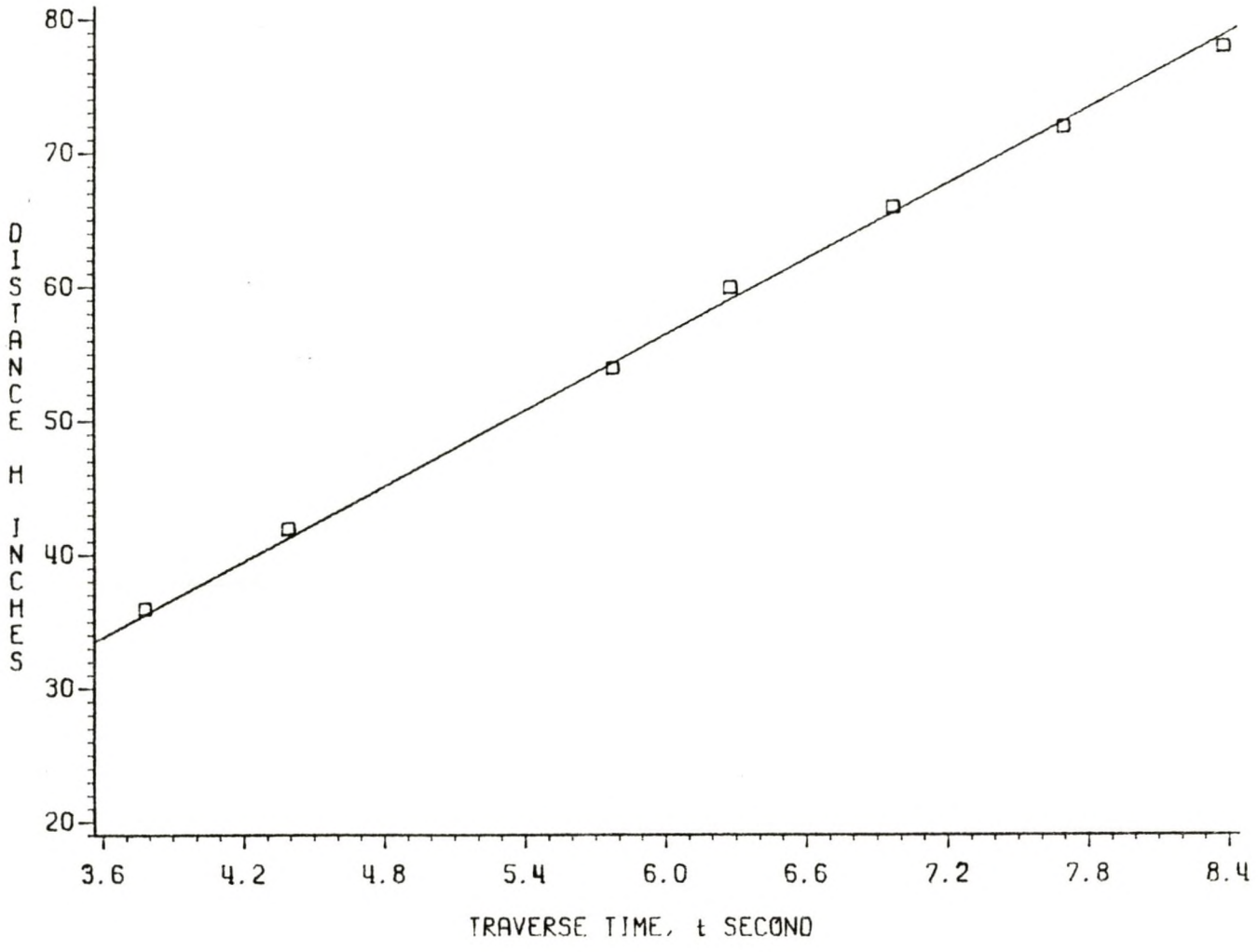

Figure 2: Effect of Liquid Height on Single Bubble Rise Velocity - No Inner Tube

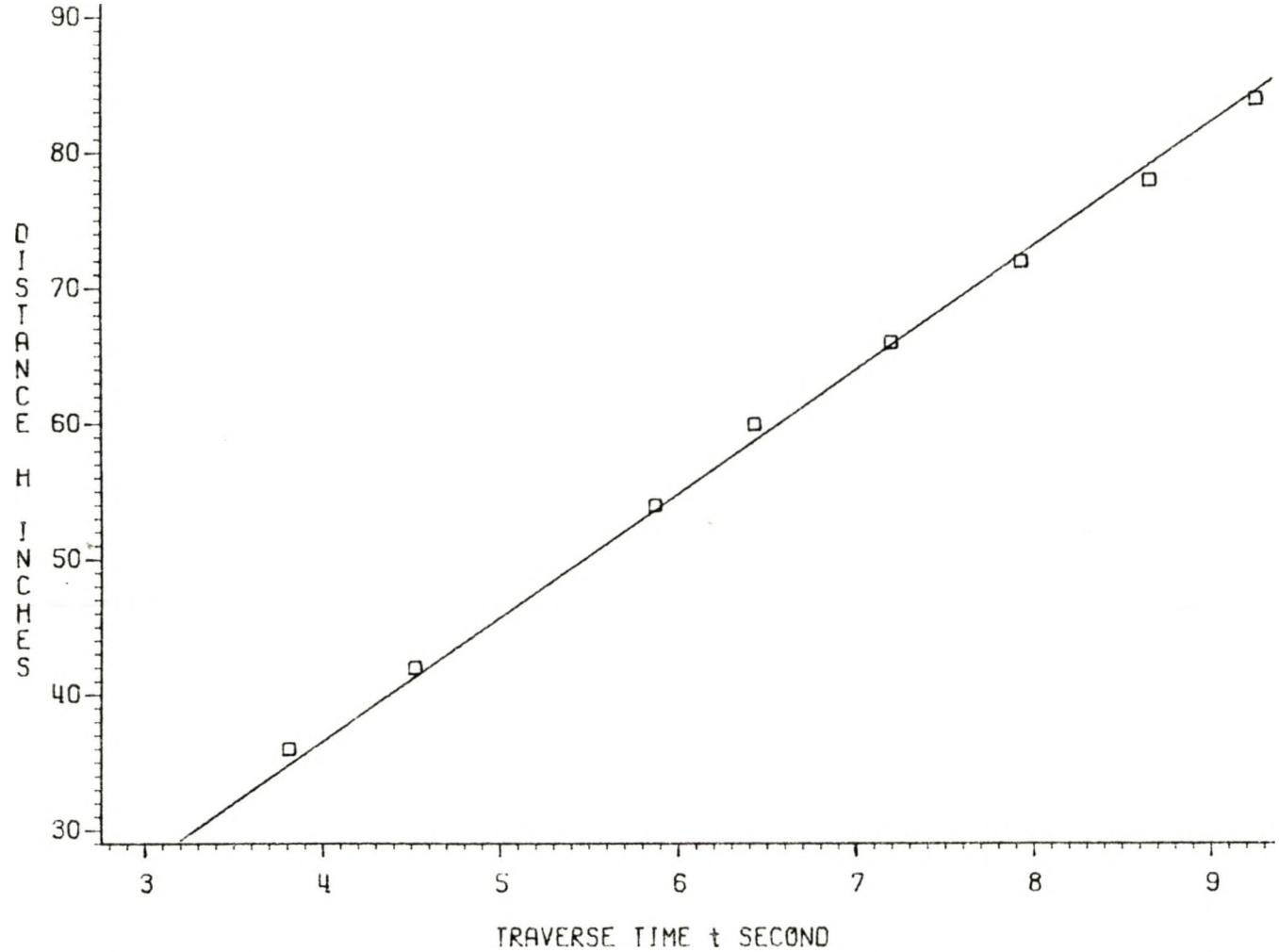

Figure 3: Effect of Liquid Height on Single Bubble Rise Velocity - 2.38 inch Inner Tube

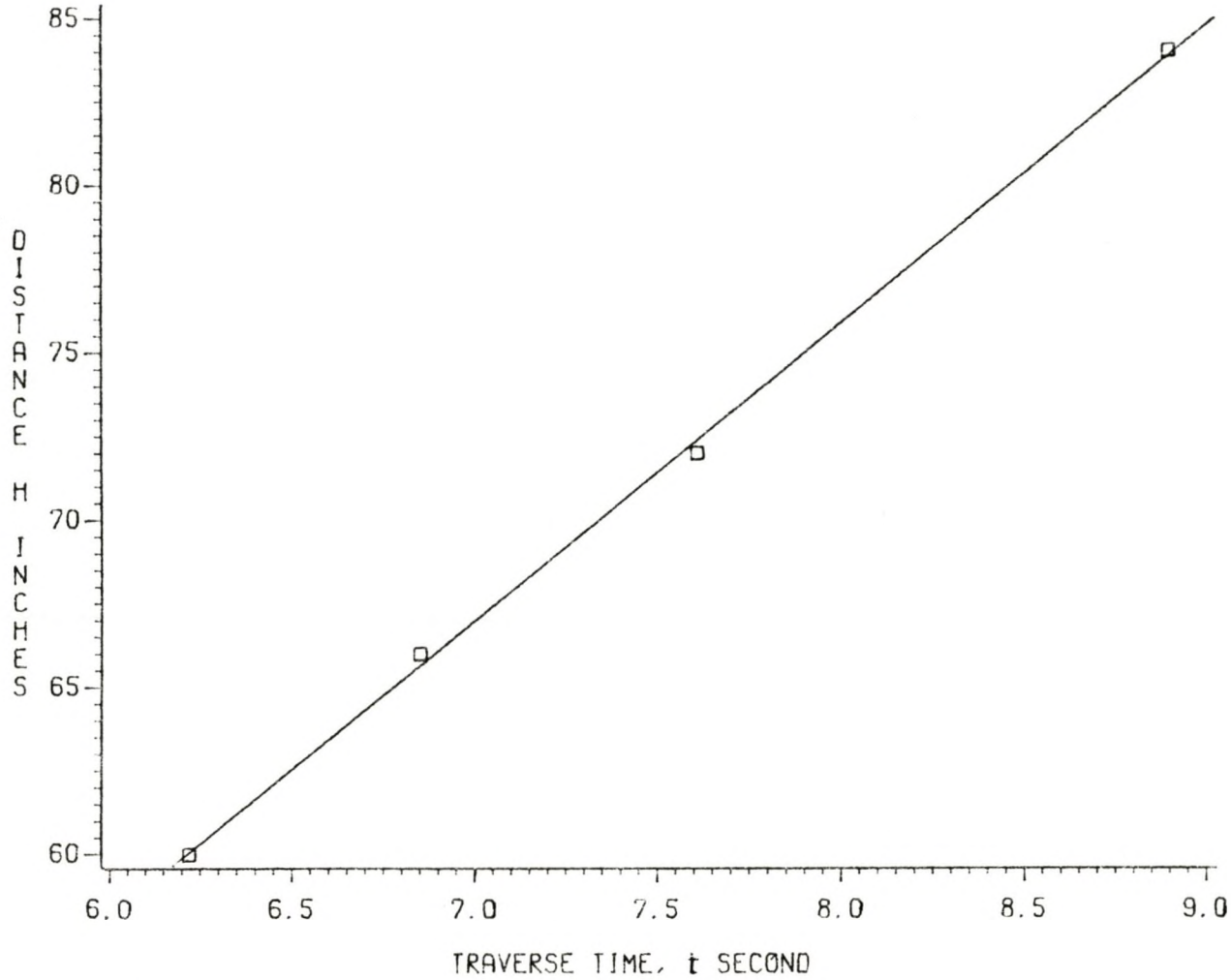

Figure 4: Effect of Liquid Height on Single Bubble Rise Velocity - 3.527 inch Inner Tube

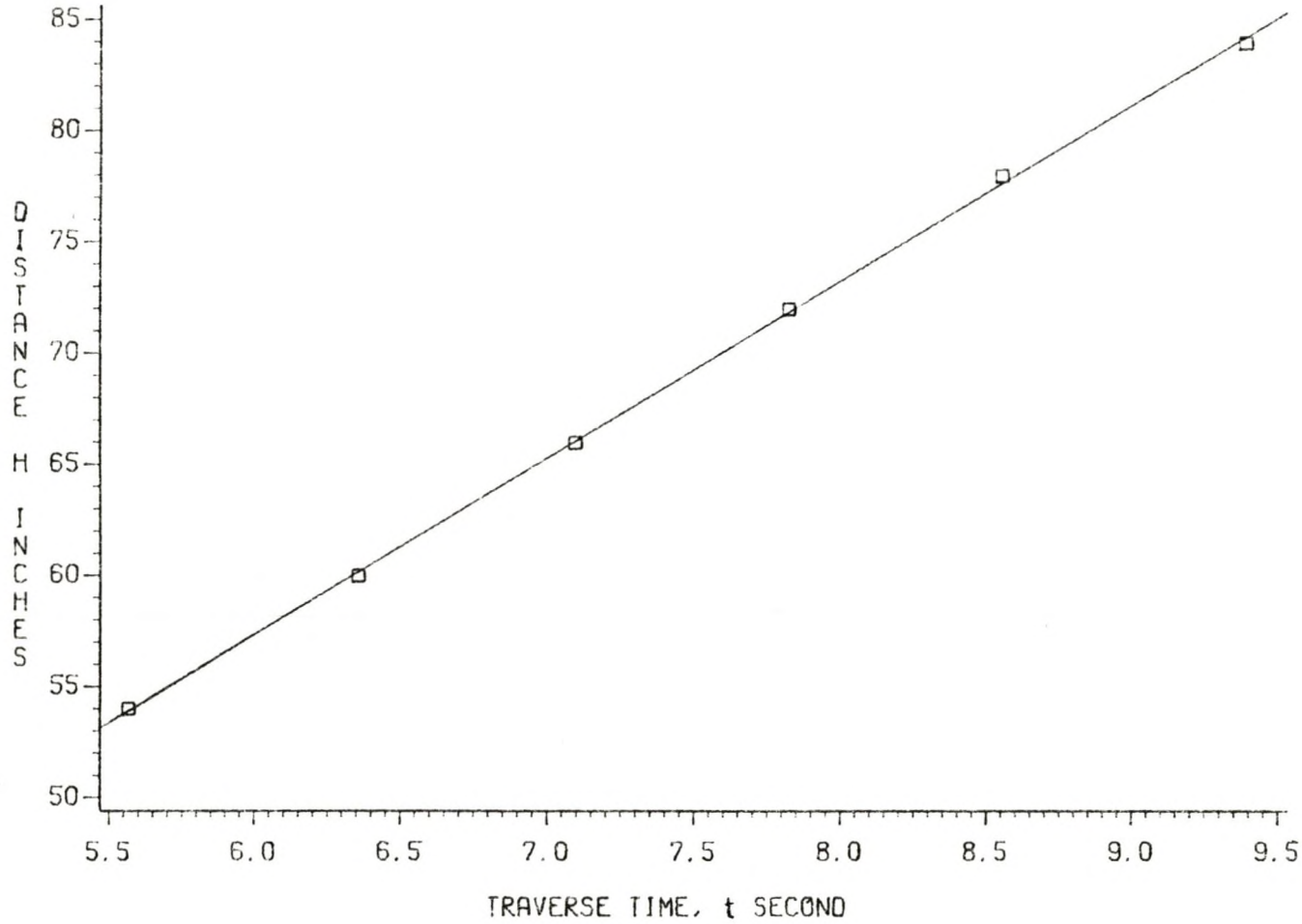

Figure 5: Effect of Liquid Height on Single Bubble Rise Velocity - 4.49 inch Inner Tube

TABLE 3

Bubble Rise Velocities For Various Channels

Casing Outside Diameter, D_c=6.515 inch
Terminal Rise Velocity, v_t=0.8184 ft/sec

Tube Diameter, D_t inch	Equivalent Diameter, D_e inch	Bubble Rise Velocity, v_b ft/sec	Correlation Coefficient, R^2	Standard Deviation, s_d	$1/D_e$ 1/inch	v_t/v_b
0	6.515	0.7660	0.9990	0.5141	0.1535	1.0684
2.380	4.135	0.7375	0.9993	0.4657	0.2418	1.1097
3.527	2.988	0.7200	0.9990	0.3191	0.3347	1.1367
4.490	2.025	0.6705	0.9997	0.2210	0.4938	1.2206

The linear relationship between distance and time required to travel that distance indicates that the velocity of a single bubble was not affected by the height of the channel. High values of the correlation coefficients, greater than 0.999, and small values of the standard deviations, maximum 0.52 (representing the sum of squares of errors between actual and predicted values) represent a very good linear least squares fit. Values of the correlation coeffecients and standard deviations are given in Table 4. It should be pointed out that the bubble rise velocity was

found to be slightly affected by the liquid level, especially for the 3.527 inch and 4.49 inch inner tubes with liquid levels less than 48 inches (4 feet). These affected data were excluded from the analysis and have been reported in the Appendix F.

For the air-water system at 70° F (s=72.03 dynes/cm, $d_{f=1gm/cm^3}$ and $d_g=0$ at 70° F), the Harmathy (15) correlation

$$v_t = 1.53\ (gs(d_f-d_g))^{1/4}\ (d_f)^{-1/2} \qquad (10)$$

gives a value of the terminal rise velocity, v_t equal to 0.8184 ft/sec. The bubble rise velocity determined for the circular channel is about 6% lower than the terminal rise velocity given by Harmathy correlation (Equation (14)). When the influence of the containing wall is accounted for according to Edger, Equation (32) in conjunction with Equation (33), the agreement comesout much better, within 1.2%. The data clearly show that bubble rise velocity is affected by the containing walls and is smaller than the terminal rise velocity. The bubble rise velocity decreased with the increase in the inner tube diameter.

To determine the validity of the suggestion that the diameter D in Edger (40) correlation be replaced by equivalent diameter D_e, the correlation was rewritten in the following form:

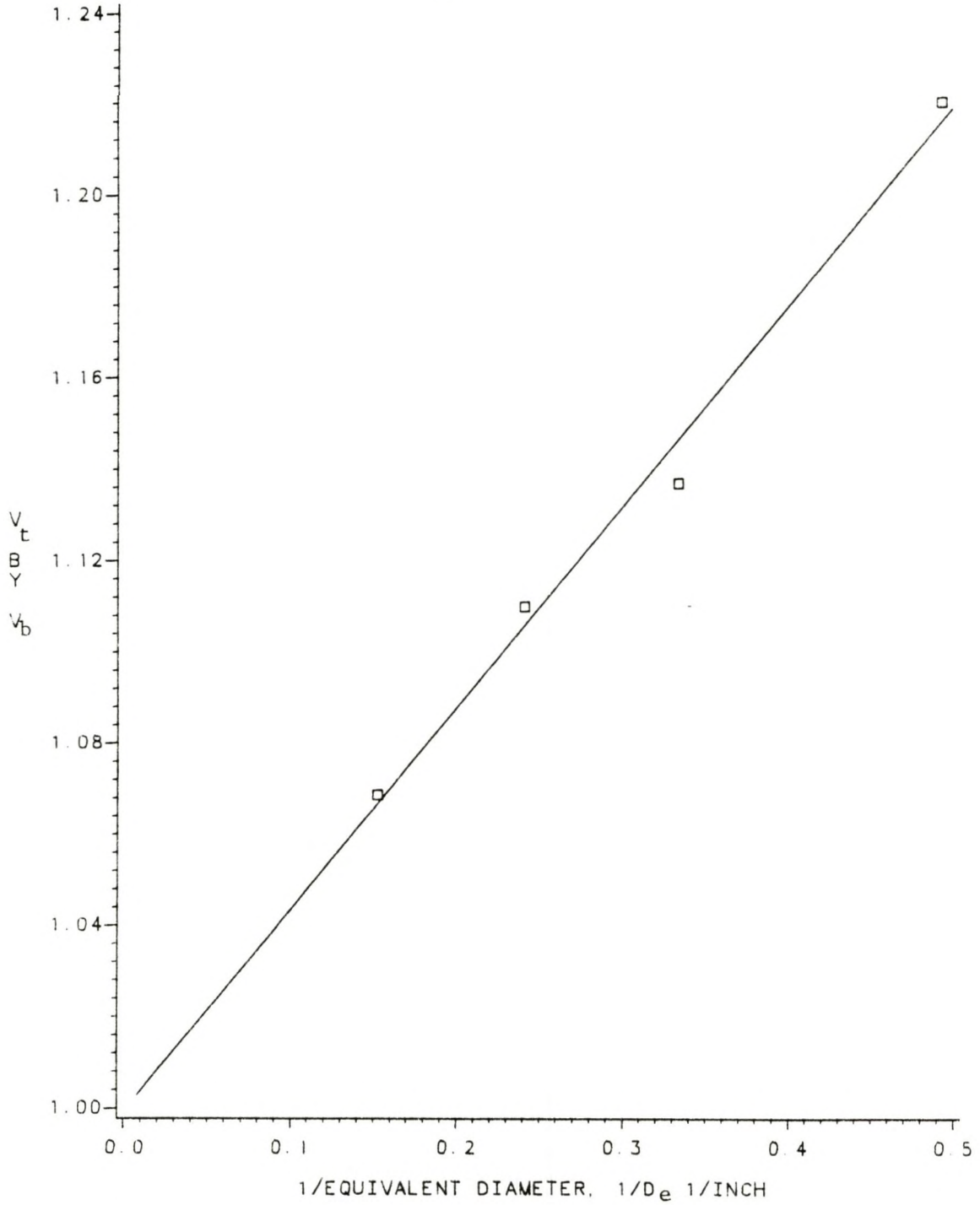

Figure 6: Variation of Bubble Rise Velocity with Equivalent Diameter

$$v_b = v_t/(1+1.6d_b/D) \qquad (32)$$

or

$$v_t/v_b = 1 + B_1/D_e \qquad (40)$$

The values of the ratio of terminal rise velocity to bubble rise velocity and the reciprocal of the equivalent diameter are shown in Table 4. Figure 6 is a plot of v_t/v_b against $1/D_e$. The values of the linear regression coefficient, 0.9860, and the standard deviation, 0.0066, indicate a very good fit between the data and Equation (40). The slope of this line gives a value for the composite parameter B_1 ($=1.6d_b$) of 0.44 inches which is slightly higher than the value of 0.36 inches obtained using Kutateladze and Styrichovich (41) correlation (Equation (33)) with r_o equal to 0.125 inches. Equation (40) can thus be written as

$$v_t/v_b = 1 + 0.44/D_e \qquad (41)$$

5.1.2 Entrance Effect

The data collected for void fraction can be separated into three groups depending upon the liquid height over which void fraction data were averaged using differential pressure measurements. Table 4 indicates the grouping of the data for the analysis involved in this section. Studying the effect of liquid height on void fraction will determine the entrance effect. The manometric method of

TABLE 4

Grouping of the Experimental Runs

Set of Experimental Runs	Liquid Height from Gas Inlet, Inch	Channel Type
First	0-21.5 21.5-43.0	Only Circular Channel
Second	21.5-43.0 43.0-64.5	Circular and Annular Channels
Third	21.5-43.0 43.0-64.5 64.5-75.75	Circular and Annular Channels

void fraction measurement yields the dependence of void fraction on the distance from the gas entrance point. Void fraction data for circular channel were first gathered at two different liquid heights - one between 0-21.5 inches and the other between 21.5-43.0 inches above the gas entrance point. The values of void fractions obtained for the two different heights and their differences at the same superficial gas velocities are tabulated in Table 27 in Appendix F. The column operating pressure was assumed to be one atmosphere. Figure 7 shows the dependence of void fraction on superficial gas velocity and liquid heights for the circular channel. The lower curve represents the void fraction data gathered at the lower height (0-21.5 inches) and the higher

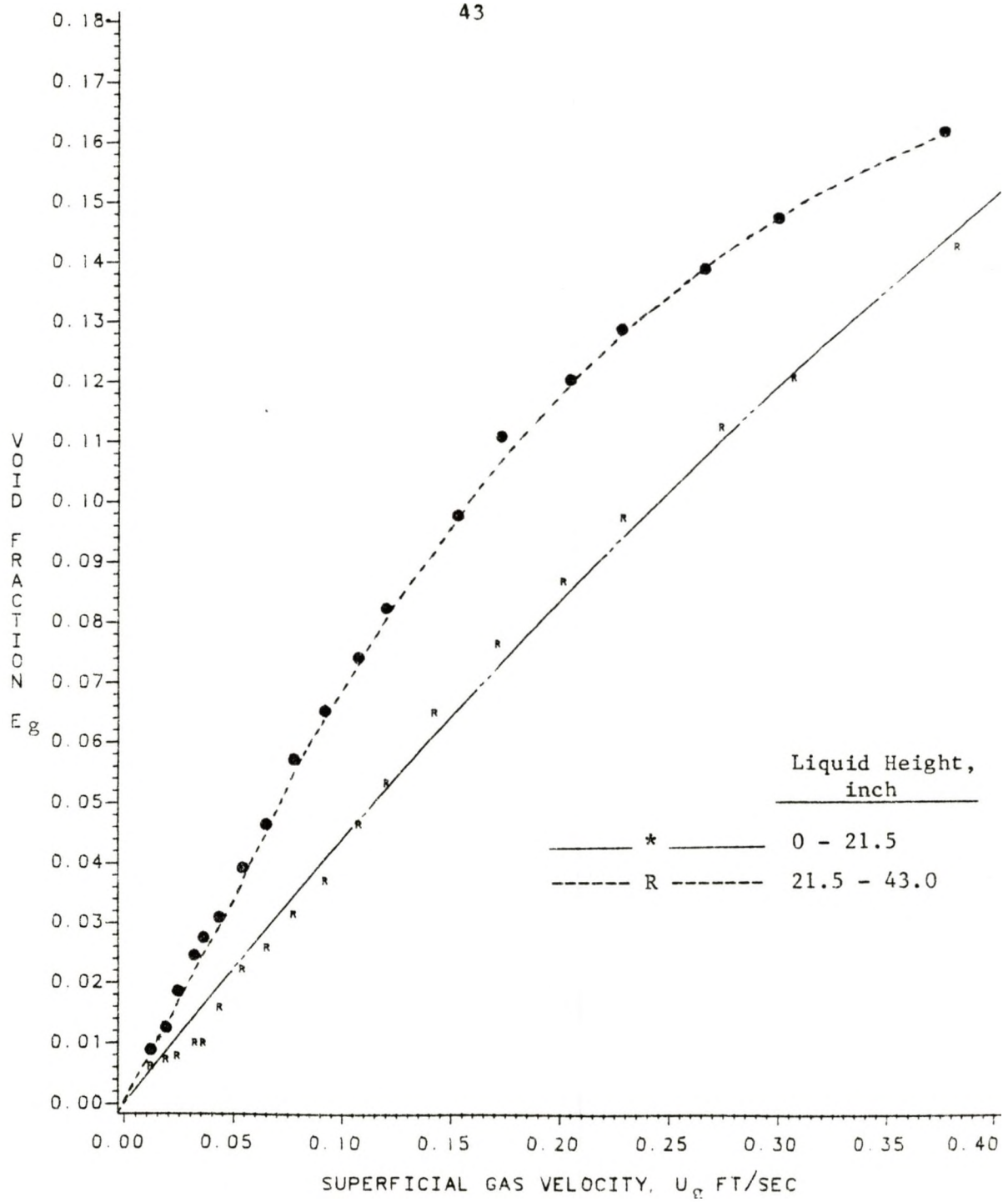

Figure 7: Dependence of Void Fraction on Superficial Gas Velocity and Liquid Height, Circular Channel - First Set

curve represents the higher liquid level (21.5-43.0 inches). The graph clearly demonstrates that void fraction increases with height for a constant superficial gas velocity. The average increase in void fraction with height for the whole range of superficial gas velocities is 72.2%. Void fraction was low for the lowest height because of the larger gas bubbles at the bottom and high bubble velocity when air enters into the column through the side-inlets. It was visually observed that a bubble breaks after travelling a short distance from the gas entrance point. This is consistent with Wallis' (9) work for gas bubbling through a soap solution. The nonlinear relationship

$$E_g = \frac{u_g}{Au_g+B} \qquad (32)$$

between void fraction and superficial gas velocity (positive values of B have been reported in the literature) does not hold for the lower liquid level, rather the relationship is linear. This shows a strong dependence of void fraction on the distance, at least up to 21.5 inches, from the gas entrance point. After observing the entrance effect for the circular channel, it was expected that the annular channels would also exhibit a similar entrance effect.

The second set of runs was then conducted with all channels at the two heights - one between 21.5-43.0 inches and the other between 43.0-64.5 inches. These runs would give a

check for the entrance effect up to 43.0 inches of column height. Tables 28 to 31 in Appendix F give the values of void fraction and superficial gas velocitiy for all four channels. Dependence of void fraction on superficial gas velocity and liquid height are shown in Figures 8 to 11. It is seen that void fraction increases with increasing gas velocity, but at a decreasing rate. This is because bubbles become larger with an increase in the gas velocity and, hence, E_g decreases. From Figures 9 to 11 (for annular channels) it is seen that void fraction values are higher at the higher liquid level (43.0-64.5 inches) for the same superficial gas velocities. The average increase in void fraction with height are 12.44%, 12.80% and 7.34% for channels with the 2.38 inch tube, the 3.527 inch tube and the 4.49 inch tube, respectively. Therefore, the entrance effect exists at least up to 43.0 inches away from the gas inlets. For circular channels (as shown in Figure 7), however, the average increase is only 1.61%. This agrees with the observation of Wallis (5), who conducted experiments using a 3.75 inch diameter tube. He noticed a positive effect of superficial gas velocity on void fraction along the column height. These effects became less important as column height increased. For liquid heights of 24 and 36 inches he obtained almost equal values for void fraction. Zahradnik (9) also found similar trends in bubble columns.

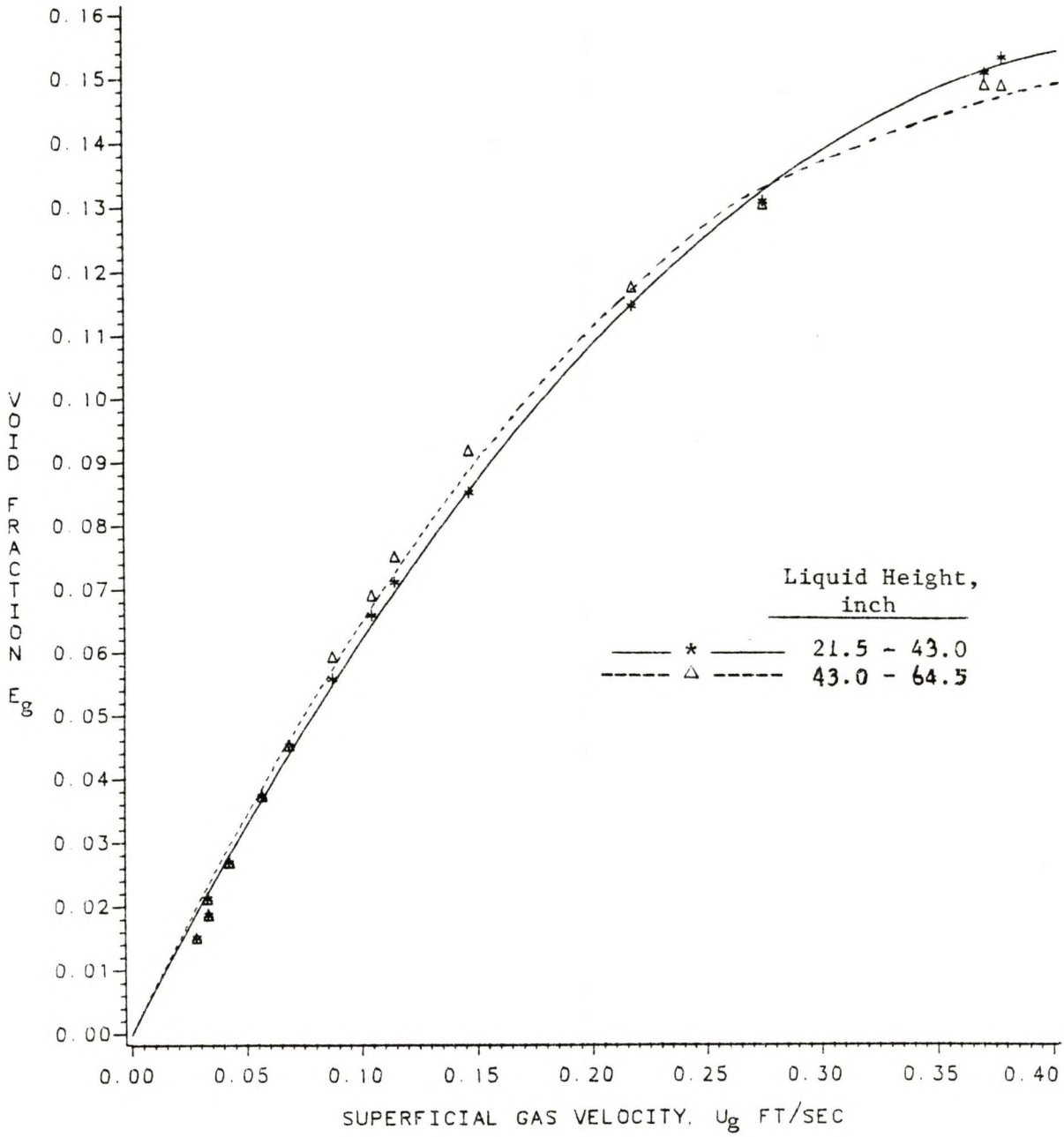

Figure 8: Dependence of Void Fraction on Superficial Gas Velocity and Liquid Height, Circular Channel - Second Set

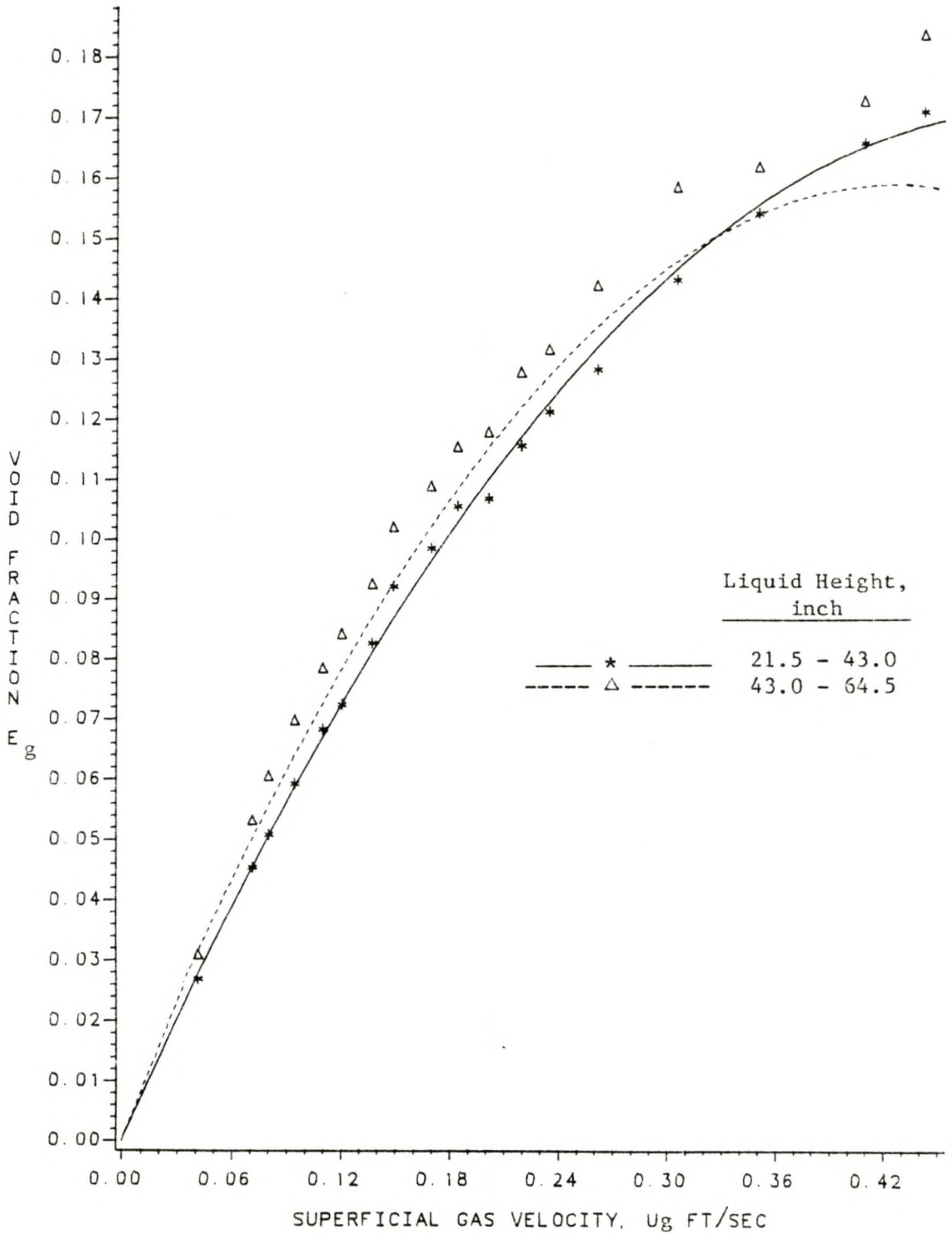

Figure 9: Dependence of Void Fraction on Superficial Gas Velocity and Liquid Height, 2.38 inch Inner Tube - Second Set

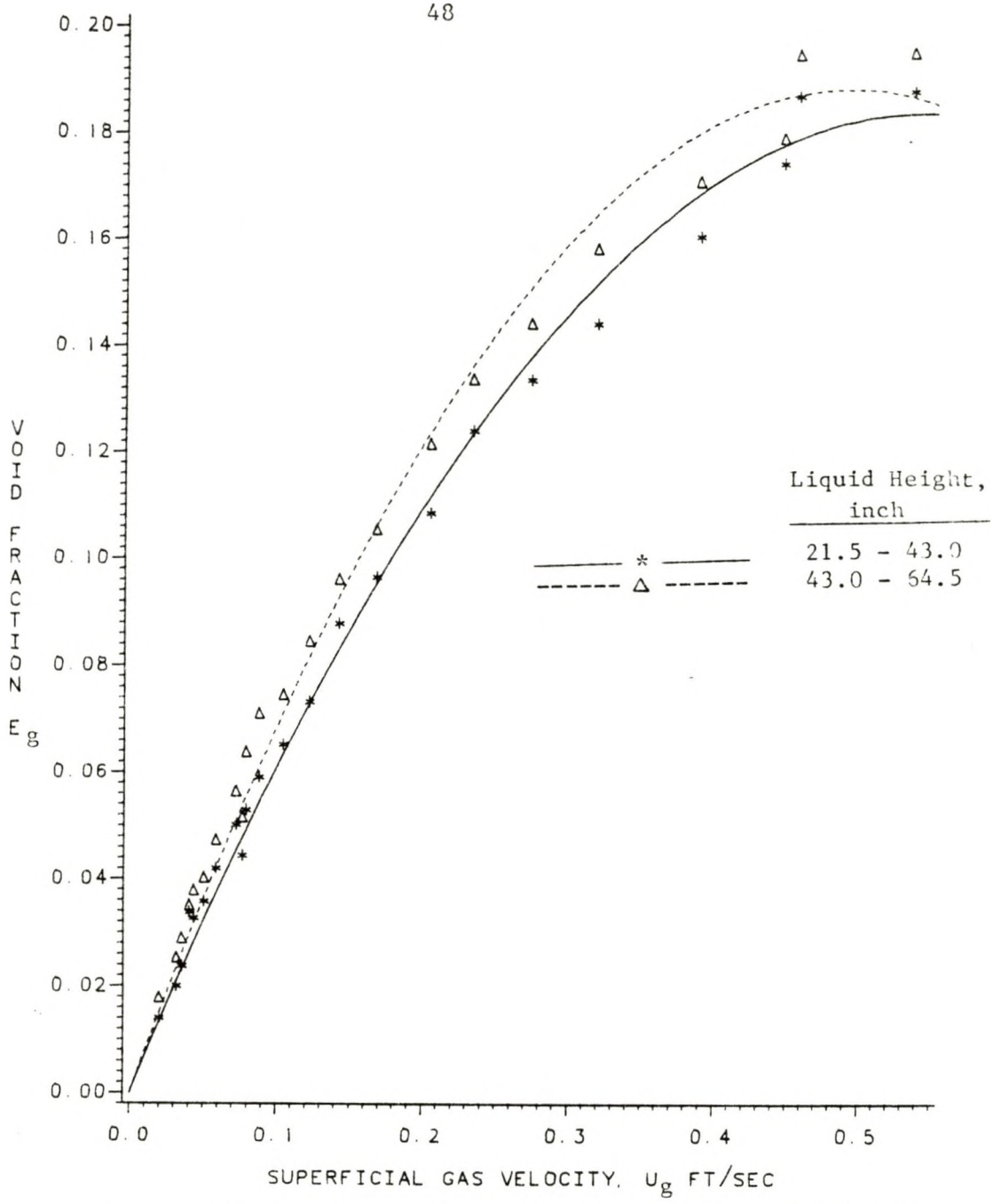

Figure 10: Dependence of Void Fraction on Superficial Gas Velocity and Liquid Height, 3.527 inch Inner Tube - Second Set

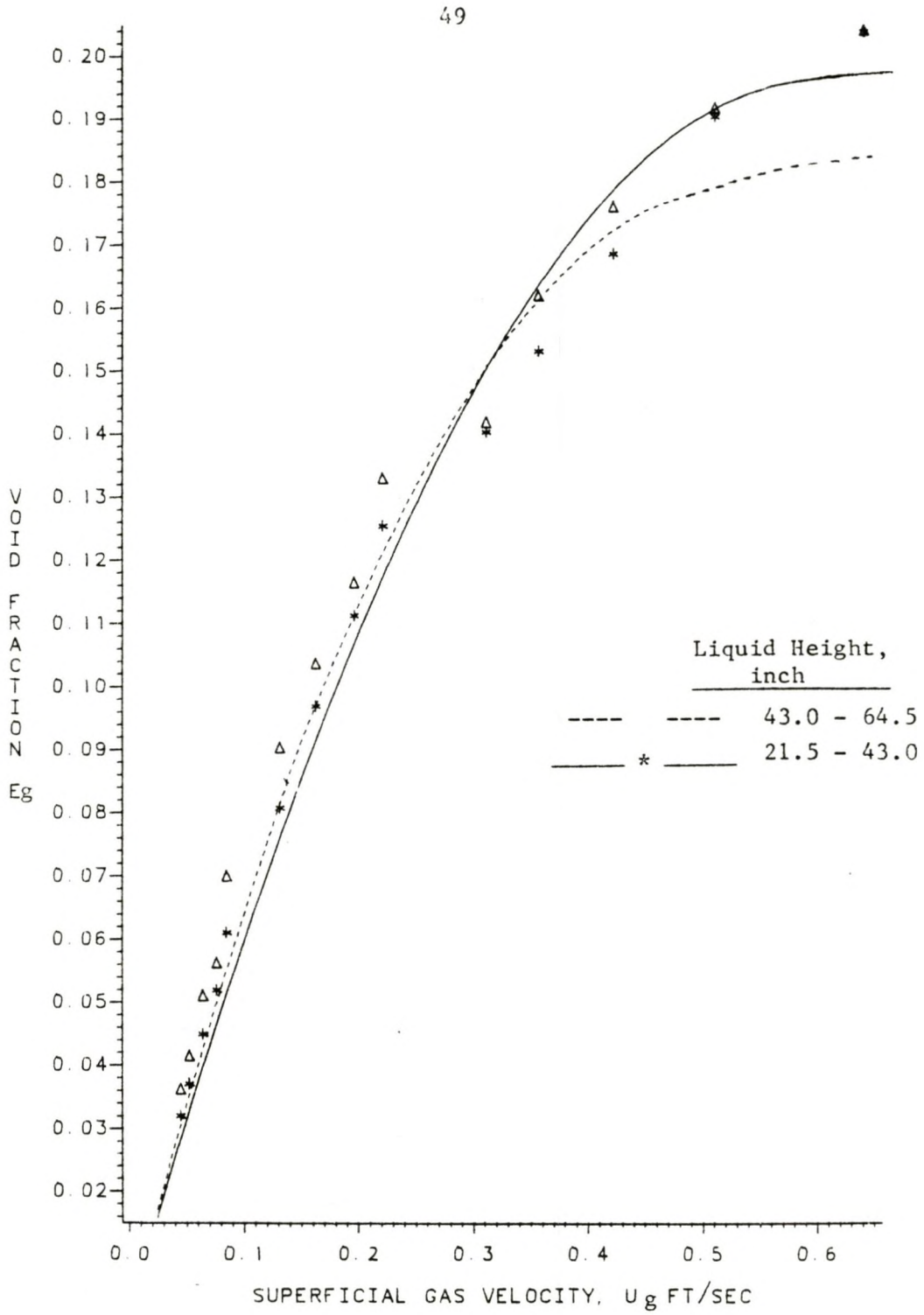

Figure 11: Dependence of Void Fraction on Superficial Gas Velocity and Liquid Height, 4.49 inch Inner Tube - Second Set

Finally, the third set of experimental data was taken at three different heights (Table 4) using all of the channels. With the column height being eight feet, it was not possible to take data beyond 6.33 feet (75.75 inches) because liquid would then splash out of the top of the column. Although void fraction data for the height between 21.5-43.0 inches were available from the second set of runs, these data were retaken along with data for the other two heights in the third set of runs to facilitate extrapolation of the data to infinite column height. The void fraction is tabulated as a function of superficial gas velocity in Tables 32 to 35 (Appendix E) for all of the channels. The plots of void fraction versus superficial gas velocities for the four different channels are illustrated in Figures 12 to 15. There is a definite increase in void fraction with liquid height for heights lower than 43.0 inches for all channels. The average increase with liquid height ranges 6.30 to 20.85%. For the second set of runs the variation was 7.34 to 12.88%. This difference is attributed to experimental error, especially fluctuations in the manometer fluid during the experimental runs. The curves for heights between 43.0-64.5 inches and 64.5-75.75 inches show that at low superficial gas velocities void fraction increased slightly with increasing column height, and at higher gas velocities void fraction decreased slightly with the increase in height. The same trend was observed for all the channels studied.

Presence of foam on the top of the gas-liquid column was observed. This increased the local values of void fraction at this height at low superficial gas velocities. This explanation is consistant with visual observation and also with Zahradnik's (9) work for bubble columns. At high velocities void fraction decreased with height probably beacause bubbles coalesced at the top of the column and the mean bubble velocity therefore increased. Wallis (5) observed a similar effect for slug flow in an air-water system in circular tubes. The net increase in void fraction with height (between 43.0-64.5 inches and 64.5-75.25 inches) varied from 1.54 to 10.36%. These results indicate that increases in void fraction with height at constant gas velocities is not significant at heights greater than 43.0 inches in the column. Hence, the entrance effect may be neglected at column heights greater than 43.0 inches from the gas entrance point.

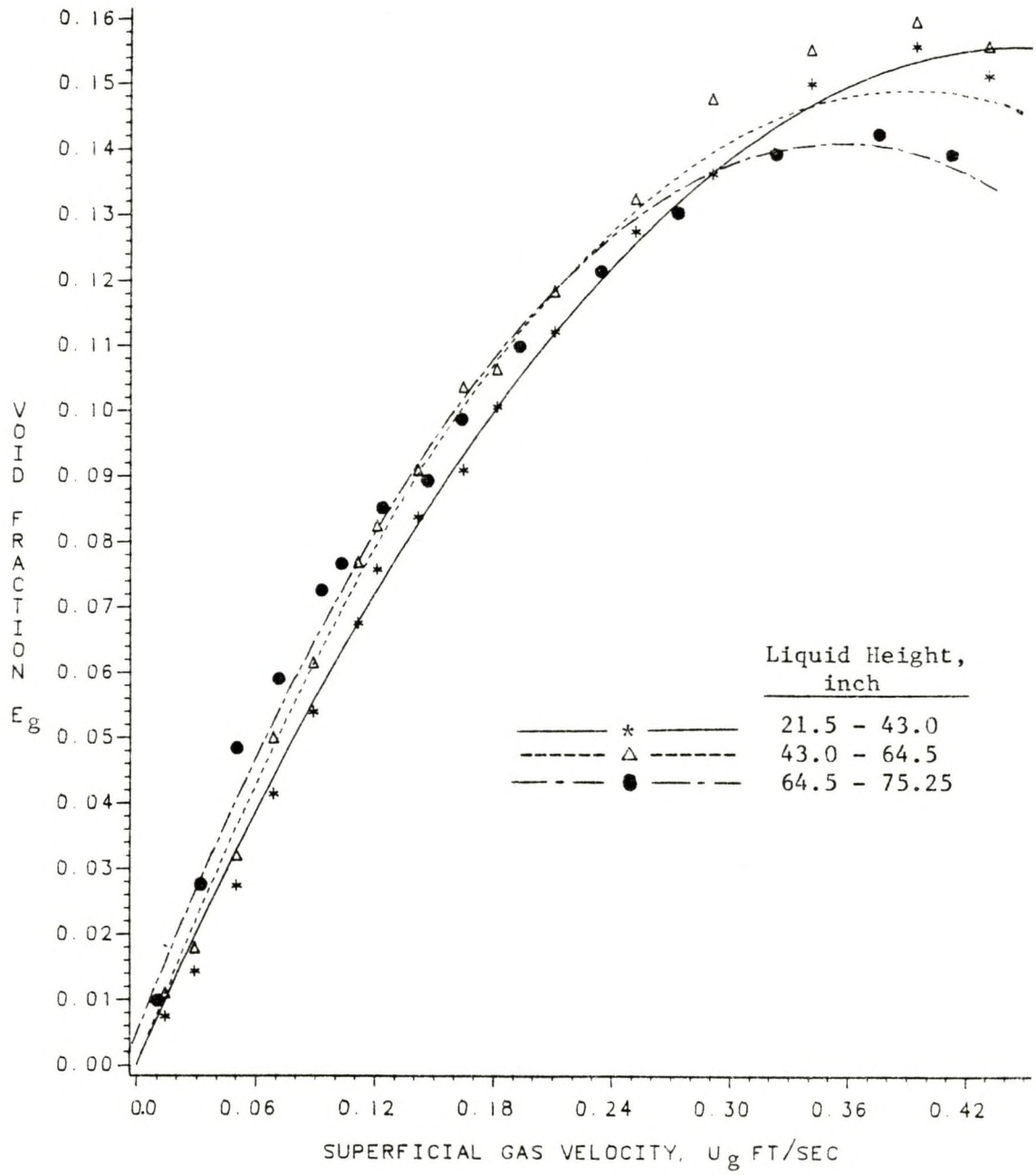

Figure 12: Dependence of Void Fraction on Superficial Gas Velocity and Liquid Height, Circular Channel - Third Set

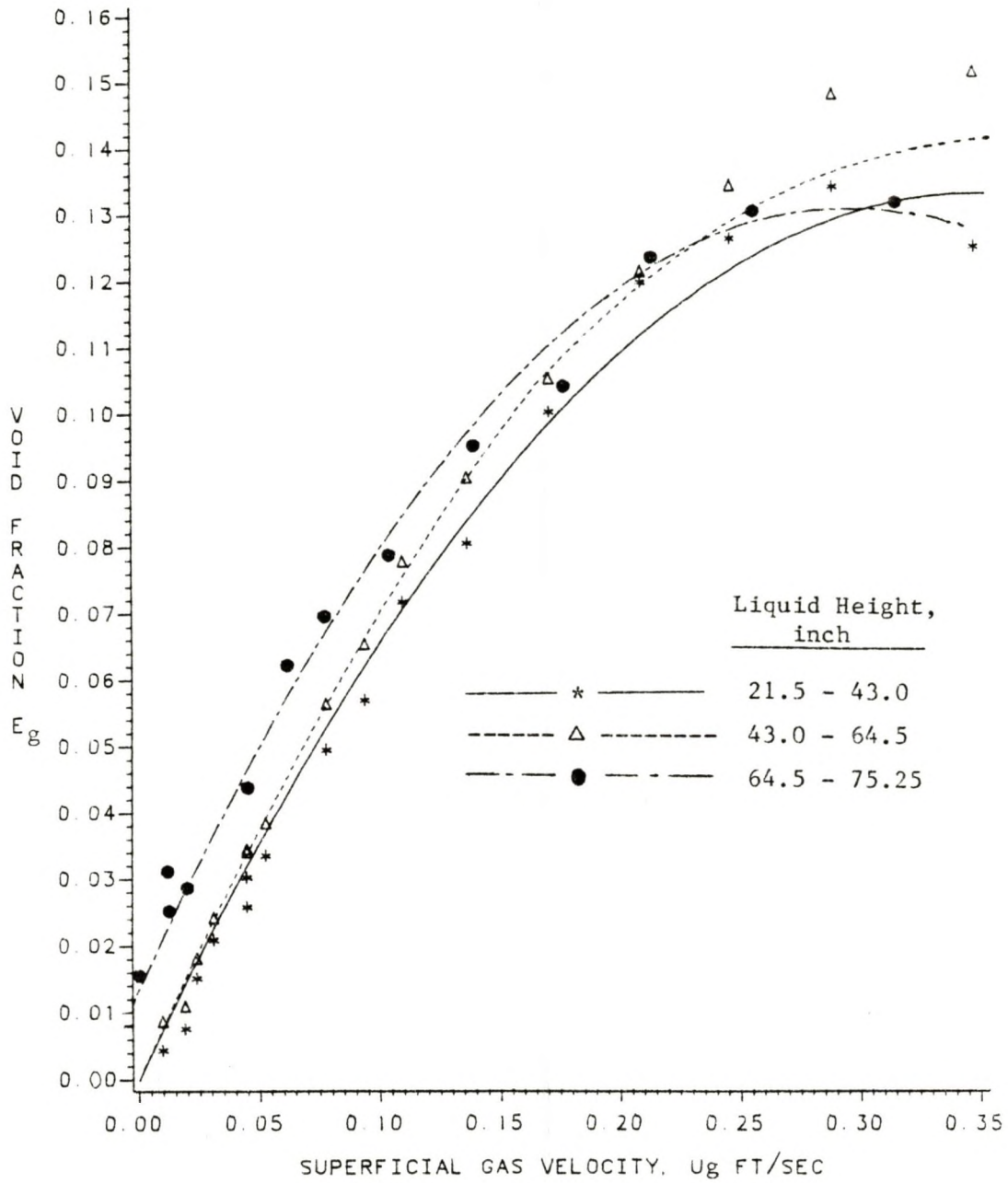

Figure 13: Dependence of Void Fraction on Superficial Gas Velocity and liquid Height, 2.38 Inch Inner Tube - Third Set

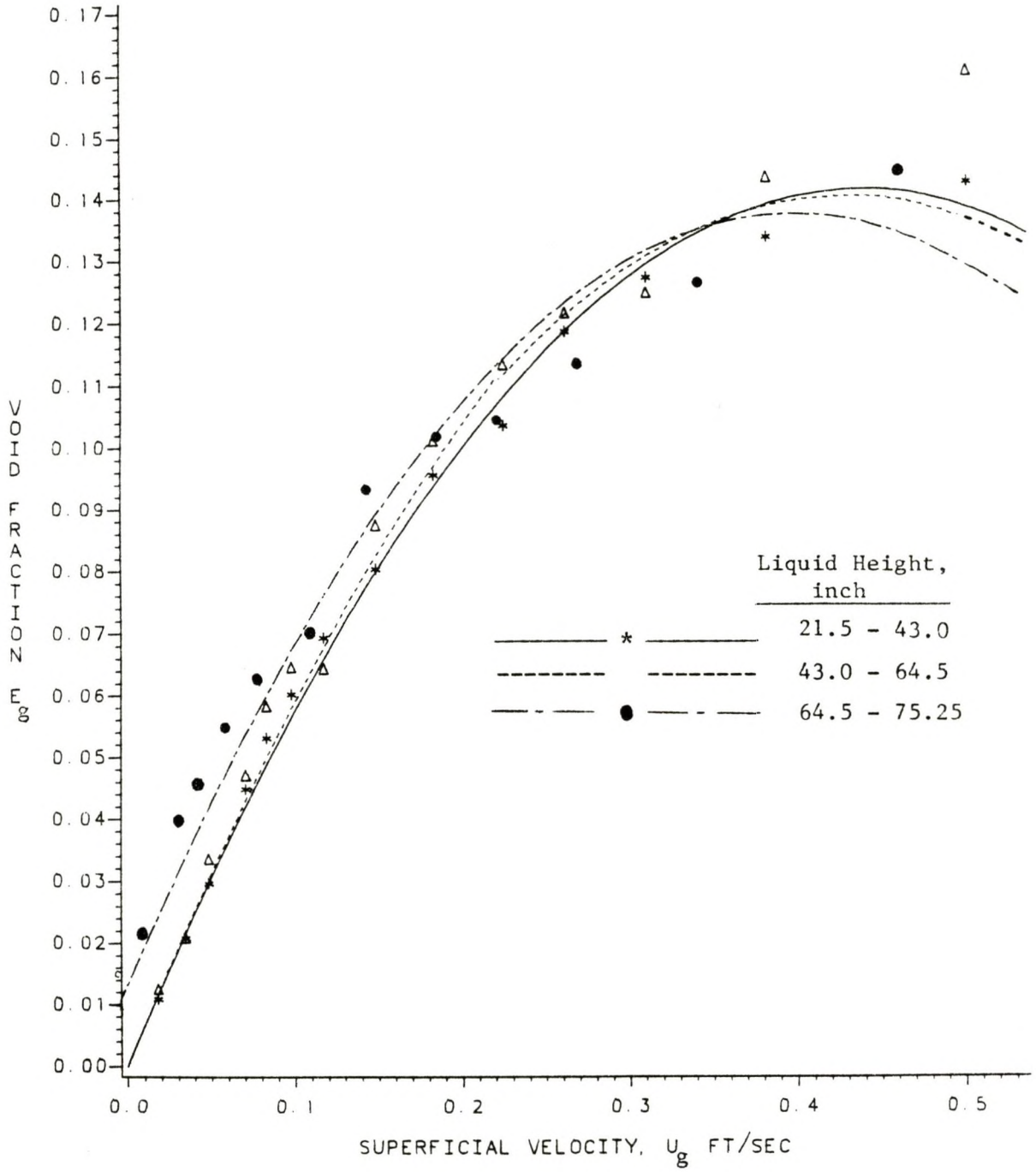

Figure 14: Depeendence of Void Fraction on Superficial Gas Velocity and Liquid Height, 3.527 inch Inner Tube - Third Set

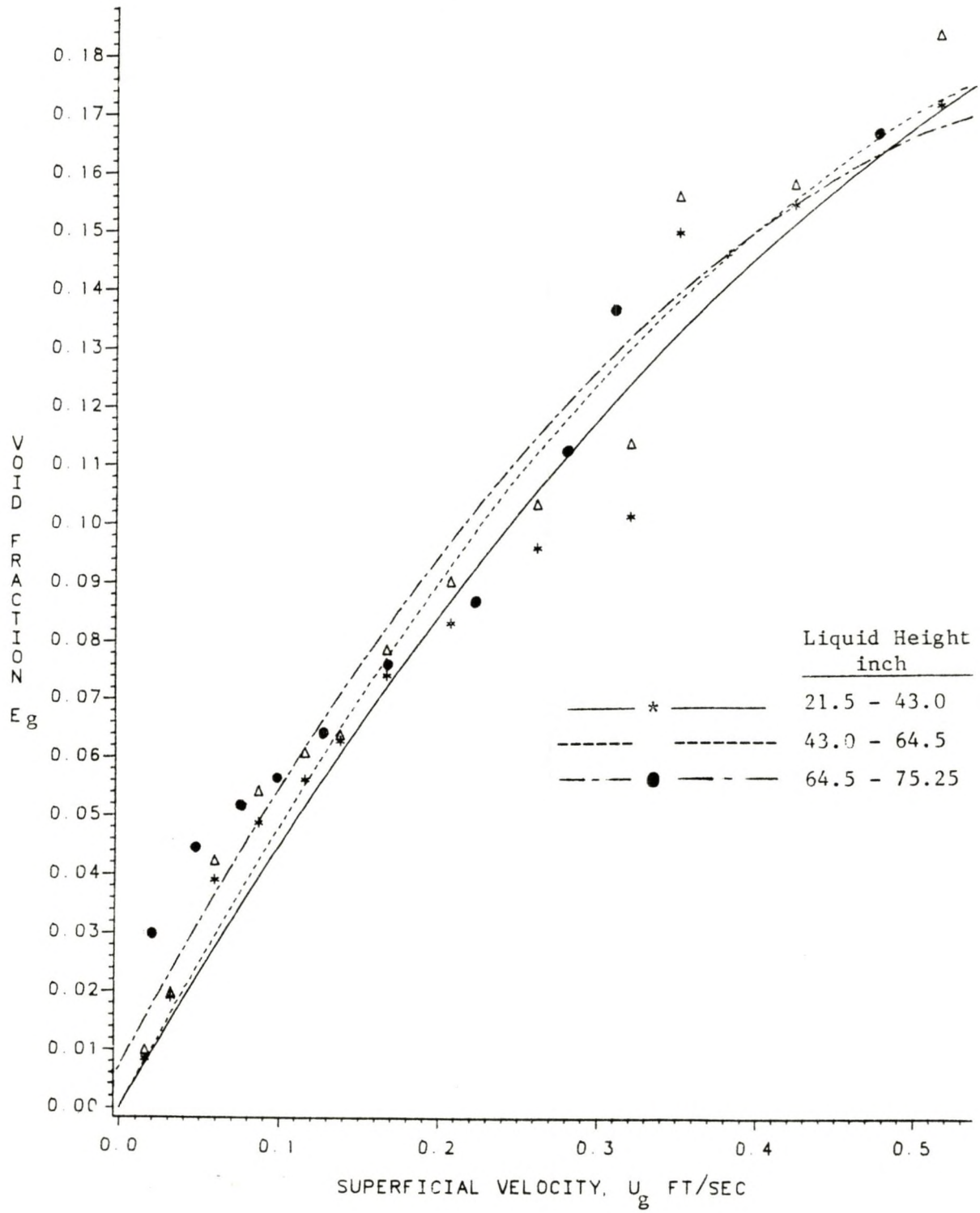

Figure 15: Dependence of Void Fraction on Superficial Gas Velocity and Liquid Height, 4.49 inch Inner Tube - Third Set

5.1.3 Void Fraction

As discussed earlier, the entrance effect was found to be negligible at about 43.0 inches away from the gas inlet. Hence, extrapolation of the void fraction data to infinite column height is not required. Because of foaming and greater experimental error on the top section of the column (64.5-75.75 inches), the void fraction data gathered at the top will not be considered in the analysis. Sufficient number of data were not taken during the third set of experimental runs primarily because the third set of runs was made to check the presence of the entrance effect between 43.0-64.5 inch height. Void fraction measurements taken between 43.0-64.5 inch height during the second set of experimental runs were used to study the effect of annulus diameter on void fraction.

Visual observation showed a bubbly flow pattern to exist during all of the experimental runs. This is consistent with the fact that the void fraction values were always lower than 0.25. Data were analyzed to estimate the parameters in the void fraction correlations for bubbly flow (Equation (30)).

To aid in the data analysis, Equation (35) (or Equation (30)) can be rearranged to give

$$u_g/E_g = Au_g+B \qquad (42)$$

Equation (42) suggests a linear relationship between u_g/E_g and u_g. Experimental results obtained with the air-water system are shown in Figures 16, 17, 18 and 19 for channels with no inner tube, and with tubes having diameters of 2.38 inches, 3.527 inches and 4.49 inches, respectively. The figures show the values of ratio of superficial gas velocity to void fraction, u_g/E_g, plotted against the superficial gas velocity, u_g. All plots yielded straight lines indicating the validity of the proposed correlation (Equation (35)). The correlation coefficients, obtained by linear regression curve fitting, were greater than 0.94 for the annular channels and was 0.814 for the circular channel. The scatter in the data at low u_g for the circular channel reflects the relatively large errors in the calculated values of u_g/E_g for small errors in reading the height of manometer fluid. The same data plotted as E_g versus u_g (figure 8) does not show as much scatter. Table 5 summarizes the values of the parameters A and B for various channels obtained from the slopes and the intercepts of the curves, along with the correlation coefficients and standard deviations. The parameter A increased with increasing tube diameter (i.e., decreasing equivalent diameter). This agrees with with the proposed correlation (Equation (31)).

Figure 20 is a plot of A versus D_t/D_c showing the validity of the linear relationship given by

$$A = A_o + A_1(D_t/D_c) \qquad (31)$$

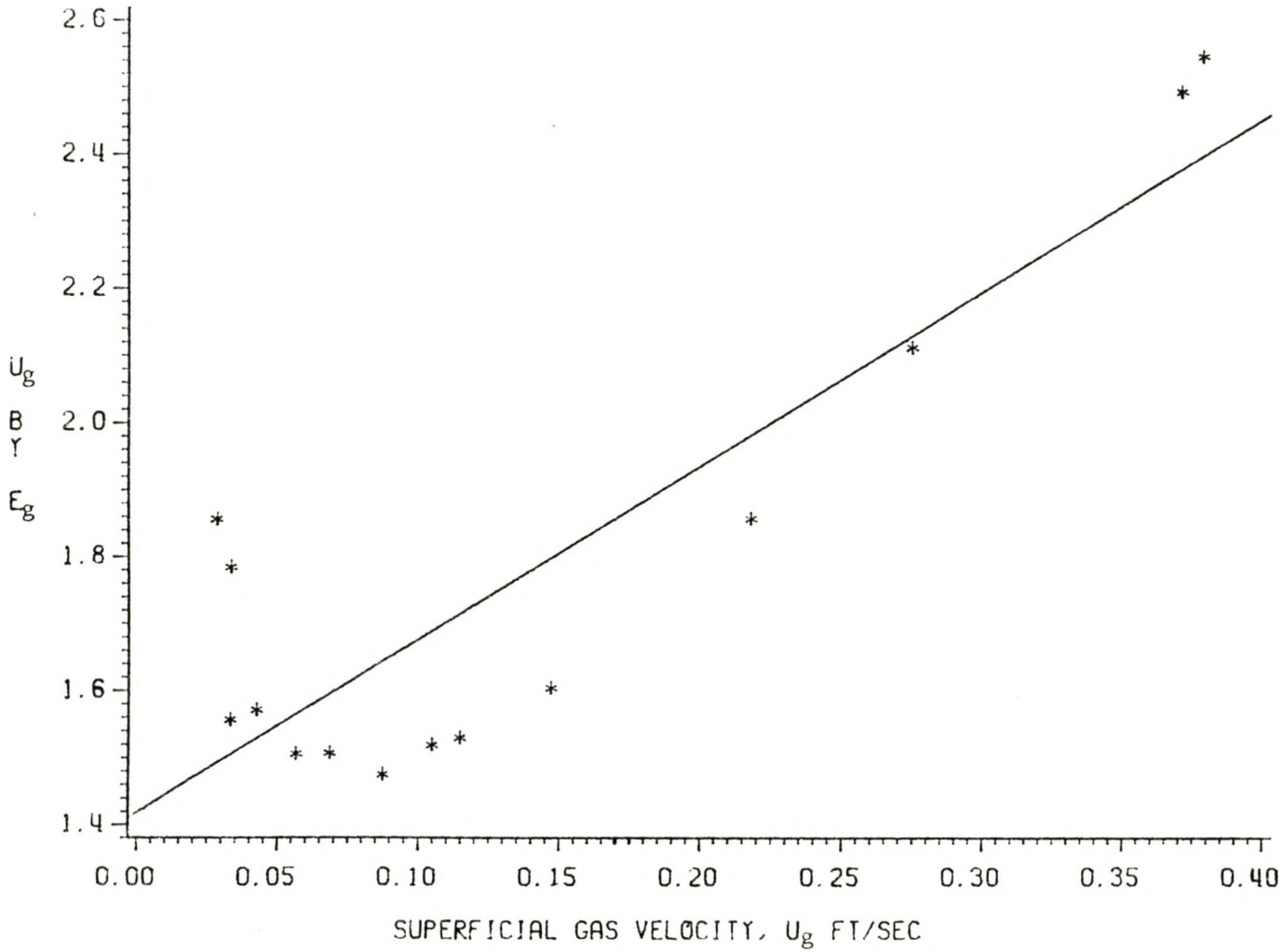

Figure 16: Ratio of Superficial Gas Velocity to Void Fraction as a Function of Gas Velocity - Circular Channel

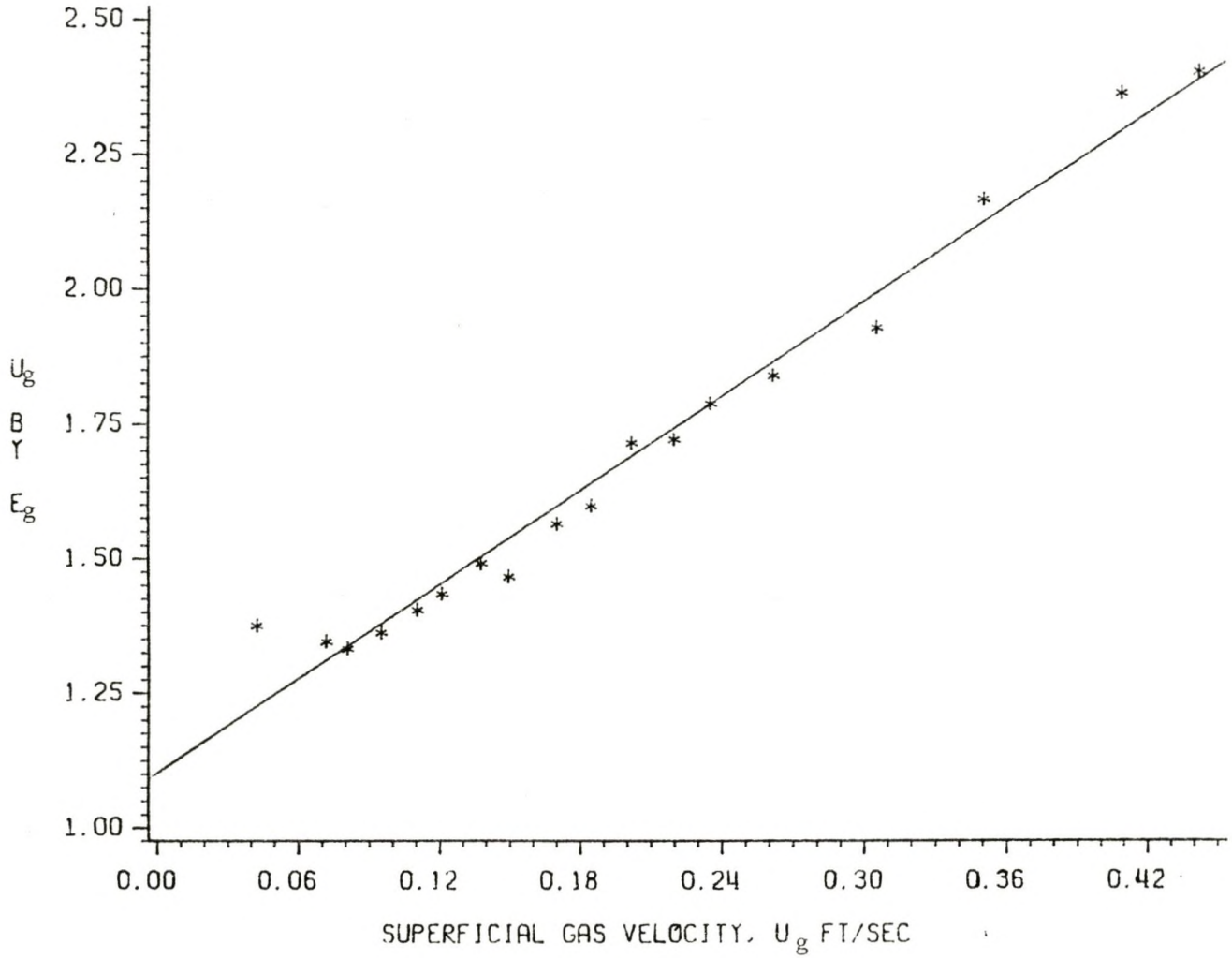

Figure 17: Ratio of Superficial Gas Velocity to Void Fraction as a Function of Superficial Gas Velocity - 2.38 inch Inner Tube

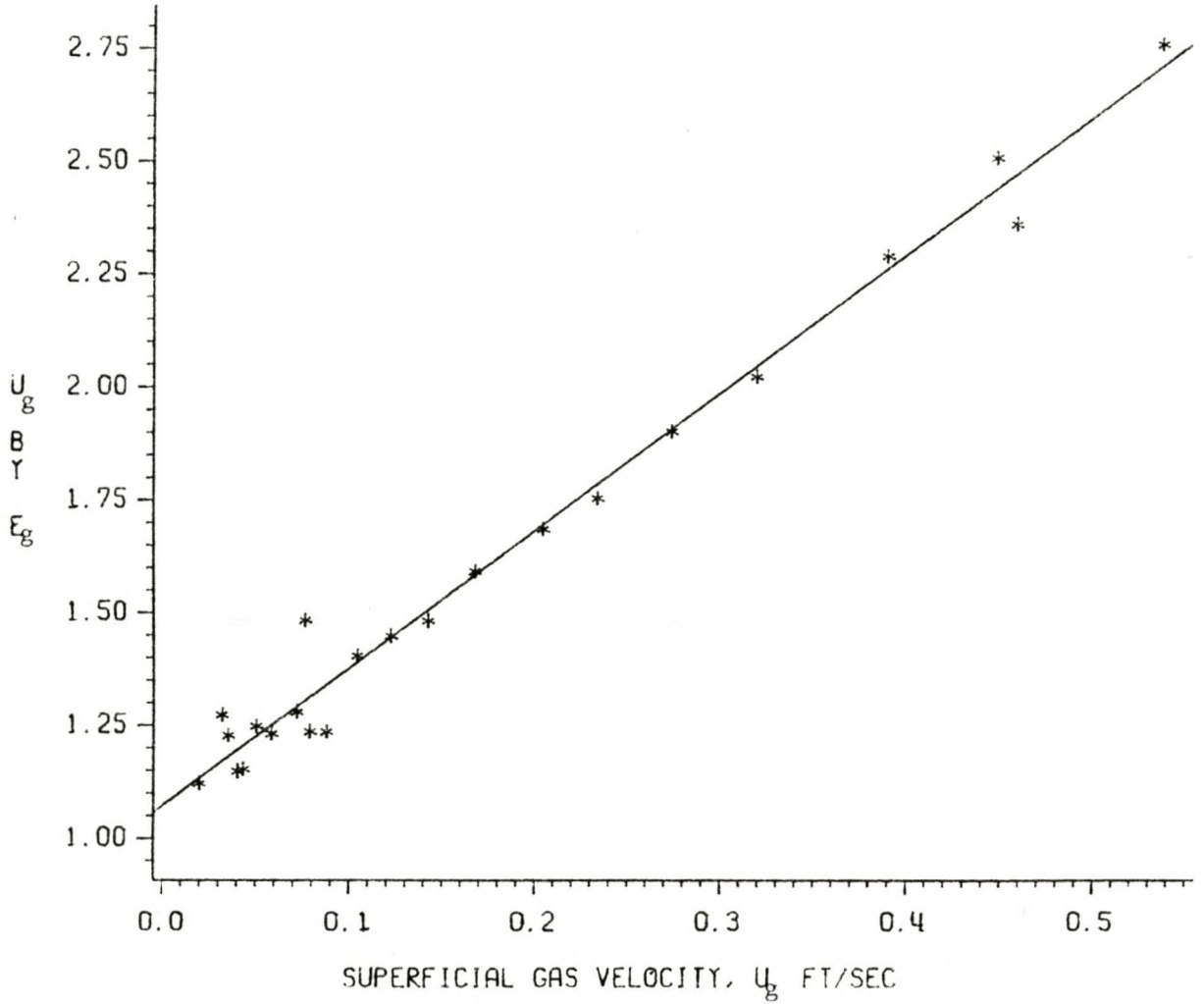

Figure 18: Ratio of Superficial Gas Velocity to Void Fraction as a Function of Superficial Gas Velocity - 3.527 inch Inner Tube

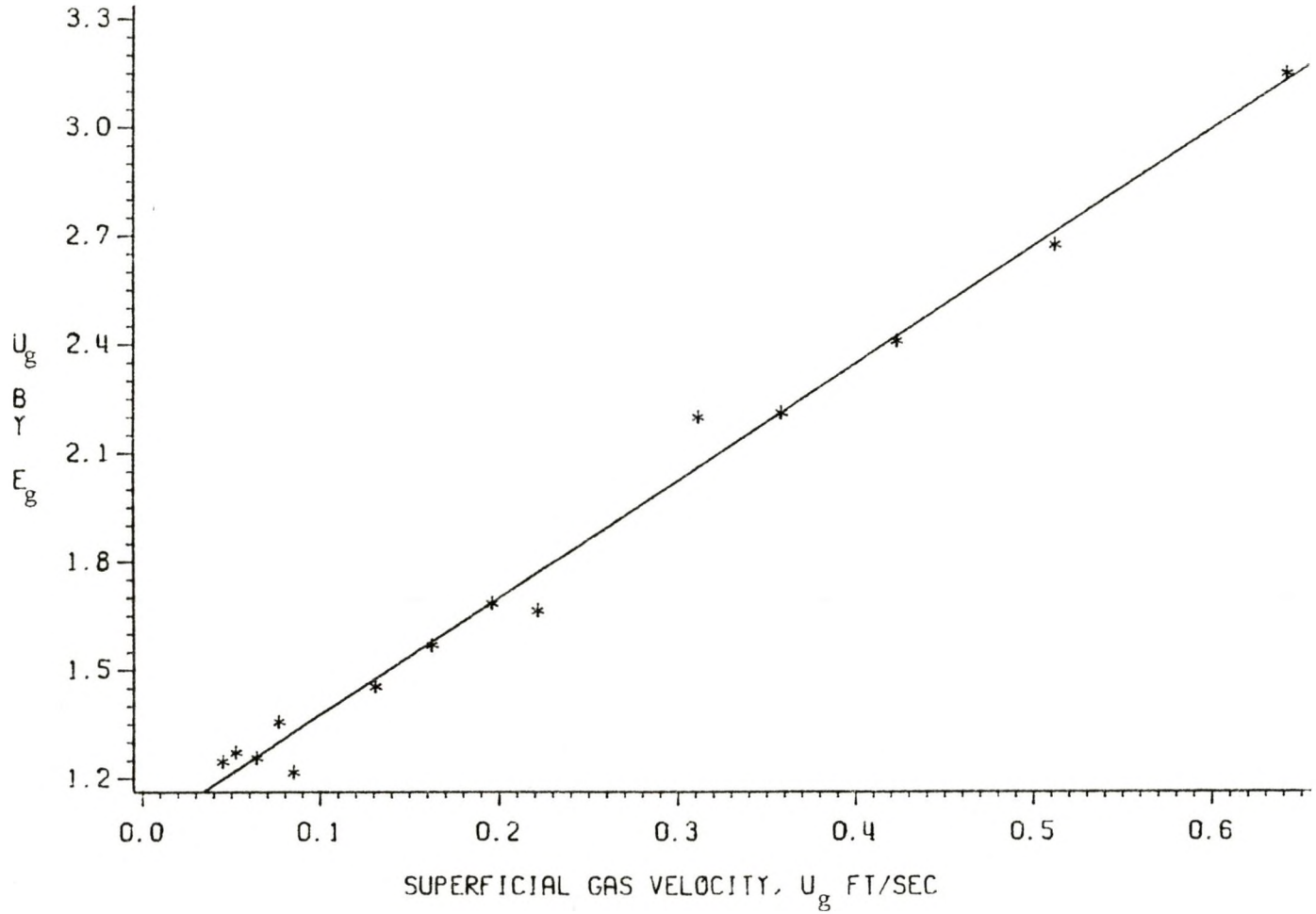

Figure 19: Ratio of Superficial Gas Velocity to Void Fraction as a Function of Superficial Gas Velocity - 4.49 inch Inner Tube

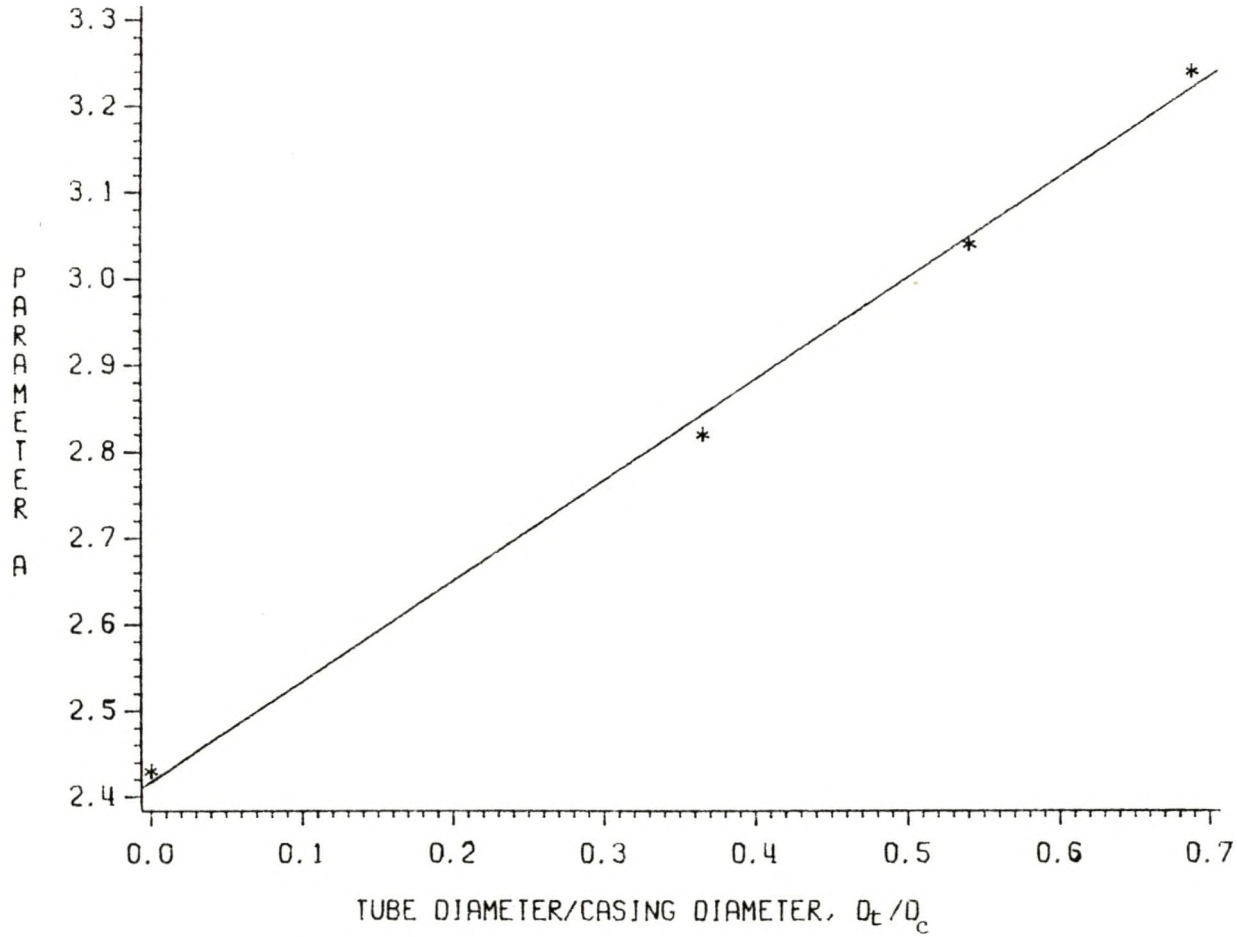

Figure 20: Effect of Annulus Diameter on the Parameter A of Equation (25)

The high value of the coefficient of correlation, 0.997, and the low value of standard deviation, 0.02, represents a very good linear least squares fit.

TABLE 5

Parameters A and B of Proposed Correlation for Void Fraction (Equation (25))

Casing Inside Diameter, D_c = 6.515 inch

Tubing Outside Diameter, D_t Inch	D_t/D_c	Parameters of Equation (35) A	Parameters of Equation (35) B	Correlation Coefficient, R^2	Standard Deviation, s_d
None	0.0	2.43	1.46	0.8140	0.1770
2.380	0.3653	2.82	1.13	0.9479	0.0516
3.527	0.5410	3.04	1.10	0.9825	0.0638
4.490	0.6890	3.24	1.08	0.9850	0.0638

The values of the parameters A_1 and A_o calculated from the slope and intercept of this curve were 1.17 and 2.42 respectively. Values of B_o were calculated from $B_o=B/v_b$. The values of B_o are 1.900, 1.523, 1.535 and 1.611 for channels with no inner tube, 2.38 inch tube, 3.527 inch tube and 4.490 inch tube, respectively. The value of B_o which should

be constant, varied somewhat, although the variation appears to be random with annular diameters. This variation in the value of B_0 reflects the scatter in the void fraction data gathered (which was indicated by the fluctuations in the manometer fluid level and is a common source of error in all two-phase flow experiments.

With an average value of B_o=1.643 and the values of the parameters B_1, A_1 and A_o of 0.44 inches, 1.17 and 2.42 respectively, the proposed correlation for void fraction during bubbly flow (Equation (35)) becomes

$$E_g = \frac{u_g}{(2.42+1.17D_t/D_c)u_g + (2.514Z/(1+0.44/D_e))} \quad (43)$$

where

$$Z = (sg/d_f)^{1/4} \text{ gm/sec}$$

and

$$D_e = (D_c - D_t) \text{ inches}$$

For the air-water system at 70° F the above equation reduces to

$$E_g = \frac{u_g}{(2.42+1.17D_t/D_c)u_g + (1.345/(1+0.44/D_e))} \quad (44)$$

In Figure 21 the experimental values of E_g are compared with those predicted by Equation (44) for the air-water system. As can be seen from the figure, the measured values of E_g are in excellent agreement with the predicted values of E_g;

TABLE 6

Comparison of Experimental Data with the Proposed Correlation for Bubbly Flow

Tube Diameter, inch	Percent Average Error	Percent Absolute Average Error	Percent of Data within 10% of Prediction	Sum of Squares of Errors $\times 10^4$	Standard Deviation $\times 10^4$
0.0	0.4056	11.27	71.43	3.30	4.828
2.380	-0.1611	6.166	100.00	9.00	7.277
3.257	-0.0874	8.453	95.65	22.48	10.108
4.490	-0.2438	7.357	100.00	10.27	8.889
Total	-0.0381	8.206	92.75	45.05	7.836

the total average error is -0.0381%. A negative value for the average deviation indicates that the proposed correlation overestimates the void fraction. The total absolute average deviation gives the deviation without regard to whether the correlation under or overestimate the void fraction. This indicates scattering of the data due to experimental errors. The average error in percent and the corresponding standard deviation (refers to the spread of the percent average deviation) are listed in Table 6. The table includes details of the analysis.

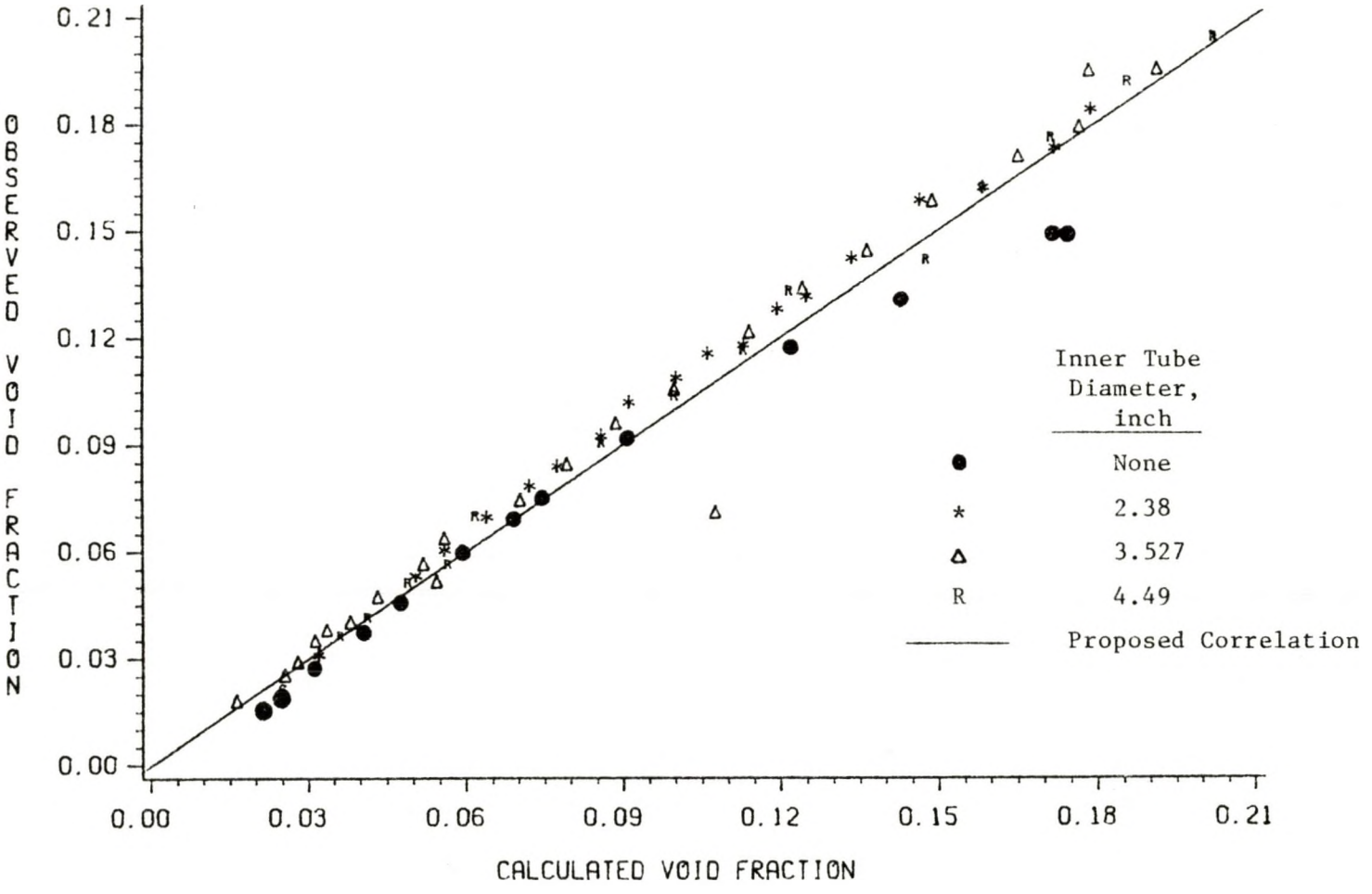

Figure 21: Comparison of Experimental and Predicted Values of Void Fraction

5.1.4 Comparison of Present Results with Previous Work

Godbey-Dimon (2) analyzed data from a pumping oil-well and obtained values of 1.2 and 0.60 ft/sec for the parameters A and B, respectively. Mashelkar (24), Haug (8) and Zahradnik (9) obtained values of 2.0 for A and 0.98 ft/sec for B. These values of the parameters are much lower than those determined in the present investigation - 2.43 and 1.46 ft/sec for A and B, respectively (for the circular channel). Figures 21 and 22 compare the present data with the above correlations. In these figures, the E_g values observed in the present work are shown as data points while the correlation is shown as a straight line. Figure 21 shows the comparison of the experimental data with the correlation proposed by Godbey and Dimon (2). It can be seen that the Godbey-Dimon correlation yields much higher E_g values for the whole range of gas velocities, especially at high velocities. The large differences between the present data and the Godbey-Dimon (2) correlation cannot be explained by the difference in the properties of crude oil (for which the correlation is suggested) and water (the present experimental medium). Earlier (in Chapter 2) it was indicated how one may arrive at the correlation from theoretical considerations. It is not very clear from the published work of Godbey-Dimon (2) whether they used actual data to derive the values of the parameters they suggest. It seems unlikely that they used experimental data.

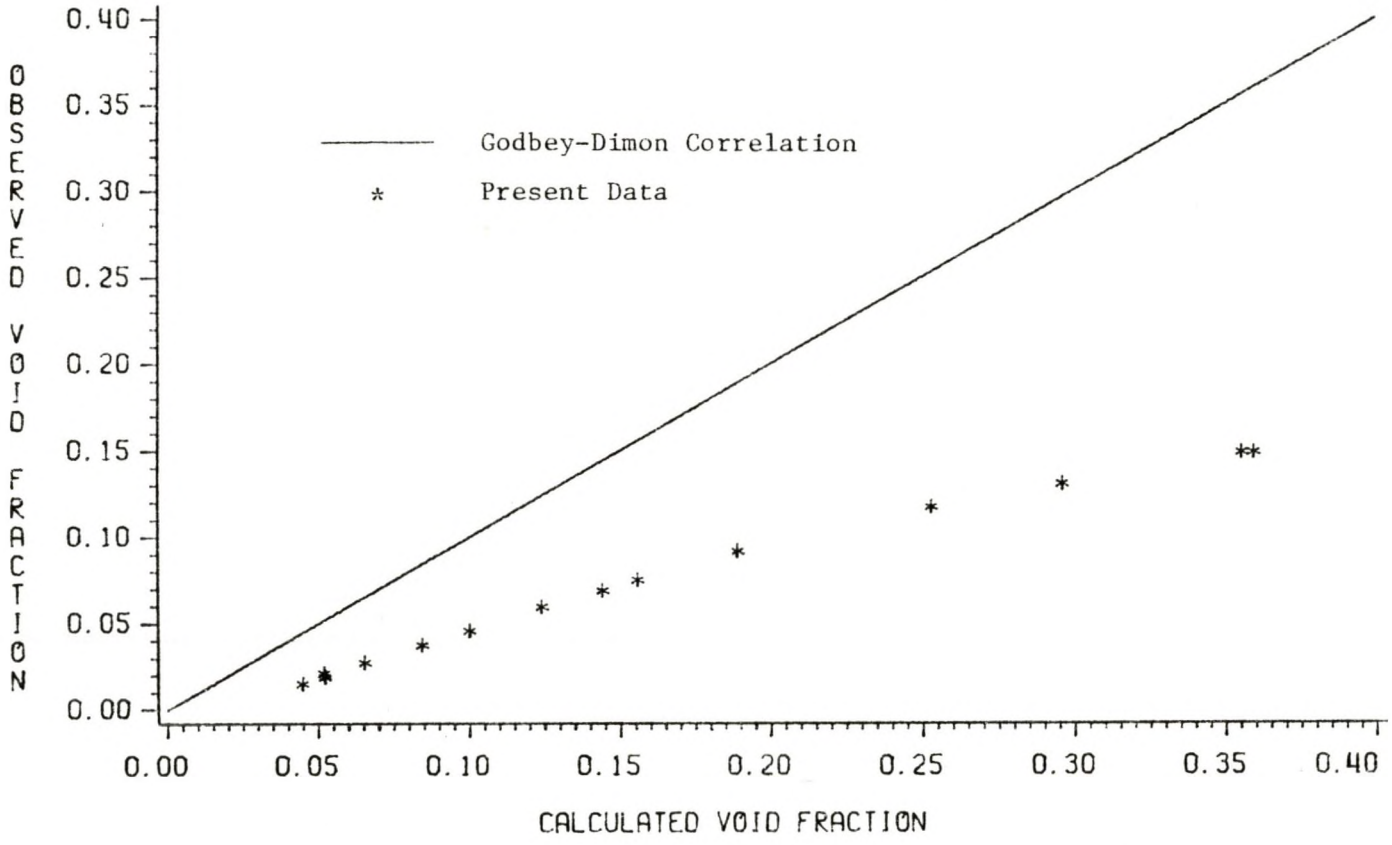

Figure 22: Comparison of the Experimental Data with the Godbey-Dimon Correlation for Void Fraction

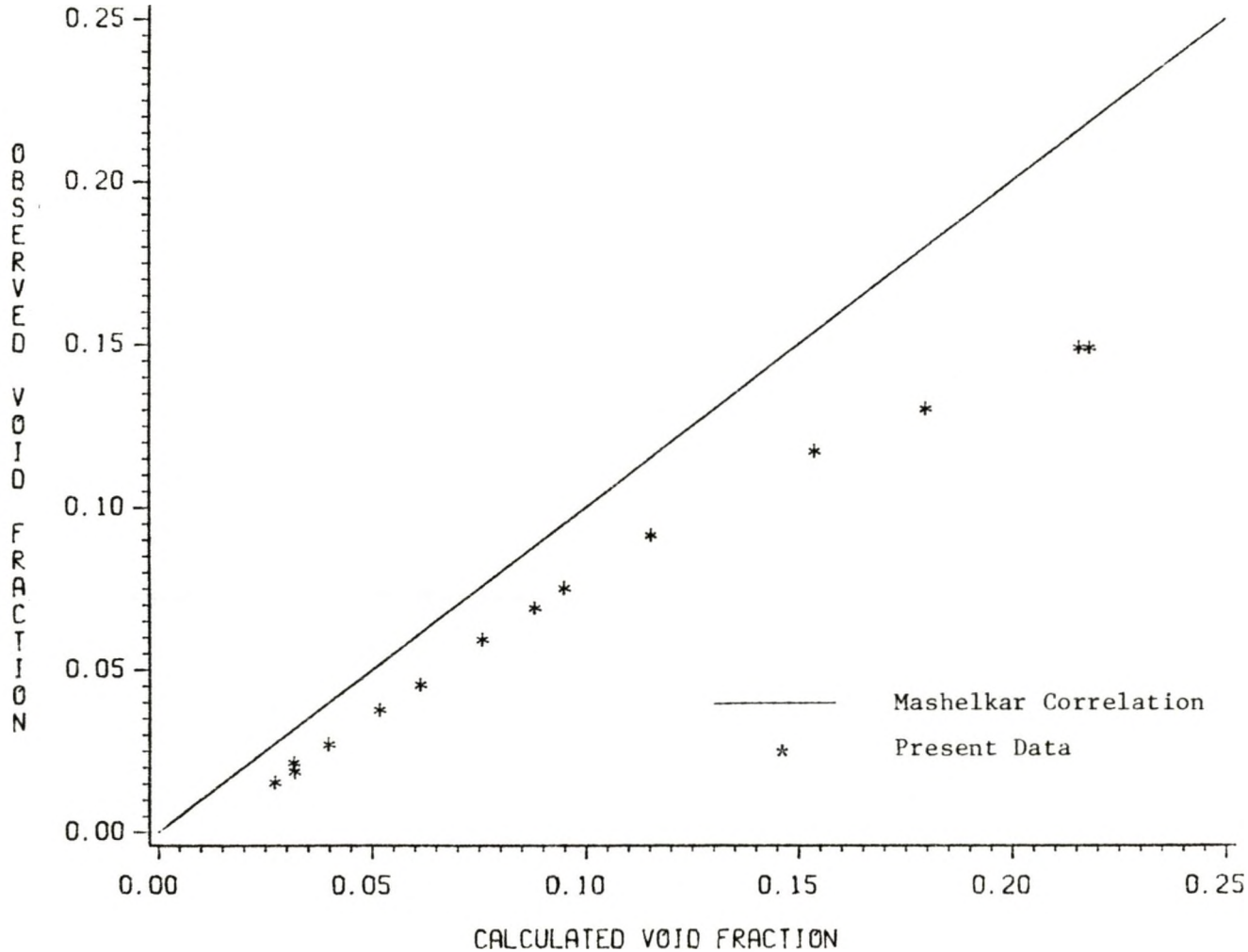

Figure 23: Comparison of the Experimental Data with the Mashelkar Correlation for Void Fraction

In Figure 22, the Mashelkar (24) correlation of the experimental data is shown. As can be seen, the data points lie below the solid line representing the correlation of Mashelkar (24). However, the Mashelkar (24) correlation is in a closer agreement with our work than is the Gobey-Dimon (2) correlation. The disagreement between the data and the Mashelkar (24) correlation may be attributed partly to differerences in the design of air-inlets around the bottom of the column casing. In this work the gas was introduced horizontally whereas most other researchers introduced gas into the channel through nozzles that project upward. Because the arrangement used in this experiment more closely approximates the way gas enters an oil-well casing, it is believed that values of the parameters obtained in this work are more appropriate for use in calculating void fraction and hence bottom-hole pressure in oil-wells. The diameter of the gas injector orifice may also account for somewhat lower values of void fraction as suggested by Equation (33). The effect of gas injector diameter, however, was not investigated in this work.

The void fraction data obtained with the air-water system for annular channels is compared with the Podio et al. (3) correlation in Figure 24. The details of this analysis are given by Tarrillion (42) in his Masters thesis. The figure shows that the measured values of E_g approximately agrees with the Podio et al. (3) correlation except at very large

flow rates. The slight difference may be due to the difference in column diameters used in the two works. It is also possible that the short column used in this work has not been entirely able to eliminate the entrance effect.

5.2 EXPERIMENTAL RESULTS USING DATA GATHERED FROM EIGHTEEN FEET HIGH COLUMN

Most of the work by previous researchers has been carried out in long columns to avoid an entrance effect. It was suspected that the entrance effect may not have been eliminated in the eight foot high column. Hence, to study the effect of annular diameter on void fraction, data were obtained using an eighteen foot high column. The experimental procedure and data analysis were similar to those performed with the shorter column. A summary of the conditions at which data were gathered is given in Table 7.

Due to vibrations of the tubing during experimental runs, data gathered with the 4.5 inch diameter inner tube was rejected. Data collected from the experiments and calculated values are tabulated in Appendix E. The computer program used to do all calculations is shown in Appendix A.

TABLE 7

Conditions of Experimental Runs

Tube Outside Diameter, inch	Liquid Height, inch
0.0	108.0-130.0
	130.0-156.0
2.875	108.0-119.5
	119.5-131.5
3.50	108.0-119.5
	119.5-131.5
4.50	108.5-119.5

5.2.1 Analysis for The Bubbly Flow

The method of measuring the bubble rise velocity using an ordinary stopwatch was thought to be crude because of the very short time required for the bubble to travel a particular distance. Data were taken with extra care using a shorter column to avoid errors in counting short time. Due to the above mentioned problem and various other difficulties, no attempts were made to measure bubble rise velocity in the larger column. Equation (41) was used to estimate the bubble rise velocity (v_b) for the purpose of data analy-

sis. The values of bubble rise velocities for various channels are listed in Table 8.

To determine the entrance effect, void fraction data obtained for the circular channel at two different heights (between 108.0-130.0 inches and 130.0-156.0 inches) were plotted against the superficial gas velocity. The column operating pressure was calculated as the sum of the pressure due to the height of water at the midpoint section through which voidage data were averaged as well as the amospheric pressure. With this estimated pressure the superficial gas velocity was calculated at the mid point of this section. Figure 25 shows the dependence of void fraction on superficial gas velocity and liquid height for the circular channel. The graph clearly indicates that the void fraction (E_g) decreases with increasing liquid height at a constant superficial gas velocity (u_g) for the whole range of gas velocities studied. The decrease in E_g was higher at larger values of u_g. The mean bubble velocity increased because the bubbles coalesced at the top of the column; and this resulted in a decrease in E_g. This argument is reinforced by Wallis' (5) observation for slug flow in the air-water system. This effect is always expected to be encountered at the top of liquid column. In this study, the liquid height was maintained at 6 inches above the top pressure tap. Data were not taken above about 130.0 inches from the gas entrance point.

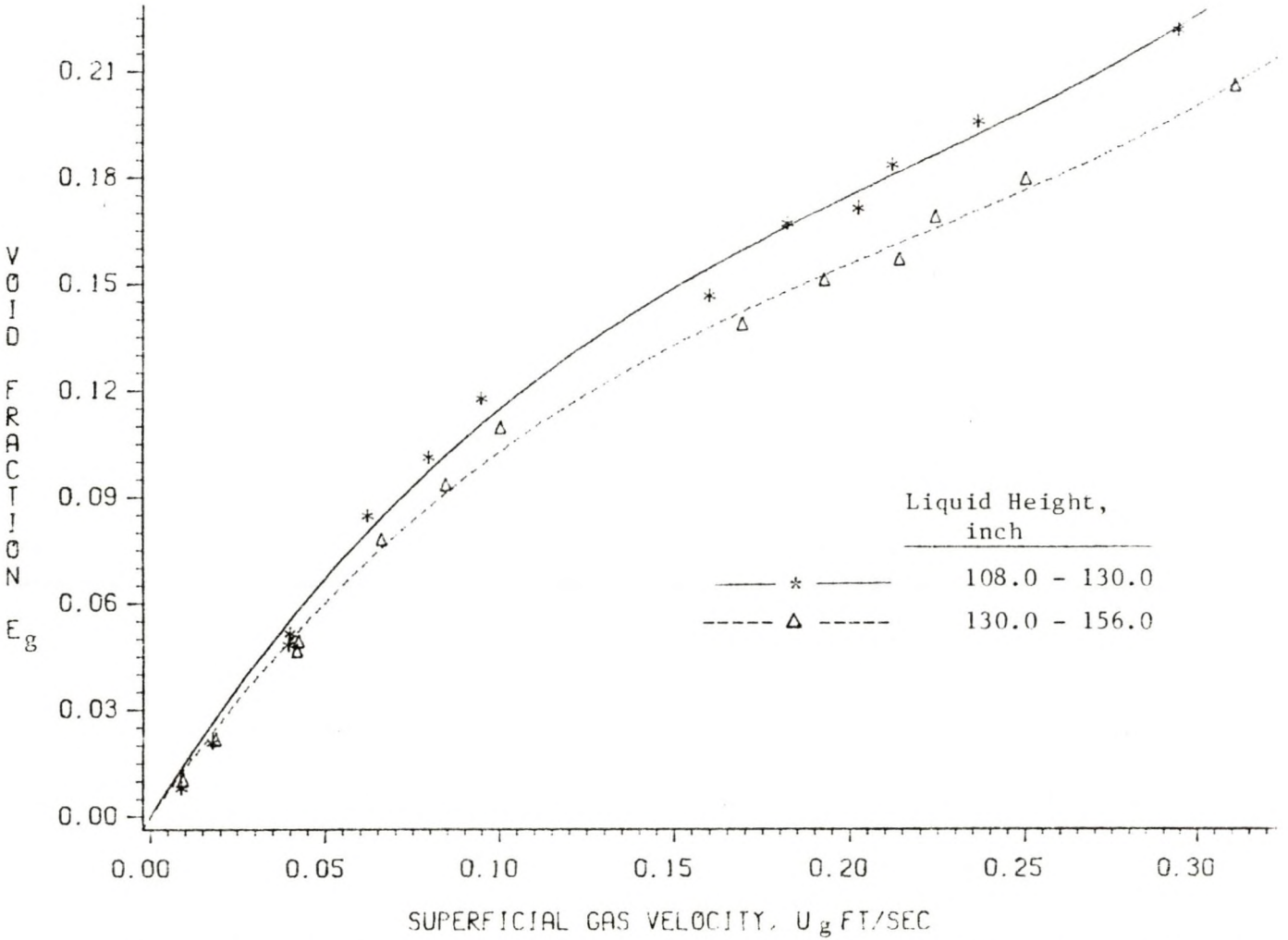

Figure 25: Dependence of Void Fraction on Superficial Gas Velocity and Liquid Height - Circular Channel

Experiments were then conducted with the annular channels at two heights - one between 108.0-119.5 inches and the other between 119.5-131.3 inches. The dependence of void fraction on liquid height and superficial gas velocity is shown in Figures 26 and 27 for channels with diameters 2.875 and 3.50 inches, respectively. Figure 26 clearly demonstrates that E_g does not change with liquid height except for a slight variation at very high gas velocities. This increase is due to high fluctuations (up to 12 cm) in the manometer fluid. For the 3.5 inch diameter tube changes in E_g with height were more prominant. This is seen in figure 27. This change may be due to the smaller number of data points obtained as compared to the number of data gathered for the 2.785 inch tube. Thus, it can be said that the entrance effect does not exist at a column height of 108.0 inches.

All the data gathered between liquid heights 108.0-131.5 inches were considered when studying the effect of annular diameter (including the circular channel) on void fraction. Figures 28, 29 and 30 illustrate the linear relationship between the ratio of superficial gas velocity to void fraction u_g/E_g, and the superficial gas velocity, u_g, for channels with no inner tube, and tubes of diameters 2.785 and 3.5 inches, respectively. The superficial gas velocity ranged from 0.02 to 0.96 ft/sec.

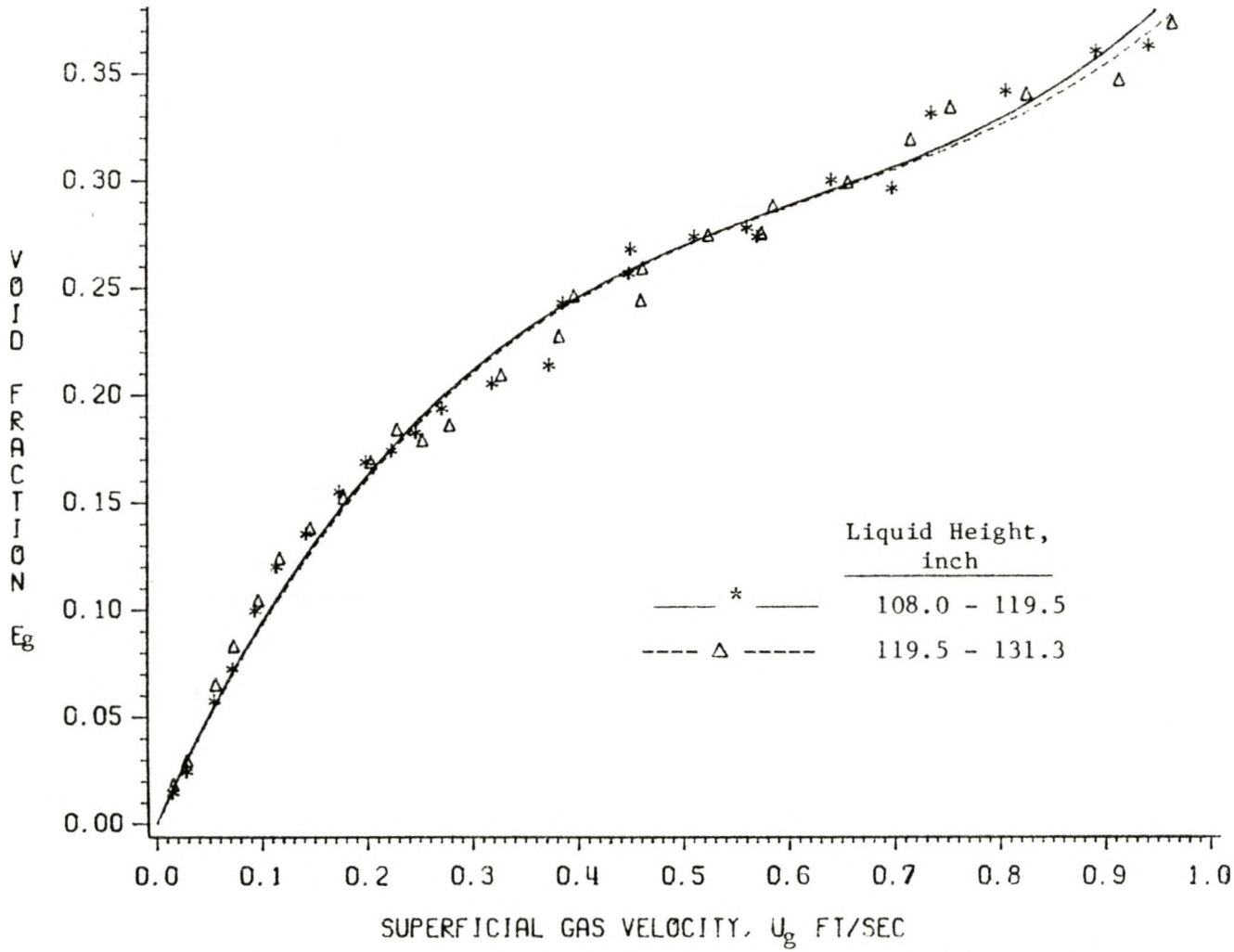

Figure 26: Dependence of Void Fraction on Superficial Gas Velocity and and Liquid Height - 2.875 inch Inner Tube

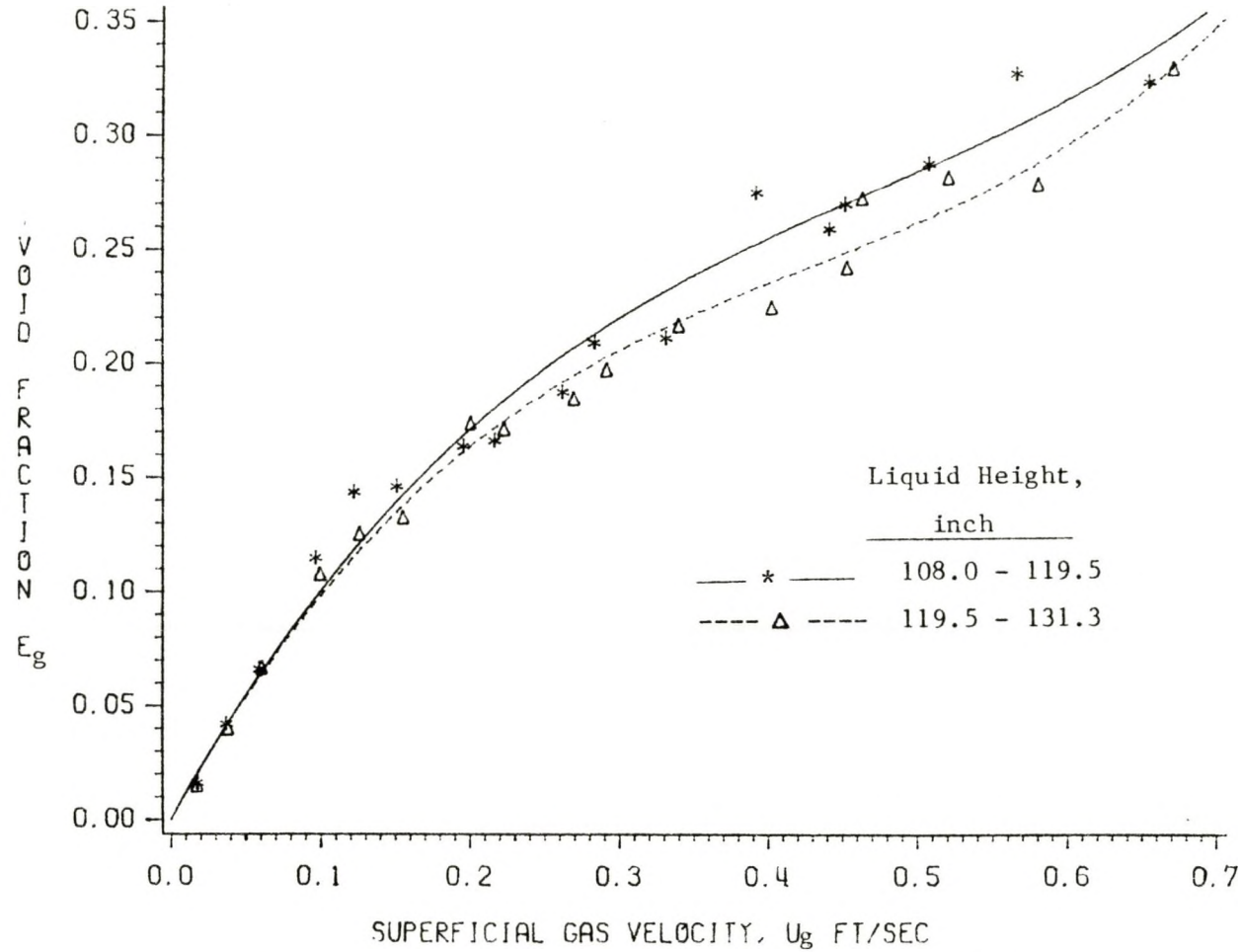

Figure 27: Dependence of Void Fraction on Superficial Gas Velocity and Liquid Height - 3.50 inch Inner Tube

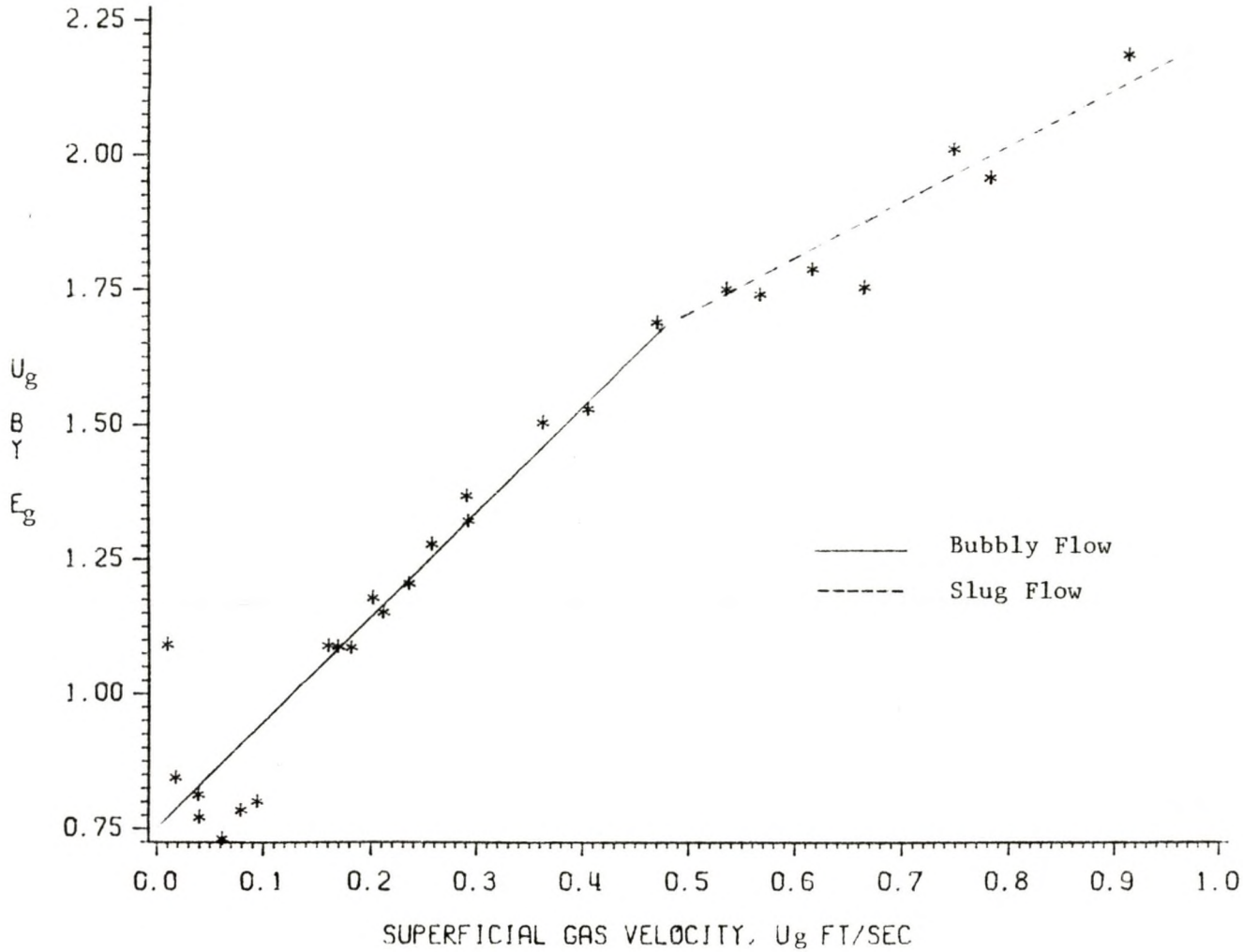

Figure 28: Ratio of Superficial Gas Velocity to Void Fraction as a Function of Gas Velocity - Circular Channel

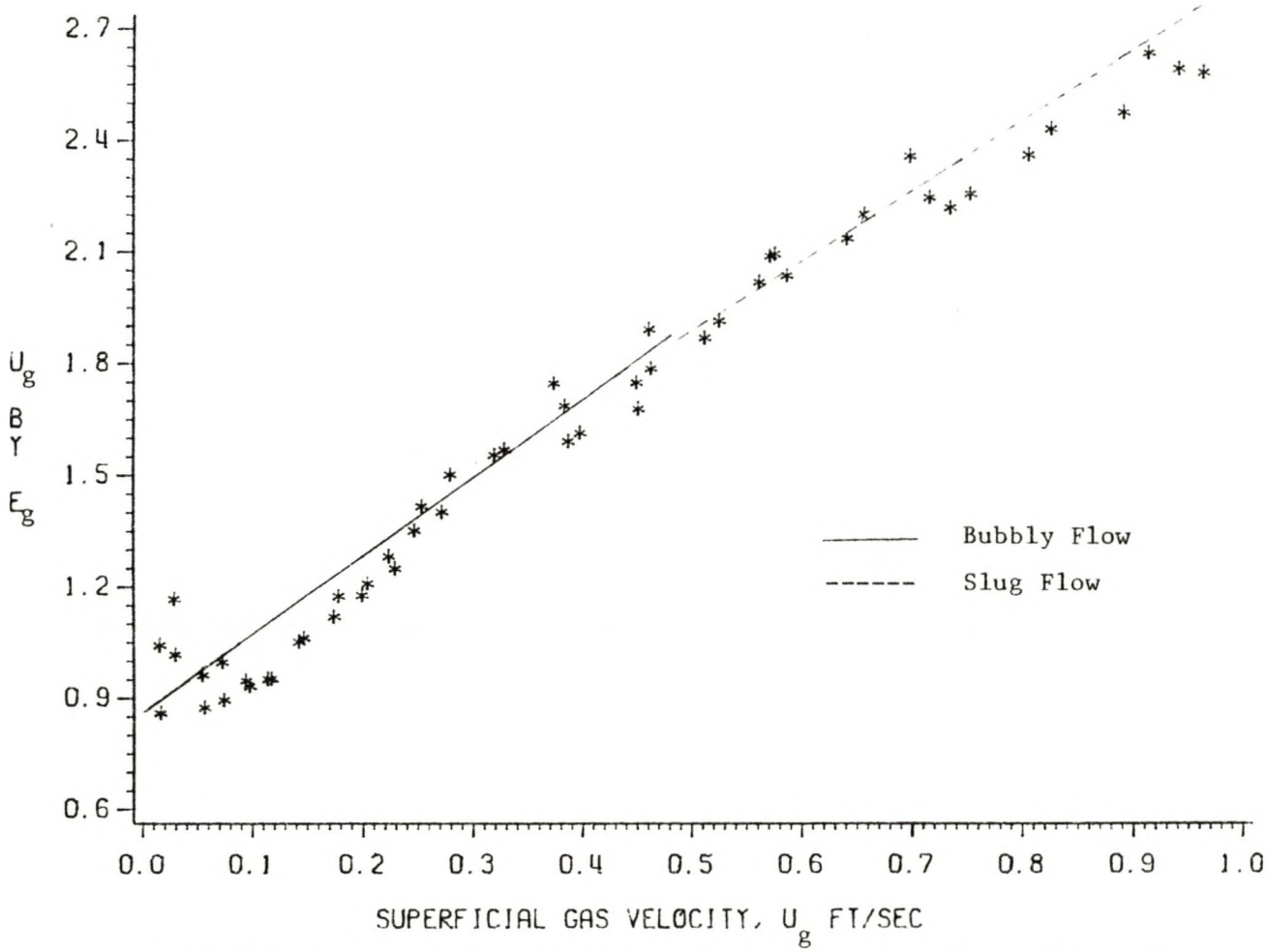

Figure 29: Ratio of Superficial Gas Velocity to Void Fraction as a Function of Gas Velocity - 2.875 inch Inner Tube

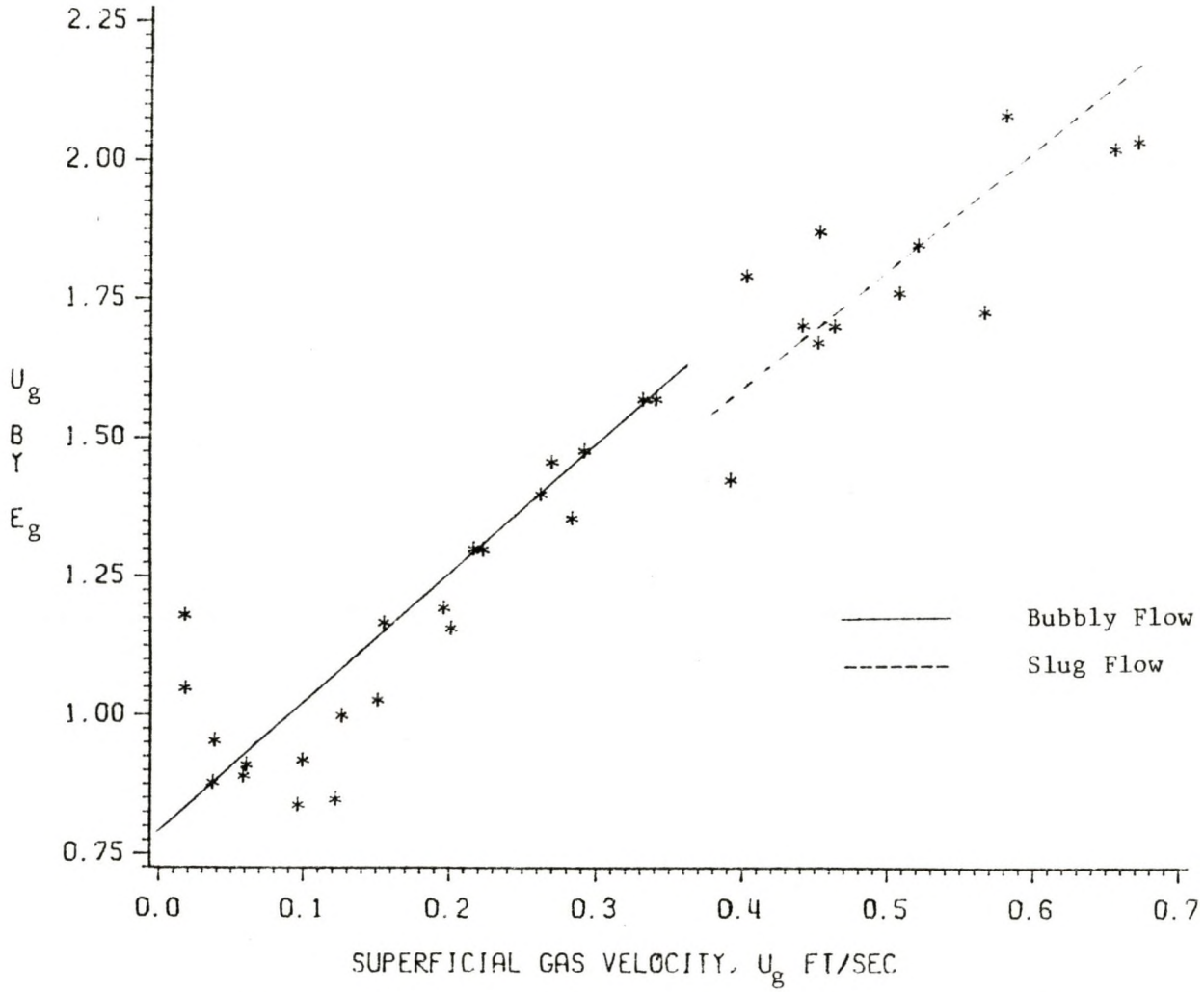

Figure 30: Ratio of Superficial Gas Velocity to Void Fraction as a Function of Gas Velocity - 3.50 inch Inner Tube

Visual observation showed a bubbly flow pattern to exist up to a void fraction of 0.25. This is consistent with the fact that transition from bubbly to slug flow occured when void fraction reached 0.25. As seen in Figures 25 to 27 (plot of u_g/E_g versus u_g), the nature of the curve changes when E_g approaches 0.25. These changes, however, are shown more clearly in Figures 28, 29 and 30. In these figures, the lower curves represent bubbly flow and the upper curves represent slug flow. Transition occurs at a superficial gas velocity of about 0.40 ft/sec. The two curves in Figures 28 adn 29 tend to intersect at the transition point (when E_g is greater than 0.25). In figure 30 the curves do not intersect due to scatter of data points indicated at low values of u_g. The scatter, as explained earlier, is due to small errors in reading the height of the manometer fluid. This results in relatively large errors in the calculated values of u_g/E_g. Analysis of the data in the bubbly flow region is tabulated in Table 8. It includes the values of parameters A and B calculated from the intercepts and the slopes of the curves in Figures 28 to 30, correlation coefficients and standard deviations obtained from the linear least aquares fit. The high values for the correlation coeffecient (larger than 0.80) for all the channels indicates a good linear least squares fit.

As expected from Equation (31), A is a linear function of D_t/D_c. The plot of A versus D_t/D_c (shown by the solid line

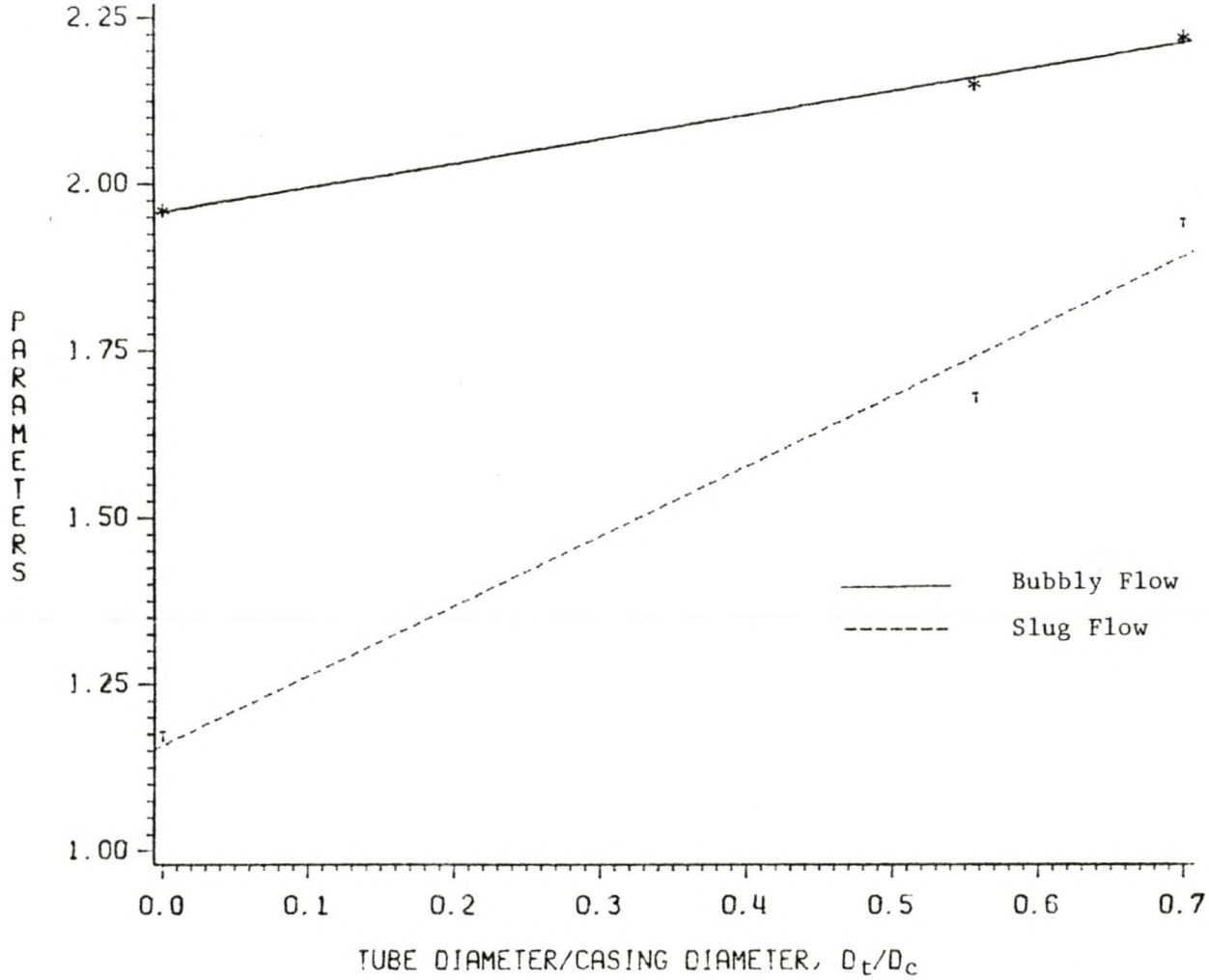

Figure 31: Parameters A and A_s as a Function of Ratio of the Tube Diameter to Casing Diameter

in Figure 31) shows the validity of Equation (31). The high value of the correlation coefficient, 0.9953, and the low value of standard deviation, 0.0092, represent a very good linear least squares fit. The values of the parameters A_1 and A_0 calculated from the slope and intercept of this curve are 0.363 and 1.96, respectively.

TABLE 8

Analysis of Correlation for Void Fraction (Equation (30)) in Bubbly Flow

Casing Outside Diameter, D_c = 5.0 inch

Tubing Outside Diameter		Bubble Rise Velocity	Parameters of Equation (35)		Correlation Coefficient	Standard Deviation
D_t inch	D_t/D_c	v_b ft/sec	A	B	R^2	s_d
0.0	0.0	0.7522	1.96	0.75	0.8088	0.1034
2.785	0.557	0.6828	2.15	0.82	0.8969	0.0938
3.500	0.700	0.6328	2.22	0.80	0.8494	0.1165

Values of $B_o(=B/v_b)$ are 0.9971 for the circular channel, and 1.201 and 1.2642 for the channels with the 2.785 and 3.50 inch tube, respectively. The variation in the values

of B_o reflects the scatter in the void fraction data gathered.

With an average value of B_o=1.1541, and the values of the parameters B_1, A_1 and A_o as 0.44 inches, 0.363 and 1.96 respectively, the proposed correlation for void fraction during bubbly flow (Equation (35)) becomes

$$E_g = \frac{u_g}{(1.96+0.363D_t/D_c)u_g + (1.766Z/(1+0.44/D_e))} \quad (45)$$

where

$$Z = (sg/d_f)1/4 \text{ gm/sec}$$

and

$$D_e = (D_c - D_t) \text{ inches}$$

For an air-water system at 70o F the above equation reduces to

$$E_g = \frac{u_g}{(1.96+0.363D_t/D_c)u_g + (0.945/(1+0.44/D_e))} \quad (46)$$

Agreement of the experimental data with the predicted values for bubbly flow are excellent throughout the range of superficial gas velocities and tube sizes tested. It is evident from Figure 32 that Equation (46) works quite well in predicting the void fraction. The average error relative to the experimental void fraction is less than 0.063%. The detailed analysis is shown in Table 9. E_g values obtained us-

ing the eighteen foot high column were higher than those obtained from the shorter column, probably because of the existance of an entrance effect in the shorter column. Hence, the correlation obtained using the data gathered from the longer column was considered to be more appropriate in predicting void fraction.

A one-way analysis of variance was performed to determine if annular diameters had a significant effect on the measured void fraction. At the 95% degree of confidence, it was seen that annular diameters did not have a significant effect on the measured void fraction. Table 10 is the analysis of variance table; the calculations are shown in Appendix D.

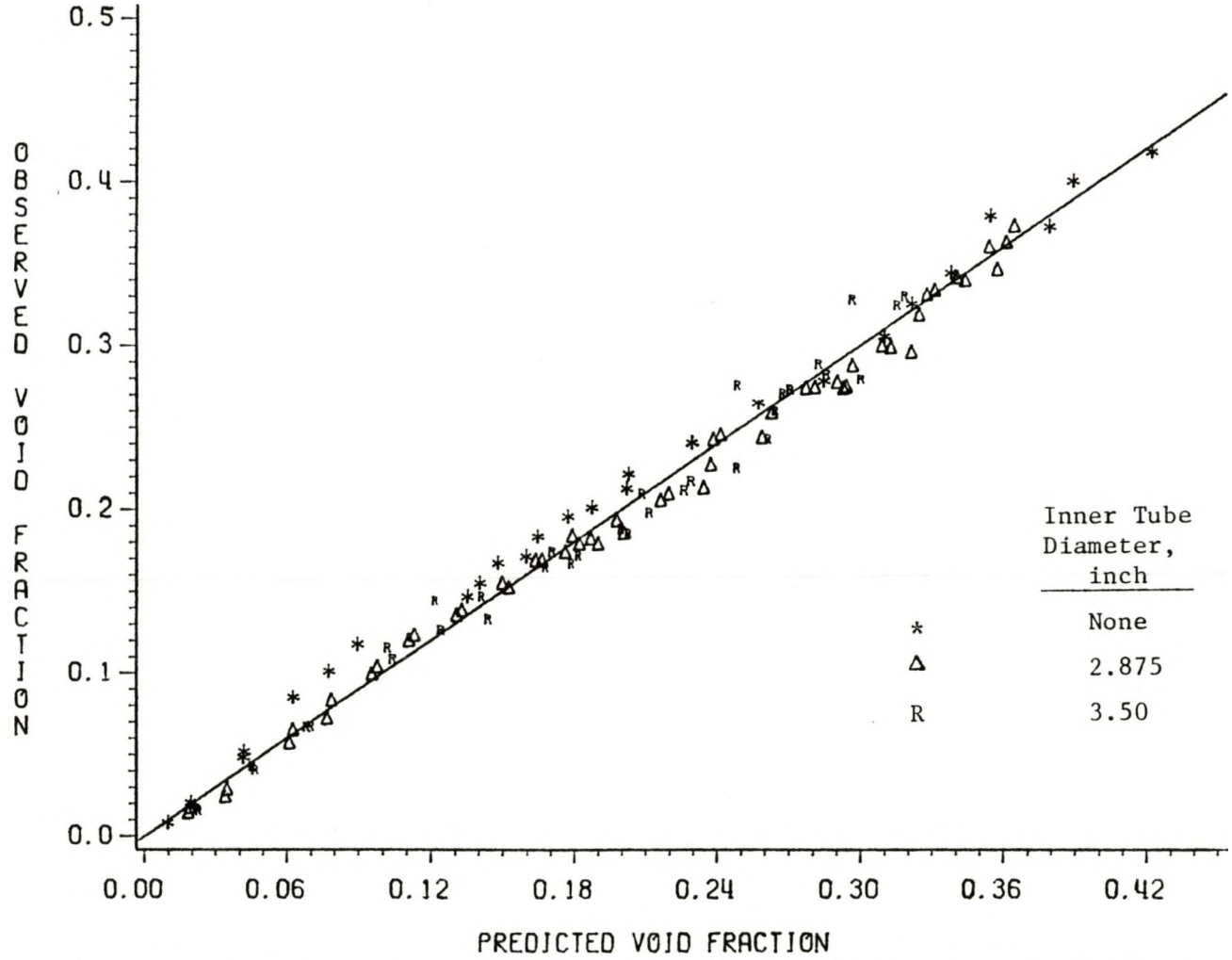

Figure 32: Comparison of Experimental and Predicted Values of Void Fraction

TABLE 9

Comparison of the Experimental Data with the Proposed Correlation for Bubbly Flow

Tube Diameter, inch	Percent Average Error	Percent Absolute Average Error	Percent of Data within 10% of Prediction	Sum of Squares of Errors $\times 10^3$	Standard Deviation $\times 10^3$
0.0	-0.2769	12.61	94.11	4.279	16.353
2.875	-0.0391	5.728	93.55	2.019	8.203
3.50	0.4358	8.561	87.50	32.73	11.930
Total	0.06294	8.298	91.67	39.028	11.610

TABLE 10

One-Way Analysis of Variance for the Effects of Annular Diameters on the Measured Void Fraction

Source of Variation	Degrees of Freedom	Sum of Squares	Mean Square	F	F_c
Mean	1	1.4196	1.4196	-.-	-.-
Tube size	2	0.0003	0.00015	0.031	3.137
Error	69	0.3410	0.0049	-.-	-.-
Total	72	1.7609	-.-	-.-	-.-

5.2.2 Analysis for The Slug Flow

The available air pressure allowed gathering only a limited data at high enough gas velocities for slug flow to be observed. As pointed out earlier, slug flow was found to exist whenever void fraction exceeded 0.25. For the purpose of data analysis, the correlation for slug flow, Equation (36), can be rewritten as

$$E_g = u_g/(A_s u_g + B_s) \qquad (47)$$

or

$$u_g/E_g = A_s u_g + B_s \qquad (48)$$

The linear relationship between the ratio of superficial gas velocity to void fraction u_g/E_g, and superficial gas velocity u_g, for the flow (E_g higher than 0.25) are shown in Figures 28 to 30 for all of the channels. Values of the parameters A_s and B_s along with values of the correlation coefficients and standard deviations are included in Table 11. The correlation coefficients, greater than 0.78 indicate a good linear least squares fit.

Nicklin experimentally determined the value of parameter $A_s (=C_o$ in Equation (36)) to be 1.2 for circular channels; this is 2.6% higher than the value obtained in this experiment. A slight variation of the parameter A_s with tubing diameter is noticed. A plot of A_s versus D_t/D_c is shown by the dotted line in figure 31. A reasonably good straight

TABLE 11

Values of the Parameters A_s and B_s (Equation (48)) for the Slug Flow

Casing Outside Diameter, D_c = 5.0 inch

Tubing Outside Diameter		Equivalent Diameter	Parameters of Equation (35)		Correlation Coefficient	Standard Deviation
D_t inch	D_t/D_c	D_e inch	A_s	B_s	R^2	s_d
0.0	0.0	5.0	1.17	1.08	0.9254	0.0535
2.875	0.557	2.215	1.68	1.04	0.9632	0.0613
3.500	0.700	1.500	1.94	0.78	0.7873	0.0935

line (correlation coefficient of 0.9795) can be fit through the data giving

$$A_s = A_{os}+A_{ls}(D_t/D_c)$$
$$= 1.16+1.05(D_t/D_c) \quad (49)$$

To determine the validity of Griffith's (28) suggestion Equation (38) is rewritten as

$$k = a+b(D_t/D_c) \quad (50)$$

and since $B_{s=v_t=k(gD_c)^{1/2}}$ (Equation (37))

$$B_s/(gD_c)^{1/2} = a+b(D_t/D_c) \quad (51)$$

The plot of $B_s/(gD_c)^{1/2}$ versus D_t/D_c (Figure 33) yields a negative value for b as indicated by the slope. This means that Griffith's suggestion of using D_c instead of D is not borne out by the present data. On the other hand, if D_e is used instead of D according to the equation

$$B_s/(gD_e)^{1/2} = a+b(D_t/D_c) \qquad (52)$$

a positive value of b is obtained from the plot of $B_s/(gD_e)^{1/2}$ versus D_t/D_c. The parameters a and b, calculated from the intercept and the slope, are 0.087 and 0.047, respectively. These values are not comparable with those obtained by Griffith (28). With the values of a and b Equation (52) becomes

$$B_s = (0.087+0.047D_t/D_c)(g(D_c-D_t))^{1/2} \qquad (53)$$

Equation (48) along with the expressions for A_s and B_s can now be written as

$$E_g = \frac{u_g}{(1.16+1.05D_t/D_c)u_g + (0.087+0.047D_t/D_c)W} \qquad (54)$$

where

$$W = (g(D_{c-D_t}))^{1/2} \text{ ft/sec}$$

When g=32.2 ft/sec, Equation (54) becomes

$$E_g = \frac{u_g}{(1.16+1.05D_t/D_c)u_g + (0.494+0.267D_t/D_c)W_1} \qquad (55)$$

where

$$W_1 = D_e{}^{1/2}$$

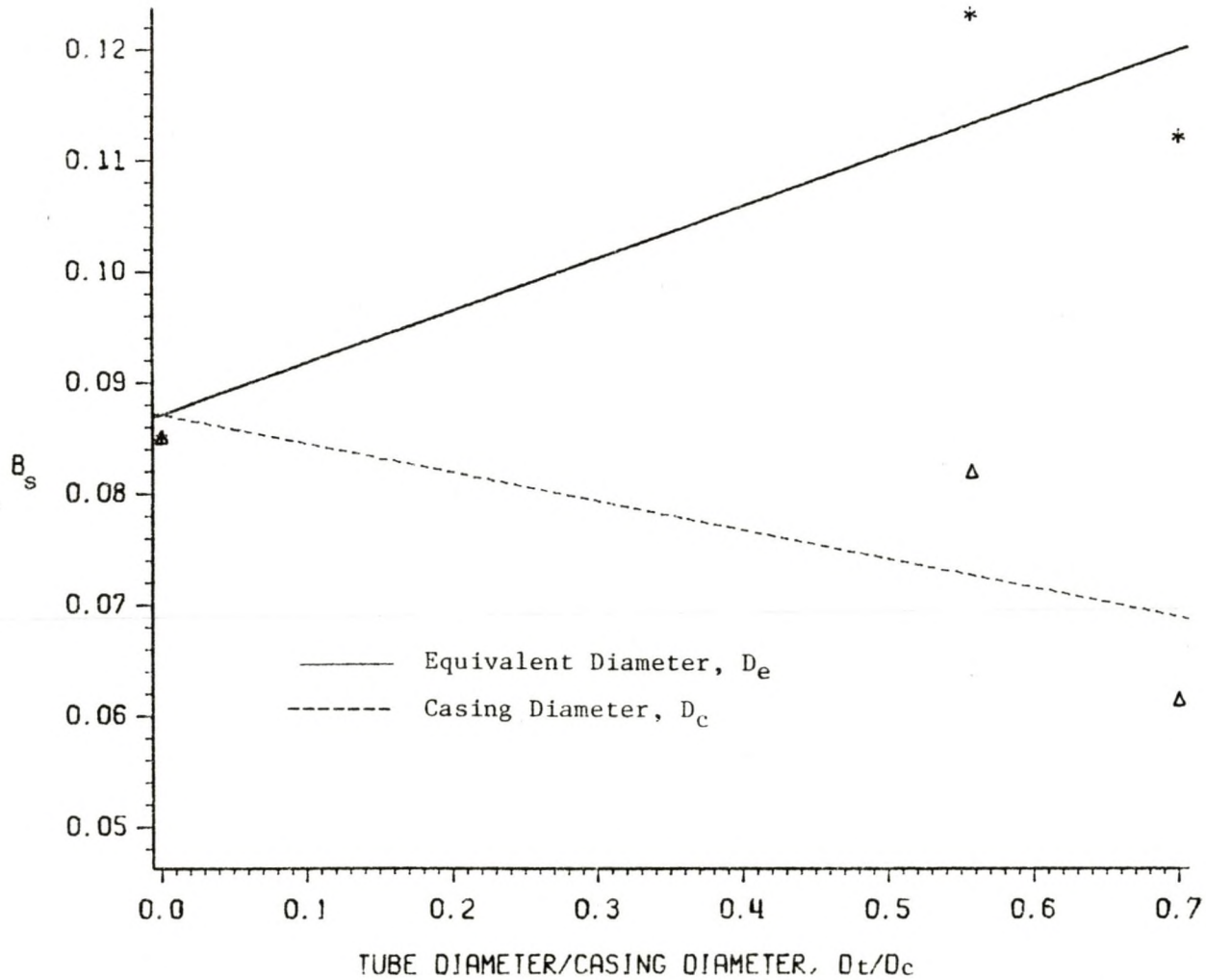

Figure 33: Effect of Annular Diameter on the Parameter B_s for Slug Flow

and

$$D_e = (D_c - D_t) \text{ inch}$$

Comparison between the measured and the predicted value of E_g is shown in Figure 32 (for E_g greater than 0.25). Good agreement exists between the data and the correlation; the average error and the absolute error relative to the experimental error are 0.053 percent and 3.01 percent, respectively.

A one-way analysis of variance was performed to study the effect of annular diameter on void fraction with 95% confidence level, 2 degrees of freedom for the treatment (tube size) and 27 degrees of freedom for the error term. The tabulated critical value of F is 3.26 and the calculated value of F is 2.76. Because the calculated value is less than the critical value we fail to reject our null hypothesis. Thus, annular diameters do not have a significant effect on the measured void fraction for the tube sizes studied.

From the few experimental data gathered, it appears that the equivalent diameter D_e is a better correlating parameter than the casing diameter, D_c, as shown in Figure 33. However, because of higher experimental errors at high velocities (very high fluctuations in the manometer fluid), these conclusions concerning the effect of annular diameters on the variation of the correlating parameters (A_s and B_s) and on E_g need further confirmation.

5.2.3 Comparison of Present Results With Previous Work

Comparison of the present data with the Godbey-Dimon (22) correlation and the Mashelkar (24) correlation are shown in Figures 34 and 35. In these figures, the data points represent the E_g values observed in the present work versus the E_g values calculated from the above correlations. The solid lines represent the correlations of the above researchers. The E_g values observed in this work are lower than those reported by Godbey-Dimon and are slightly higher than those reported by Mashelkar. The discrepency between the Godbey-Dimon correlation and the present data cannot be attributed to one specific reason, because no literature is available regarding the derivation of the Godbey-Dimon correlation. The difference between the present data and the Mashelkar correlation may be due to the differences in the column diameters and design of the air inlet orifices.

Figure 36 compares the present data with the Podio et al. (3) correlation. The agreement between the present data and their data is very good although the Podio et al. correlation slightly underperdicts the void fraction. This slight difference may be due to the differences in column diameters and possibly due to the different methods of measuring void fraction.

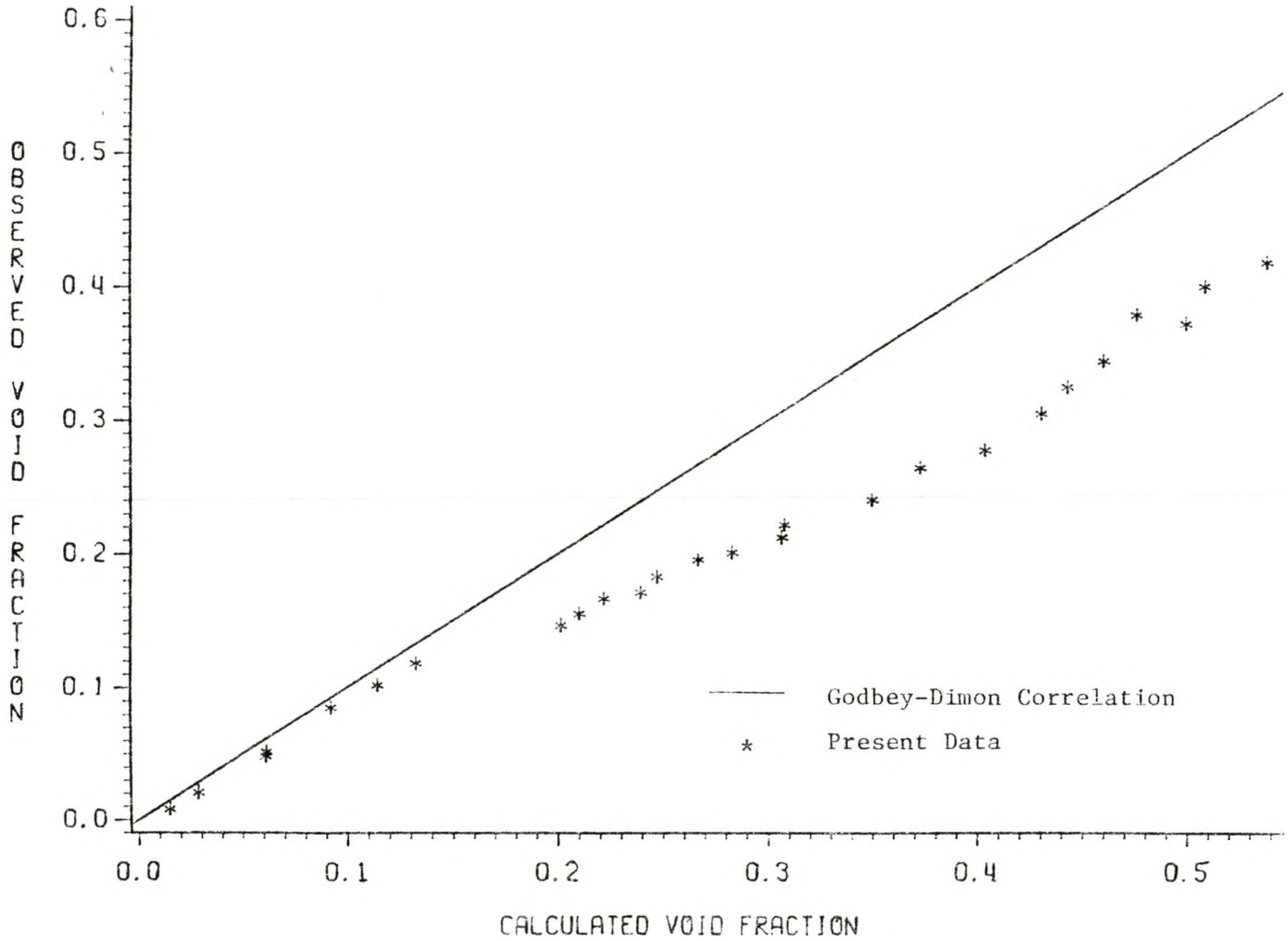

Figure 34: Comparison of the Experimental Data with the Godbey-Dimon Correlation for Void Fraction

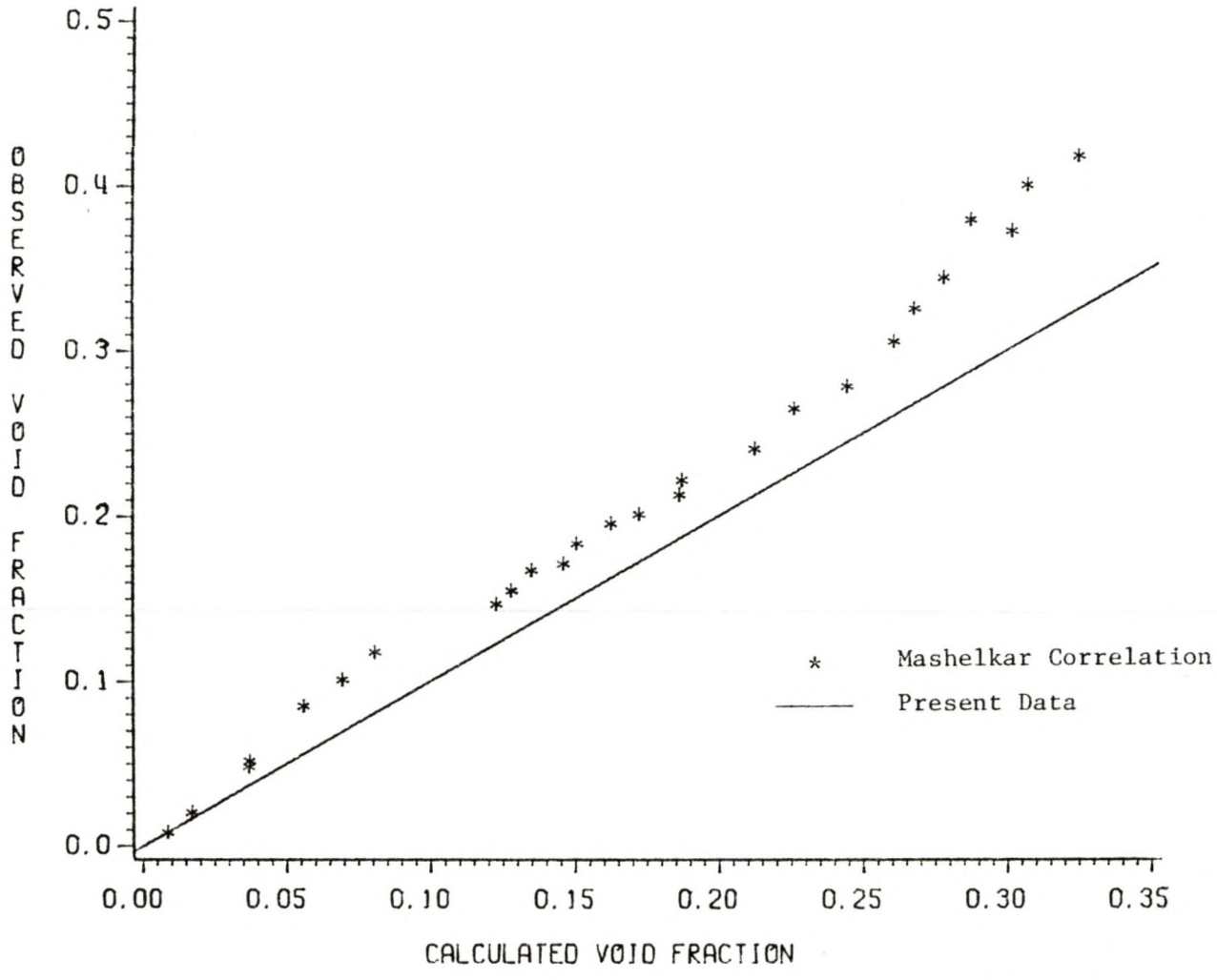

Figure 35: Comparison of the Experimental Data with the Mashelkar Correlation for Void Fraction

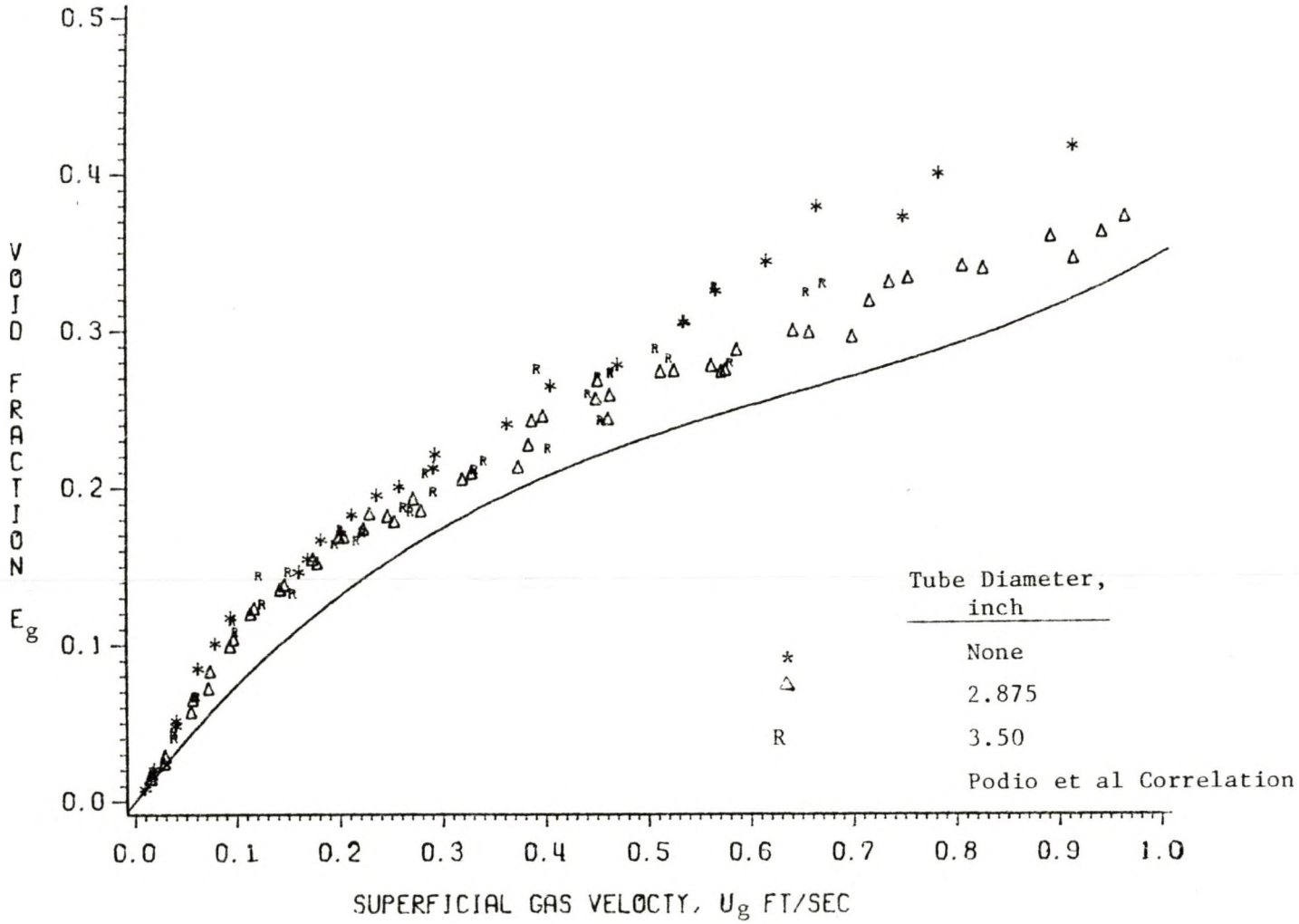

Figure 36: Comparison of the Experimental Data with the Podio et al. Correlation for Void Fraction

Chapter VI

CONCLUSION AND RECOMMENDATION

6.1 CONCLUSION

Based on the experimental data gathered and the analysis presented the following conclusions are presented:

1. The gas void fraction during bubbly flow may be correlated with superficial gas velocity by a modification of the Zuber and Hench equation. However, the parameter A was found to increase with the tubing to casing diameter ratio while the parameter B decreased with a decrease in equivalent diameter (i.e., increase in tube diameter). Single bubble rise velocity appears to be well represented by the Edger correlation.
2. A similar equation (modified from Walli's suggestion) well represents the void fraction data during slug flow. The dependence of the parameters on annular diameters was similar to that in bubbly flow.
3. The dependence of void fraction on annular diameters, for both bubbly and slug flow, was found to be insignificant.

4. Visual observation as well as data analysis indicated that the transition between bubbly and slug flow occurs at a value of void fraction of about 0.25.
5. Experimental runs from the two columns indicated that void fraction data gathered at less than nine feet away from the gas inlets is likely to be affected by the entrance effect.

6.2 RECOMMENDATION

The present study was preliminary in nature. It is urged that more data be gathered for the slug flow region to study the effect of annular diameters on void fraction. It is also urged that tests similar to those reported in this study with a 1.5 inch diameter inner tube be conducted.

It would be of interest and importance to perform experiments similar to this study with higher column operating pressures.

The effect of liquid properties (viscosity and surface tension) on void fraction would constitute a major part of a future study.

In most pumping oils the oil bore casing is inclined. Very little work has been published on the effect of inclination on two-phase flow in pipes. The effect of inclinations on void fraction would be an interesting aspect.

The experimental procedure used in this work can be improved. The inner tubes should be provided with strong mechanical support to avoid vibrations during experimental runs. An integrator should be used to record the average deflection of manometer fluid with time.

APPENDICES

Appendix A

SAMPLE CALCULATIONS

Computer Program 'CALCN' in FORTRAN to Convert the Raw Data to Superficial Gas Velocity and Void Fraction.

The program listed here calls the data file 'DATAN0' as the input data and stores the output into the file 'CALCN0'. The raw data was processed by this program. The program can also be modified for specific purposes.

```
 10 *    NOMENCLATURES FOR THE SYMBOLS USED IN THE PROGRAM  *

 20 *    '(I)' IS USED TO MAKE THE VARIABLES SUBSCRIPTED
 30 *    S:1-SPECIFIC GRAVITY OF MANOMETER FLUID
 40 *    AREA:X-SECTIONAL AREA OF THE CAHNNEL, FT**2
 50 *    H1,H2:HEIGHTS OF MANOMETER FLUID, CM
 60 *    P,Q:PRESSURE AND FLOWRATE INDICATED BY THE FLOW
 70 *            -meter, PSIG AND FT**3/MIN RESPECTIVELY
 80 *    T:COLUMN OPERATING TEMPERATURE, 70 DEG F.(530 DEG
R.)
 90 *    HI:INTITIAL HEIGHT OF LIQUID COLUMN,INCH
100 *    HF:FINAL HEIGHT OF LIQUID WHEN GAS BUBBLES
110 *            THROUGH THE COLUMN, INCH
120 *    L1,L2:SECTIONS OF LIQUID HEIGHTS THROUGH WHICH
130 *            VOIDAGE MEASUREMENTS WERE TAKEN
140 *            BY USING MANOMETERS, INCH
150 *    F:MULTIPLICATION FACTOR FOR CORRECTION OF Q
160 *    H1P,H2P:HEIGHTS OF LIQUID ABOVE THE MID POINTS OF
170 *            SECTIONS THROUGH WHICH VOIDAGE MEASUREMENTS
180 *            ARE AVERAGED, INCH
190 *    P1,P2:IMPROVED ESTIMATION OF COLUMN PRESSURES
200 *            AT THE MID POINT OF THE SECTIONS,PSIA
210 *    U1,U2:CORRESPONDING SUPERFICIAL GAS VELOCITIES,
220 *            FT/SEC
210 *    TB:BASE TEMP AT WHICH FLOWRATE WAS INDICATED,
220 *            60 DEG F. (520 DEG R.)

230       DIMENSION
H1(40),H2(40),AL1(40),AL2(40),HF(40),F(40)
240       DIMENSION
H1P(40),H2P(40),P1(40),P2(40),U1(40),U2(40)
250       DIMENSION P(40),Q(40),T(40)
260       REAL L1,L2
270       DATA S,AREA,L1,L2/0.300,0.13640,22.0,26.0/

280 *    CALLS DATA FILE 'DATAN0' AND
290 *    STORES THE CALCULATED DATA

300       CALL OPSYS('ALLOC','DATAN0',7)
310       READ(7,100) N
```

```
320       WRITE(6,800)
330       CALL OPSYS ('ALLOC','CALCN0',9)
340       DO 307 I=1,N
350       READ(7,900) P(I),Q(I),H1(I),H2(I)

360 *    CALCULATION OF VOID FRACTION

370       AL1(I)=S*H1(I)/(2.54*22.0)
380       AL2(I)=S*H2(I)/(2.54*26.0)

390 *    IMPROVED CALCULATION OF COLUMN PRESSURE
400 *    NUMERICAL VALUES ARE USED IN THE CALCULATION
410 *            OF P1 AND P2 TO HAVE UNIT CONSISTENCY;

420 *    THE VALUES 108 AND 130 ARE THE
430 *            LOWER LIQUID LEVELS IN
440 *    INCHES FOR EACH SECTION L1 AND L2
450 *            AND CHANGE DEPENDING UPON THE DATASET

460       HF(I)=HI/(1-(AL1(I)+AL2(I))/2)

470 *    CALCULAITON OF LIQUID HEIGHT BELOW
480 *            THE MIDPOINT OF THE SECTION OF INTEREST
490       H1P(I)=(L1/2.0)*(1-AL1(I))+108
500       H2P(I)=(L2/2.0)*(1-AL2(I))+130

510 *    CALCULAITON OF LIQUID HEIGHT ABOVE
520 *            THE MIDPOINT OF THE SECTION OF INTEREST

530       H1P(I)=(HF(I)-H1P(I))
540       H2P(I)=(HF(I)-H2P(I))
560       P1(I)=(H1P(I)/12.0)*14.7/30.0+14.7
570       P2(I)=(H2P(I)/12.0)*14.7/30.0+14.7

580 *    CORRECTION FOR AIR FLOW RATE INDICATED BY THE
FLOWMETER

590       F(I)=0.00146*(P(I)+14.7)+0.8985
600       Q(I)=Q(I)*F(I)

610 *    CALCULATION OF SUPERFICIAL GAS VELOCITIES
620 *            THE NUMERICAL VALUES ARE USED TO
630 *            HAVE UNIT CONSISTENCY

640       TB=520
650
U1(I)=(P(I)+14.7)*Q(I)*(T(I)+460.0)/(AREA*P1(I)*60.0*TB)
660
U2(I)=(P(I)+14.7)*Q(I)*(T(I)+460.0)/(AREA*P2(I)*60.0*TB)

670 *    CALCULATION OF THE RATIO OF GAS VELOCITIES TO
680 *            VOID FRATION AND PRINTING THE OUTPUT

690       UAL1=U1(I)/AL1(I)
```

```
      UAL2=U1(I)/AL2(I)
      WRITE(9,700) U1(I),U2(I),AL1(I),AL2(I),UAL1
  307 CONTINUE

  100 FORMAT(I4)
  700 FORMAT(5(1X,F6.4),2(1X,F8.4))
  800 FORMAT(1X,'U1
(F/S)',3X,'U2(F/S)',3X,'AL1',4X,'AL2')
  900 FORMAT(4(2X,F10.6))
      STOP
      END
```

Program 'LINEAR' for Linear Regression of the Calculated Results

```
 10       DIMENSION X(100),Y(100),YP(100)
 20       DIMENSION U(100),V(100),GCF(100),GCFP(100)
 30       CALL OPSYS('ALLOC','DFLOW',9)
 40      N=22
 50       DO 303 I=1,N
 60      READ(9,400) X(I),U(I),V(I),YP(I),Y(I)
 70   303 CONTINUE
 80   101 CONTINUE
 90       WRITE(6,500) N
100       XSUM=0
110       X2SUM=0
120       YSUM=0
130       XYSUM=0
140       Y2SUM=0
150       DO 102 I=1,N
160       XSUM=XSUM+X(I)
170       YSUM=YSUM+Y(I)
180       X2SUM=X2SUM+X(I)**2
190       XYSUM=XYSUM+X(I)*Y(I)
200       Y2SUM=Y2SUM+Y(I)**2
200   102 CONTINUE
210       DEN=X2SUM*N-XSUM**2
220       SLOPE=(XYSUM*N-XSUM*YSUM)/DEN
230       C=(X2SUM*YSUM-XYSUM*XSUM)/DEN
240       CORCOF=DEN*SLOPE**2/(N*Y2SUM-YSUM**2)
250       DO 103 I=1,N
260       YP(I)=C+SLOPE*X(I)
270   103 CONTINUE
280       WRITE(6,300) SLOPE,C
290       SS=0.0
300       DO 202 J=1,N
310       ERROR=YP(J)-Y(J)
320       PCERR=ERROR/YP(J)
330       SS=SS+ERROR**2
340   202 CONTINUE
350       STDEV=(SS/(N-1))**0.5
360       WRITE(6,600) STDEV,CORCOF

370   700
FORMAT(8X,F12.6,5X,F12.6,5X,F12.6,5X,F12.6,5X,F12.6)
380   100 FORMAT(I4)
390   400 FORMAT(3(1X,F7.4))
400   200 FORMAT(5X,F6.4,5X,F6.4)
410   300
FORMAT(//,15X,'SLOPE=',E14.6,5X,'INTERCEPT=',F10.5,//)
420   500 FORMAT(//,20X,'NUMBER OF DATA POINTS',I5)
430   600 FORMAT(/,12X,'STANDARD DEVIATION=',E14.6,5X,
              'CORRELATION COEFF=',F10.5)
440       STOP
450       END
```

Appendix B

DERIVATION OF EQUATIONS FOR CALCULATING VOID FRACTION

The derivation of expressions for calculating void fraction are as follows

B.1 VOID FRACTION CALCULATED FROM LIQUID HEIGHT

Void Fraction = Fraction of Volume Occupied by the Gas in the Gas Liquid Column

$$E_g = \frac{\text{(Final Volume of Gas-liquid mixture)} - \text{(Initial Volume of liquid)}}{\text{Final Volume of Gas-liquid Mixture}}$$

For a constant cross-sectional area of liquid column

$$E_g = \frac{H_f - H_i}{H_f} \tag{56}$$

where H_f is the final height of the gas-liquid column and H_i is the initial height of the liquid column.

B.2 VOID FRACTION CALCULATED FROM DIFFERENTIAL PRESSURE DATA

Points A and B in Figure 37 represent the height of the liquid levels between which data were taken. Let p_a and p_b be the pressure at points A and B, d_f and d_c are the densities of water and manometer fluid respectively and h the deflection of the manometer fluid. Force balance on the two arms of the manometer at the same lavel (indicated by dotted line) gives

$$p_a + hd_c + z_1 d_f = p_b + zd_f + hd_f + z_1 d_f$$

or

$$(p_a - p_b) = zd_f + h(d_f - d_c) \qquad (57)$$

The difference in pressures between points A and B is due to the height of the gas liquid column. Neglecting the pressure exerted by the gas column

$$p_a - p_b = (1 - E_g)zd_f \qquad (58)$$

Combining the above two equations

$$zd_f + h(d_f - d_c) = (1 - E_g)zd_f$$

$$E_g zd_f = h(d_c - d_f)$$

$$E_g = h(s - 1)/z \qquad (59)$$

where s is the specific gravity of the manometer fluid.

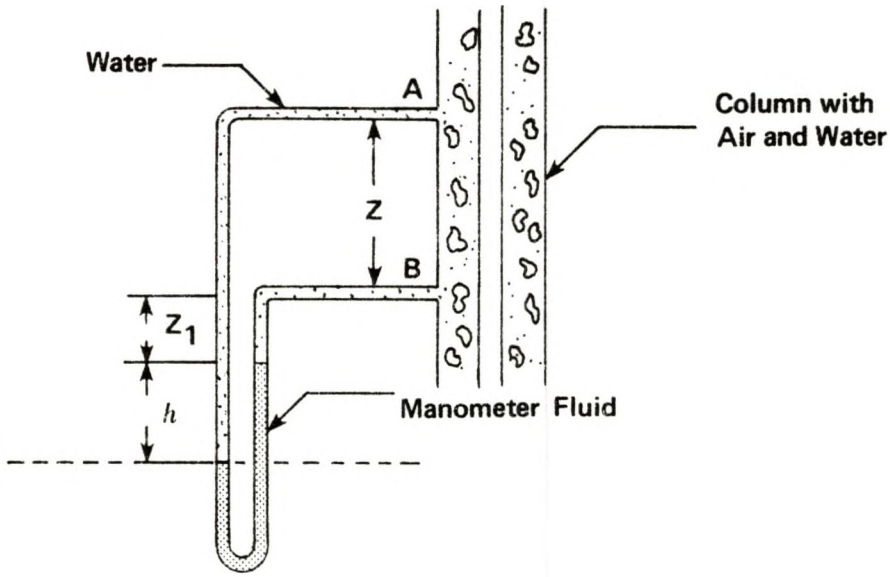

Figure 37: Schematic of the Manometer showing Liquid Levels

Appendix C

CALIBRATION OF THE DISC FLOWMETER

The disc flowmeter used to measure the flow rate of air entering the column was temperature compensated at a base temperature of 60° F. Although the flowmeter was capable of operating at wide range of pressures, it was not known whether the flowmeter was pressure compensated. This flowmeter was calibrated using another disc flowmeter which gave accurate readings up to pressures of 5 psig. The method of calibration is discussed below.

C.1 METHOD OF CALIBRATION

Air from the supply line was allowed to flow through the larger disc flowmeter (used for taking experimental data) to the smaller disc flowmeter and was then blown into the atmosphere. A pressure reducer valve (also indicates the pressure) was placed in between the outlet of the larger flowmeter and the inlet of the smaller flowmeter. The two flowmeters were thus connected in series and the air inlet pressure on entering the smaller flowmeter was kept constant at 3 psig with the help of a reducer valve. The following data were then recorded

1. the flow rate (V_1) in ft^3/min across the larger flowmeter
2. the pressure (P_1) at the outlet of the larger flowmeter
3. the flow rate (V_2) in ft^3/min across the smaller flowmeter. The fow rate indicated by the smaller

flowmeter was assumed to be at a constant air temperature of 70° F.

Flow rates of air measured with the two flowmeters at their respective pressures and temperatures were then converted to same temperature and pressure conditions. A multiplication factor was then obtained by taking the ratio of V_1 to V_2. The calibration curve was drawn by plotting the multiplication factor against the pressure of the larger gas flowmeter. Values of pressures, flow rates and multiplication factors are tabulated in Table 12, Appendix E.

Figure 38 shows the linear calibration curve which has a slope of 0.001462 and an intercept of 0.8985. The vlaues of the correlation coefficient, 0.9587, and standard deviation 0.0067 show a very good linear least square fit. Although the variation in the multiplication factor with pressure was very low, a linear increase in the multiplcation factor with pressure explains that the larger flowmeter was not truly pressure compensated. Flow rates indicated by the larger flowmeter were corrected by multiplying with the multiplication factor. These were then used to calculate the superficial gas velocities.

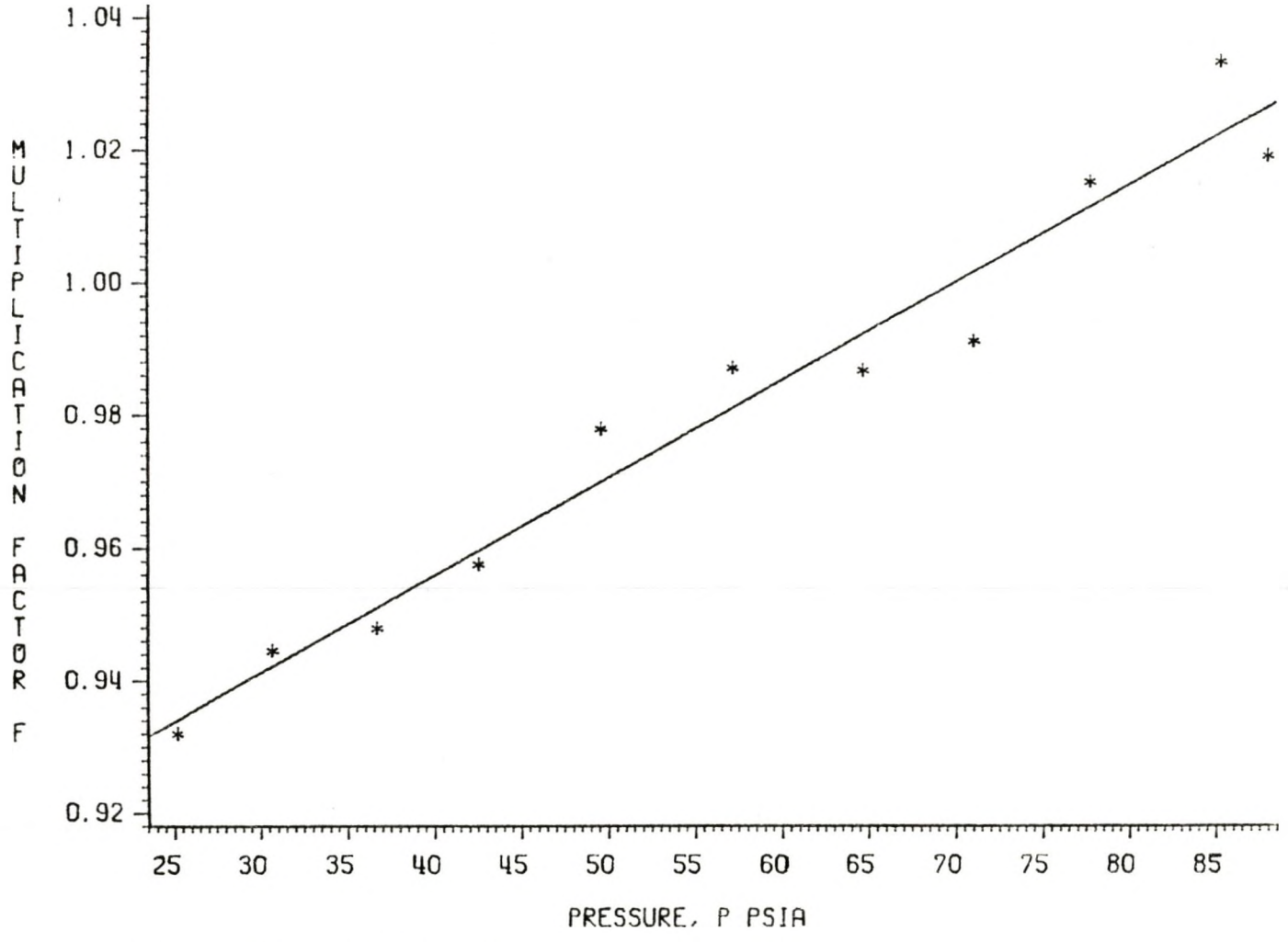

Figure 38: Calibration Curve for the Disc Flowmeter

C.2 CALCULATION OF MULTIPLICATION FACTOR

(Data from Table 12 Appendix E)

P_1 = Pressure at the outlet of larger flowmeter = 57.2 psia

P_2 = Constant pressure at the inlet of smaller flowmeter = 17.7 psia

V_1 = Volumetric flow rate across the larger Flowmeter = 0.2816 ft^3/min

V_2 = Volumetric flow rate across the smaller Flowmeter = 0.9397 ft^3/min

T_1 = Base temperature of the larger gas flowmeter = 60° F = 520° R

T_2 = Air Temperature = 70° F

Let T_s and P_s be any reference temperature and pressure. Assuming the ideal gas law holds for air

$$V_{1s} = \frac{P_1 V_1}{T_1} \frac{T_s}{P_s} \tag{60}$$

$$V_{2s} = \frac{P_2 V_2}{T_2} \frac{T_s}{P_s} \tag{61}$$

Dividing Equation (60) by Equation (61) the dimensionless multiplication factor is

$$F = \frac{V_{1s}}{V_{2s}} = \frac{P_1 V_1}{T_1} \frac{T_2}{P_2 V_2}$$

$$= \frac{(57.2 \text{ psia})(0.2816 \text{ ft}^3/\text{min})(530^\circ \text{ R})}{(19.7 \text{ psia})(0.9397 \text{ ft}^3/\text{min})(520^\circ \text{ R})}$$

$$= 0.9871$$

Appendix D

STATISTICAL ANALYSIS

A simple program 'AOV' was used to perform the calculations involved in preparing the ANOVA table. The following are the calculated values

i = number of observations in each treatment

j = number of treatments

Total number of observations

$= N_1+N_2+N_3$

$= 17+31+24 = 72$

Sum of each treatment (column)

$TT1 = sumy_{i1} = 2.3281$

$TT2 = sumy_{i2} = 4.4159$

$TT3 = sumy_{i3} = 3.3659$

Total sum of observations

$ysum = TT1+TT2+TT3 = 10.1099$

Total sum of squares

$y2sum = sum\ (y_{ij})^2 = 1.7609$

Mean sum of squares

$S_A = N(ybar^2) = N(ysum/n)(S'2.)$

$= 1.4196$

$S_D = y2sum-S_A = 0.3413$

Treatment sum of squares

$S_T = sum(TT_j**2/N_j)-S_A$

$= 0.0003$

Error or residual sum of squares

$$S_R = S_D - S_T$$
$$= 0.3410$$

$$F_{statistic} = F_{calc}$$
$$= S_T/S_R = 0.031$$

$F_{critical}$ = 3.37 from tables at a confidence level of 0.95

0.031 less than 3.37

Annular diameters does not have a significant effect on the measured pressure drop at a confidence level of 0.95.

```
 10 *    PROGRAM 'AOV' FOR MAKING ANOVA TABLE

 20      DIMENSION Y1(50),Y2(50),Y3(50),U7(50)
 30      DIMENSION AL2(50),AL3(50),AL4(50),AL7(50)
 40      REAL MSA,MST,MSR
 50      CALL OPSYS('ALLOC', 'TABAOV',7)
 60      DATA N1,N2,N3/17,31,24/
 70      N=N1+N2+N3

 80      DO 101 I=1,31
 90      READ(7,100) Y1(I),Y2(I),Y3(I)
100  101 CONTINUE

110       DO 102 I=1,N1
120       TT1=TT1+Y1(I)
130       Y12SUM=Y12SUM+Y1(I)**2.0
140  102 CONTINUE

150       DO 103 I=1,N2
160       TT2=TT2+Y2(I)
170       Y22SUM=Y22SUM+Y2(I)**2.0
180  103 CONTINUE

190       DO 104 I=1,N3
200       TT3=TT3+Y3(I)
210       Y32SUM=Y32SUM+Y3(I)**2.0
220  104 CONTINUE

230       YSUM=TT1+TT2+TT3
240       Y2SUM=Y12SUM+Y22SUM+Y32SUM
250       YBAR=YSUM/N
260       SA=N*(YBAR**2.0)
270       SD=Y2SUM-SA
280       ST=(TT1**2.0/N1+TT2**2.0/N2+TT3**2.0/N3)-SA
290       SR=SD-ST
300       WRITE(6,200)
310       WRITE(6,300) TT1,TT2,TT3
320       WRITE(6,300) YSUM,Y2SUM,YBAR
330       WRITE(6,300) SA,SD,ST,SR
340       PRINT *,N

350  100 FORMAT(3(F7.4))
360  200 FORMAT(//,7X,'SA,ST,SR,MSA,MST,MSR',/)
370  300 FORMAT(2X,5(2X,F10.6))
380       STOP
390       END
```

Appendix E

RAW DATA AND CALCULATED VALUES

TABLE 12

Data for Calibration of Disc Flowmeter and Calculated Values of Multiplication Factors

Larger Flowmeter		Smaller Flowmeter		Multiplication Factor
Pressure	Volumetric Flow rate	Pressure	Volumetric Flow rate	
P_1	V_1	P_2	V_2	F
psia	ft^3/min	psia	ft^3/min	
57.20	0.2816	17.7	0.9397	0.9871
64.75	0.2502	17.7	0.9456	0.9866
71.10	0.2238	17.7	0.9246	0.9910
77.80	0.2151	17.7	0.9494	1.0151
85.30	0.1969	17.7	0.9360	1.0332
88.05	0.1861	17.7	0.9259	1.0191
49.60	0.3223	17.7	0.9414	0.9778
42.55	0.3608	17.7	0.9234	0.9574
36.70	0.4173	17.7	0.9304	0.9479
30.70	0.4870	17.7	0.9115	0.9445
25.20	0.6162	17.7	0.9594	0.9320

TABLE 13

Bubble Rise Velocity Data For Various Channels

Tubing Outside Diameter D_t inch	Distance Travelled, H inch	Traverse Time t sec
	3.780	36.00
	4.390	42.00
	5.780	54.00
0.0	6.280	60.00
	6.970	66.00
	7.700	72.00
	8.380	78.00
	9.254	84.00
	8.660	78.00
	7.935	72.00
2.38	7.200	66.00
	6.430	60.00
	5.870	54.00
	4.520	42.00
	3.810	36.00
	8.900	84.00
	7.610	72.00
3.527	6.850	66.00
	6.220	60.00
	5.570	54.00
	4.320	42.00
	9.390	84.00
	8.560	78.00
	7.830	72.00
4.49	7.100	66.00
	6.360	60.00
	5.570	54.00
	4.270	42.00
	3.600	36.00

TABLE 14

Void Fraction Data for Circular Channel

Experimental Run: First
Casing Inside Diameter, D_c = 6.515 inch
Specific Gravity of the Manometer Fluid = 1.30

Air Inlet Pressure, P	Air Flow Rate, Q	Temperature, T	Height of Manometer Fluid	
			0-21.5*	21.5-43.0*
			h_o	h_1
psig	ft^3/min	^oF	cm	cm
20.80	0.0722	75.50	1.10	1.60
20.60	0.1144	75.50	1.30	02.30
20.00	0.1489	75.50	1.40	3.40
19.93	0.1983	75.50	1.80	4.50
19.75	0.2237	75.50	1.80	5.05
19.60	0.2722	75.50	2.90	5.65
18.60	0.3474	75.50	4.05	7.15
18.07	0.4264	75.30	4.70	8.45
16.70	0.5300	75.00	5.70	10.40
16.00	0.6438	74.80	6.70	11.90
14.15	0.8031	74.70	8.40	13.50
13.50	0.9202	74.20	9.65	15.00
15.85	1.0000	73.80	11.80	17.30
19.00	1.0900	73.40	13.90	19.90
22.75	1.1477	72.80	15.80	22.30
26.05	1.1935	72.20	17.75	24.30
31.95	1.2388	71.50	20.50	26.70
36.03	1.2717	70.80	22.00	28.10
45.85	1.3083	69.50	26.00	31.80

* Numbers represent the liquid heights in inch between which voidage data were taken.

TABLE 15

Void Fraction Data For Circular Channel

Experimental run: Second
Casing Inside Diameter, D_c = 6.515 inch
Specific Gavity of the Manometer Fluid = 1.238

Final Height of Liquid, H_2	Air Inlet Pressure, p	Air Flow Rate, Q	Temperature, T	Height of Manometer Fluid	
				21.5-43.0 h_1	43.0-64.5 h_2
Inch	Psia	ft^3/min	^oF	cm	cm
73.00	70.70	0.0811	73.50	3.50	3.50
73.40	70.65	0.0958	73.50	4.30	4.30
73.60	49.65	0.1398	73.50	4.90	4.90
73.90	41.10	0.2184	73.80	6.20	6.20
74.80	40.55	0.2946	73.80	8.60	8.60
75.60	39.60	0.3655	73.80	10.40	10.40
77.10	37.30	0.4995	72.75	12.80	13.60
77.50	36.10	0.6186	72.50	15.10	15.80
77.70	35.10	0.6991	72.50	16.28	17.20
78.60	31.00	1.0191	72.75	19.50	21.00
82.00	39.50	1.1707	72.75	26.20	26.90
83.00	46.70	1.2420	71.00	30.00	29.90
85.00	58.70	1.3110	70.70	34.601	34.17
86.50	60.50	1.2962	69.90	35.15	34.14

TABLE 16

Void Fraction Data For Channel With 2.38 Inch Inner Tube

Experimental run: Second
Casing Inside Diameter, D_c = 6.515 inch
Specific Gavity of the Manometer Fluid = 1.238

Final Height of Liquid, H_2 Inch	Air Inlet Pressure, p Psia	Air Flow Rate, Q ft^3/min	Temperature, T ^oF	Height of Manometer Fluid	
				21.5-43.0	43.0-64.5
				h_1 cm	h_2 cm
67.70	60.90	0.1251	70.00	6.15	7.10
69.20	51.60	0.2511	71.40	10.40	12.20
69.80	51.10	0.2863	71.40	11.65	13.90
70.20	50.75	0.3380	73.60	13.60	16.00
70.70	50.35	0.3954	73.60	15.65	18.00
70.90	49.20	0.4442	73.30	16.60	19.30
71.50	48.68	0.5127	73.30	18.95	21.20
72.00	46.90	0.5805	71.90	21.10	23.40
72.60	46.00	0.6754	71.00	22.60	24.95
73.00	43.70	0.7745	70.80	24.20	26.50
73.50	42.60	0.8720	70.50	24.50	27.05
74.10	39.50	1.0300	70.10	26.55	29.35
74.40	37.70	1.1580	69.80	27.85	30.20
76.30	40.73	1.1870	69.80	29.45	32.65
76.70	45.40	1.2361	69.20	32.90	36.40
77.30	0.70	1.2625	68.80	35.45	37.20
79.00	56.80	1.3037	68.30	38.15	39.75
79.50	60.55	1.3156	67.90	39.35	42.25

TABLE 17

Void Fraction Data For Channel With 3.527 Inch Inner Tube

Experimental run: Second
Casing Inside Diameter, D_c = 6.515 inch
Specific Gavity of the Manometer Fluid = 1.238

Final Height of Liquid, H_2	Air Inlet Pressure, p	Air Flow Rate, Q	Temperature, T	Height of Manometer Fluid	
				21.5-43.0	43.0-64.5
				h_1	h_2
Inch	Psia	ft^3/min	^oF	cm	cm
68.50	23.20	0.2249	67.20	7.35	8.30
68.90	23.20	0.2618	68.30	8.5	9.50
69.60	22.75	0.3254	68.85	10.30	11.70
69.90	22.65	0.3881	69.70	11.90	12.90
71.00	19.70	0.4993	70.70	14.00	16.05
72.50	22.78	0.6616	71.00	18.50	20.70
73.00	24.35	0.7643	71.30	22.20	23.75
75.00	25.90	0.8656	71.30	25.50	26.70
76.50	26.45	0.9560	71.00	28.75	30.50
78.00	34.10	1.0667	53.60	32.15	32.50
79.50	36.39	1.1405	55.50	35.10	37.15
82.00	40.64	1.1944	57.80	38.65	40.35
83.00	46.50	1.2470	59.90	43.65	43.95
85.00	55.00	1.3000	61.70	46.75	46.80

TABLE 18

Void Fraction Data For Channel With 4.49 Inch Inner Tube

Experimental run: Second
Casing Inside Diameter, D_c = 6.515 inch
Specific Gavity of the Manometer Fluid = 1.238

Final Height of Liquid, H_2	Air Inlet Pressure, p	Air Flow Rate, Q	Temperature, T	Height of Manometer Fluid	
				21.5-43.0 h_1	43.0-64.5 h_2
Inch	Psia	ft^3/min	^oF	cm	cm
68.50	23.20	0.2249	67.20	7.35	8.30
68.89	23.20	0.2618	68.30	8.50	9.50
69.60	22.75	0.3254	68.85	10.30	11.70
69.89	22.65	0.3881	69.70	11.90	12.90
71.00	19.70	0.4993	70.70	14.00	16.05
72.50	22.78	0.6616	71.00	18.50	20.70
73.00	24.35	0.7643	71.30	22.20	23.75
75.00	25.89	0.8656	71.30	25.50	26.70
76.50	26.45	0.9560	71.00	28.75	30.50
78.00	34.10	1.0667	53.60	32.15	32.50
79.50	36.39	1.1405	55.50	35.10	37.14
82.00	40.64	1.1944	57.80	38.65	40.35
83.00	46.50	1.2470	59.89	43.65	43.95
85.00	55.00	1.3000	61.70	46.75	46.80

TABLE 19

Void Fraction Data for Circular Channel

Experimental Run: Third
Casing Inside Diameter, D_c = 6.515 inch
Specific Gravity of the Manometer Fluid = 1.30

Air Inlet Pressure, P	Air Flow Rate, Q	Temperature, T	Height of Manometer Fluid		
			21.5-43.0	43.0-64.5	64.5-75.25
			h_1	h_2	h_3
psig	ft^3/min	°F	cm	cm	cm
27.94	0.1435	76.19	2.60	3.25	1.80
28.05	0.0695	76.19	1.35	2.00	0.90
29.00	0.2415	76.00	5.00	5.85	3.50
26.00	0.3545	75.89	7.55	9.10	5.50
24.75	0.4769	75.60	9.80	11.20	6.50
23.00	0.6265	75.19	12.30	14.00	7.80
19.85	0.7480	74.19	13.80	15.00	8.20
19.89	0.8739	74.19	15.25	16.55	9.00
17.89	1.0833	73.60	16.55	18.85	9.40
18.19	1.1855	73.50	18.30	19.35	10.30
21.30	1.2512	73.10	20.39	21.55	11.35
26.00	1.3140	72.60	23.19	24.10	12.45
30.00	1.3679	74.00	24.80	26.85	13.30
35.80	1.4090	73.80	27.30	28.25	14.15
41.69	1.4476	72.80	28.35	29.05	14.45
45.89	1.4730	69.89	27.55	28.38	14.15

TABLE 20

Void Fraction Data for Channel with 2.38 inch Inner Tube

Experimental Run: Third
Casing Inside Diameter, D_c = 6.515 inch
Specific Gravity of the Manometer Fluid = 1.30

Air Inlet Pressure, P	Air Flow Rate, Q	Temperature, T	Height of Manometer Fluid		
			21.5-43.0	43.0-64.5	64.5-75.25
			h_1	h_2	h_3
psig	ft^3/min	^oF	cm	cm	cm
15.00	0.1202	69.50	1.40	2.00	1.60
15.40	0.0607	70.20	0.80	1.60	0.90
15.10	0.1487	70.80	2.75	3.30	2.30
14.80	0.1971	71.20	3.80	4.40	2.80
14.00	0.2929	71.50	4.70	6.20	4.30
14.25	0.2878	73.00	5.50	6.30	3.75
14.20	0.3402	73.50	6.10	7.00	4.05
12.70	0.5316	73.50	9.00	10.25	5.50
11.20	0.6800	73.70	10.35	11.90	7.25
10.25	0.8261	74.00	13.05	14.15	7.95
11.90	0.9613	74.00	14.65	16.45	8.80
14.80	1.0808	74.00	18.25	19.15	10.40
18.25	1.1794	73.50	21.80	22.10	11.25
21.93	1.2430	73.50	23.00	24.45	13.10
31.93	1.3590	72.70	22.80	27.60	13.90
26.10	1.3024	73.40	24.45	27.00	13.75

TABLE 21

Void Fraction Data for Channel with 3.527 Inch Inner Tube

Experimental Run: Third
Casing Inside Diameter, D_c = 6.515 inch
Specific Gravity of the Manometer Fluid = 1.30

Air Inlet Pressure, P	Air Flow Rate, Q	Temperature, T	Height of Manometer Fluid		
			21.5-43.0	43.0-64.5	64.5-75.25
			h_1	h_2	h_3
psig	ft^3/min	^oF	cm	cm	cm
12.20	0.2008	65.60	3.80	3.83	2.75
11.35	0.1096	68.00	2.00	2.30	1.50
12.15	0.2763	69.60	5.40	6.10	3.35
11.85	0.4088	70.30	8.15	8.55	5.10
10.25	0.5133	71.00	9.65	10.60	5.65
9.750	0.6166	71.50	10.95	11.75	6.53
9.00	0.7604	71.89	12.60	11.70	7.30
10.70	0.8955	73.00	14.60	15.90	8.00
13.00	1.0108	73.00	17.40	18.40	10.20
15.95	1.1158	73.00	18.85	20.65	11.00
18.50	1.1957	73.00	21.60	22.15	11.25
22.30	1.2648	73.00	23.20	22.75	12.10
27.95	1.3389	72.50	24.40	26.15	13.40
37.40	1.4187	72.50	26.00	29.25	15.10

TABLE 22

Void Fraction Data for Channel with 4.49 inch Inner Tube

Experimental Run: Third
Casing Inside Diameter, D_c = 6.515 inch
Specific Gravity of the Manometer Fluid = 1.30

Air Inlet Pressure, P	Air Flow Rate, Q	Temperature, T	Height of Manometer Fluid		
			21.5-43.0	43.0-64.5	64.5-75.25
			h_1	h_2	h_3
psig	ft^3/min	^oF	cm	cm	cm
13.70	0.0652	68.39	1.55	1.85	1.20
13.05	0.1335	66.60	3.45	3.60	2.30
11.75	0.2578	66.50	7.10	7.70	4.20
11.95	0.3729	67.80	8.90	9.90	5.60
10.80	0.5200	69.80	10.25	11.10	6.30
9.80	0.6453	70.69	11.45	11.65	6.75
9.40	0.7943	71.80	13.50	14.30	7.50
11.00	0.9171	73.00	15.15	16.44	8.60
13.75	1.0341	78.00	17.50	18.85	9.65
19.00	1.2050	57.80	27.35	28.50	14.45
22.90	1.2850	61.80	28.25	28.90	15.33
28.60	1.3352	66.50	31.35	33.55	17.35
16.00	1.1765	74.80	18.50	20.80	12.10

TABLE 23

Void Fraction Data for Circular Channel

Casing Inside Diameter, D_c = 5.0 inch
Specific Gravity of the Manometer Fluid = 1.30
Column Operating Temperature, T = 70° F

Air Inlet Pressure, P psig	Air Flow Rate, Q ft^3/min	Height of Manometer Fluid: 108-130 h_1 cm	Height of Manometer Fluid: 130-156 h_2 cm
Initial Height of Liquid, H_i = 162.0 inch			
8.15	0.2872	9.00	10.25
8.00	0.1269	3.85	4.75
8.00	0.2930	9.60	10.85
8.00	0.4641	15.80	17.14
8.00	0.5993	18.85	20.60
8.00	0.7191	21.94	24.10
19.83	0.9157	31.10	33.25
18.19	0.8375	27.30	30.50
23.39	0.9699	34.19	37.14
22.47	1.0030	36.44	39.50
26.50	1.2651	41.30	45.35
15.50	1.1740	31.89	34.50
8.70	0.0615	1.50	2.25

TABLE 23
(Continued)

Air Inlet Pressure, P psig	Air Flow Rate, Q ft^3/min	Height of Manometer Fluid 108-119.5 h_1 cm	Height of Manometer Fluid 130-156 h_2 cm
Initial Height of Liquid, H_i = 152.7 inch			
7.50	1.3201	15.10	**
8.25	2.2690	20.70	-
8.25	1.9945	19.60	-
9.50	3.0830	25.80	-
12.25	4.4270	33.55	-
11.10	3.9122	29.75	-
10.40	3.4736	27.10	-
9.25	2.7469	23.45	-
11.80	4.0910	31.70	-
16.15	6.0370	40.75	-
14.10	5.4725	39.00	-
13.80	5.1697	36.30	-
12.40	4.8649	36.95	-

** 12.922 lb water was taken out from the Bottom of The Column to avoid splashing out of water through the top of the column

TABLE 24

Void Fraction Data for Channel with 2.875 inch Inner Tube

Casing Inside Diameter, D_c = 5.0 inch
Specific Gravity of the Manometer Fluid = 1.30
Column Operating Temperature, T = 70° F
Initial Height of Liquid, H_i = 152.7 inch

Air Inlet Pressure, P	Air Flow Rate, Q	Height of Manometer Fluid	
		108-119.5 h_1	119.5-131.3 h_2
psig	ft^3/min	cm	cm
7.70	0.1400	2.40	2.90
7.70	0.2739	5.60	6.50
7.70	0.4768	9.70	10.40
7.70	0.7333	13.20	13.80
7.70	0.9002	15.10	15.20
7.70	1.1716	16.94	18.35
7.70	1.4326	18.85	18.55
8.20	1.6648	20.00	20.89
8.20	1.9600	20.80	22.69
8.75	2.3420	25.00	24.35
9.15	2.6614	26.64	27.39
9.75	2.9111	26.64	28.75
11.15	4.0400	33.25	33.94
7.70	0.0732	1.40	1.80
7.70	0.3610	7.05	8.30
7.70	0.5834	11.70	12.35
7.75	1.0353	16.44	16.85
7.75	1.2919	17.75	17.85
7.75	2.1027	23.64	24.55
8.20	2.4279	26.10	25.85
11.00	3.4409	28.85	31.85
8.50	3.0000	27.05	27.45**
9.90	3.2745	29.20	29.85
10.50	3.7487	32.25	33.35
11.90	4.3698	35.10	34.65
13.50	4.3905	35.35	37.30

** 5.563 lb water was taken out from the Bottom of The Column to avoid splashing out of water through the top of the column

TABLE 25

Void Fraction Data for Channel with 3.50 inch Inner Tube

Casing Inside Diameter, D_c = 5.0 inch
Specific Gravity of the Manometer Fluid = 1.30
Column Operating Temperature, T = 70° F
Initial Height of Liquid, H_i = 152.7 inch

Air Inlet Pressure, P	Air Flow Rate, Q	Height of Manometer Fluid	
		108-119.5[2] h_1	119.5-131.3 h_2
psig	ft^3/min	cm	cm
7.50	0.0643	1.60	1.50
7.70	0.2230	6.45	6.65
7.70	0.3726	11.20	10.80
7.70	0.5894	14.25	13.25
7.70	0.7773	15.95	17.35
7.90	1.0419	18.25	18.44
7.90	1.3379	20.55	21.64
7.97	1.6128	26.80	22.44
8.05	1.8753	26.30	27.19
8.05	2.1268	28.05	28.14
8.20	2.3845	31.89	27.85
8.70	2.7434	31.55	32.94
7.70	1.1480	20.35	19.69
7.70	0.8601	16.19	17.10
8.00	1.8146	25.25	24.19
7.50	0.4808	14.00	12.55
7.45	0.1401	4.10	4.00

TABLE 26

Void Fraction as a Function of Superficial Gas Velocity - Circular Channel

Experimental Run: First
Raw Data Taken from Table 14

Superficial Gas Velocity u_g ft/sec	Void Fraction 0-21.5 E_g	Void Fraction 21.5-43.0 E_g
0.0121	0.0060	0.0088
0.0190	0.0071	0.0126
0.0243	0.0077	0.0187
0.0323	0.0099	0.0247
0.0362	0.0099	0.0277
0.0438	0.0159	0.0310
0.0542	0.0222	0.0393
0.0654	0.0258	0.0464
0.0777	0.0313	0.0571
0.0921	0.0368	0.0654
0.1077	0.0461	0.0742
0.1204	0.0530	0.0824
0.1424	0.0648	0.0950
0.1715	0.0764	0.1093
0.2017	0.0868	0.1225
0.2291	0.0975	0.1335
0.2744	0.1126	0.1467
0.3078	0.1209	0.1544
0.3825	0.1428	0.1747

TABLE 27

Void Fraction as a Function of Superficial Gas Velocity - Circular Channel

Experimental Run: Second
Raw Data Taken from Table 15

Superficial Gas Velocity, u_g ft/sec	Void Fraction Calculated from Liquid Height E_g	Void Fraction 21.5-43.0 E_g	Void Fraction 43.0-64.5 E_g	Superficial Velocity by Void Fraction 43.0-64.5 u_g/E_g ft/sec
0.0283	0.0959	0.0153	0.0153	1.8563
0.0334	0.1008	0.0187	0.0187	1.7834
0.0332	0.1033	0.0214	0.0214	1.5559
0.0424	0.1069	0.0270	0.0270	1.5706
0.0564	0.1176	0.0375	0.0375	1.5057
0.0683	0.1270	0.0453	0.0453	1.5064
0.0874	0.1440	0.0558	0.0593	1.4747
0.1045	0.1484	0.0658	0.0689	1.5179
0.1147	0.1506	0.0710	0.0750	1.5298
0.1468	0.1603	0.0850	0.0915	1.6038
0.2177	0.1951	0.1142	0.1172	1.8567
0.2751	0.2048	0.1307	0.1303	2.1113
0.3714	0.2235	0.1508	0.1489	2.4942
0.3789	0.2370	0.1532	0.1488	2.5461

TABLE 28

Void Fraction as a Function of Superficial Gas Velocity - 2.380 Inch Inner Tube

Experimental Run: Second
Raw Data Taken from Table 16

Superficial Gas Velocity, u_g ft/sec	Void Fraction Calculated from Liquid Height E_g	Void Fraction 21.5-43.0 E_g	Void Fraction 43.0-64.5 E_g	Superficial Velocity by Void Fraction u_g/E_g ft/sec
0.0425	0.0251	0.0268	0.0309	1.3741
0.0715	0.0462	0.0453	0.0532	1.3448
0.0807	0.0544	0.0508	0.0606	1.3318
0.0949	0.0598	0.0593	0.0697	1.3614
0.1101	0.0665	0.0682	0.0784	1.4037
0.1206	0.0691	0.0723	0.0841	1.4338
0.1376	0.0769	0.0826	0.0924	1.4895
0.1493	0.0833	0.0920	0.1020	1.4643
0.1699	0.0909	0.0985	0.1087	1.5624
0.1844	0.0959	0.1055	0.1155	1.5963
0.2019	0.1020	0.1068	0.1179	1.7126
0.2199	0.1093	0.1157	0.1279	1.7192
0.2352	0.1129	0.1214	0.1316	1.7870
0.2617	0.1350	0.1283	0.1423	1.8389
0.3056	0.1395	0.1434	0.1586	1.9261
0.3510	0.1462	0.1545	0.1621	2.1652
0.4094	0.1646	0.1663	0.1732	2.3635
0.4426	0.1698	0.1715	0.1841	2.4036

TABLE 29

Void Fraction as a Function of Superficial Gas Velocity - 3.527 inch Inner Tube

Experimental Run: Second
Raw Data Taken from Table 17

Superficial Gas Velocity, u_g ft/sec	Void Fraction Calculated from Liquid Height E_g	Void Fraction 21.5-43.0 E_g	Void Fraction 43.0-64.5 E_g	Superficial Velocity by Void Fraction u_g/E_g ft/sec
0.0322	0.0251	0.0200	0.0253	1.2722
0.0200	0.0251	0.0139	0.0179	1.1204
0.0356	0.0337	0.0238	0.0290	1.2267
0.0403	0.0435	0.0338	0.0351	1.1479
0.0437	0.0504	0.0327	0.0379	1.1523
0.0503	0.0558	0.0357	0.0403	1.2471
0.0583	0.0625	0.0421	0.0473	1.2320
0.0765	0.0665	0.0445	0.0516	1.4822
0.0721	0.0756	0.0501	0.0564	1.2782
0.0788	0.0808	0.0530	0.0638	1.2345
0.0878	0.0859	0.0591	0.0710	1.2353
0.1046	0.0884	0.0652	0.0745	1.4031
0.1225	0.0922	0.0732	0.0845	1.4486
0.1423	0.0971	0.0878	0.0961	1.4811
0.1678	0.1020	0.0965	0.1054	1.5916
0.2048	0.1165	0.1085	0.1216	1.6843
0.2347	0.1316	0.1240	0.1338	1.7543
0.2744	0.1462	0.1336	0.1443	1.9024
0.3200	0.1538	0.1443	0.1582	2.0230
0.3910	0.1646	0.1606	0.1708	2.2889
0.4494	0.1852	0.1743	0.1791	2.5091
0.4599	0.2000	0.1870	0.1948	2.3609
0.5391	0.2143	0.1881	0.1952	2.7610

TABLE 30

Void Fraction as a Function of Superficial Gas Velocity - 4.49 inch Inner Tube

Experimental Run: Second
Raw Data Taken from Table 18

Superficial Gas Velocity, u_g ft/sec	Void Fraction Calculated from Liquid Height E_g	Void Fraction 21.5-43.0 E_g	Void Fraction 43.0-64.5 E_g	Superficial Velocity by Void Fraction u_g/E_g ft/sec
0.0451	0.0365	0.0320	0.0362	1.2473
0.0526	0.0421	0.0370	0.0414	1.2712
0.0642	0.0517	0.0449	0.0510	1.2585
0.0763	0.0558	0.0519	0.0562	1.3573
0.0852	0.0704	0.0610	0.0699	1.2174
0.1312	0.0897	0.0806	0.0902	1.4541
0.1625	0.0959	0.0968	0.1035	1.5697
0.1962	0.1200	0.1111	0.1164	1.6861
0.2214	0.1373	0.1253	0.1329	1.6653
0.3117	0.1538	0.1401	0.1416	2.2004
0.3583	0.1698	0.1530	0.1619	2.2129
0.4236	0.1951	0.1684	0.1759	2.4090
0.5125	0.2048	0.1902	0.1915	2.6758
0.6423	0.2235	0.2037	0.2040	3.1491

TABLE 31

Void Fraction as a Function of Superficial Gas Velocity - Circular Channel

Experimental Run : Third
Raw Data from Table 19

Superficial Gas Velocity,	Void Fraction			Superficial Gas Velocity by Void Fraction
	21.5-43.0	43.0-64.5	64.5-75.25	43.0-64.5
u_g	E_g	E_g	E_g	u_g/E_g
ft/sec				ft/sec
0.0291	0.0143	0.0179	0.0189	1.6319
0.0141	0.0074	0.0110	0.0094	1.2875
0.0503	0.0275	0.0321	0.0367	1.5652
0.0684	0.0415	0.0500	0.0577	1.3691
0.0890	0.0538	0.0615	0.0682	1.4469
0.1114	0.0676	0.0769	0.0819	1.4483
0.1211	0.0758	0.0824	0.0861	1.4691
0.1417	0.0838	0.0909	0.0945	1.5580
0.1647	0.0909	0.1036	0.0987	1.5910
0.1820	0.1005	0.1063	0.1081	1.7122
0.2110	0.1121	0.1184	0.1192	1.7826
0.2521	0.1274	0.1324	0.1307	1.9044
0.2908	0.1362	0.1475	0.1396	1.9714
0.3412	0.1500	0.1552	0.1486	2.1988
0.3943	0.1557	0.1596	0.1517	2.4706
0.4314	0.1513	0.1559	0.1486	2.7671

TABLE 32

Void Fraction as a Function of Superficial Gas Velocity - 2.380 inch Inner Tube

Experimental Run : Third
Raw Data from Table 20

Superficial Gas Velocity, u_g ft/sec	Void Fraction 21.5-43.0 E_g	Void Fraction 43.0-64.5 E_g	Void Fraction 64.5-75.25 E_g	Superficial Gas Velocity by Void Fraction 43.0-64.5 u_g/E_g ft/sec
0.0190	0.0077	0.0110	0.0168	1.7281
0.0097	0.0044	0.0088	0.0094	1.1077
0.0236	0.0151	0.0181	0.0241	1.3034
0.0310	0.0209	0.0242	0.0294	1.2830
0.0448	0.0258	0.0341	0.0451	1.3155
0.0446	0.0302	0.0346	0.0394	1.2873
0.0526	0.0335	0.0385	0.0425	1.3683
0.0778	0.0494	0.0563	0.0577	1.3812
0.0939	0.0569	0.0654	0.0761	1.4357
0.1097	0.0717	0.0777	0.0835	1.4117
0.1365	0.0805	0.0904	0.0924	1.5104
0.1710	0.1003	0.1052	0.1092	1.6251
0.2093	0.1198	0.1214	0.1181	1.7239
0.2466	0.1264	0.1343	0.1375	1.8360
0.3480	0.1253	0.1516	0.1459	2.2949
0.2896	0.1343	0.1483	0.1444	1.9524

TABLE 33

Void Fraction as a Function of Superficial Gas Velocity - 3.527 inch Inner Tube

Experimental Run : Third
Raw Data from Table 21

Superficial Gas Velocity,	Void Fraction			Superficial Gas Velocity by Void Fraction
	21.5-43.0	43.0-64.5	64.5-75.25	43.0-64.5
u_g	E_g	E_g	E_g	u_g/E_g
ft/sec				ft/sec
0.0348	0.0209	0.0210	0.0289	1.6536
0.0184	0.0110	0.0126	0.0157	1.4602
0.0481	0.0297	0.0335	0.0352	1.4367
0.0705	0.0448	0.0470	0.0535	1.5009
0.0831	0.0530	0.0582	0.0593	1.4268
0.0978	0.0602	0.0645	0.0686	1.5155
0.1169	0.0692	0.0643	0.0766	1.8185
0.1482	0.0802	0.0873	0.0840	1.6970
0.1831	0.0956	0.1011	0.1071	1.8116
0.2247	0.1036	0.1134	0.1155	1.9807
0.2618	0.1187	0.1217	0.1181	2.1518
0.3105	0.1274	0.1250	0.1270	2.4843
0.3818	0.1340	0.1437	0.1407	2.6576
0.5013	0.1428	0.1607	0.1585	3.1195

TABLE 34

Void Fraction as a Function of Superficial Gas Velocity - 4.49 inch Inner Tube

Experimental Run : Third
Raw Data from Table 22

Superficial Gas Velocity,	Void Fraction			Superficial Gas Velocity by Void Fraction
	21.5-43.0	43.0-64.5	64.5-75.25	43.0-64.5
u_g	E_g	E_g	E_g	u_g/E_g
ft/sec				ft/sec
0.0162	0.0085	0.0102	0.0126	1.5972
0.0323	0.0190	0.0198	0.0241	1.6349
0.0594	0.0390	0.0423	0.0441	1.4038
0.0868	0.0489	0.0544	0.0588	1.5957
0.1160	0.0563	0.0610	0.0661	1.9028
0.1384	0.0629	0.0640	0.0709	2.1619
0.1678	0.0742	0.0786	0.0787	2.1356
0.2075	0.0832	0.0904	0.0903	2.2967
0.2626	0.0961	0.1036	0.1013	2.5361
0.3517	0.1502	0.1566	0.1512	2.2465
0.4242	0.1552	0.1588	0.1612	2.6722
0.5167	0.1722	0.1843	0.1816	2.8034
0.3216	0.1016	0.1143	0.1270	2.8146

TABLE 35

Void Fraction as a Function of Superficial Gas Velocity - Circular Channel

Raw Data from Table 23

Superficial Gas Velocity		Void Fraction		Superficial Gas Velocity by Void Fraction
108-130 u_g ft/sec	130-156 u_g ft/sec	108-130 E_g	130-156 E_g ft/sec	130-156 u_g/E_g ft/sec
0.0393	0.0418	0.0483	0.0466	0.8137
0.0175	0.0186	0.0207	0.0216	0.8454
0.0398	0.0422	0.0515	0.0493	0.7728
0.0621	0.0659	0.0848	0.0779	0.7323
0.0796	0.0844	0.1012	0.0936	0.7866
0.0947	0.1003	0.1178	0.1095	0.8039
0.1822	0.1928	0.1670	0.1510	1.0910
0.1600	0.1693	0.1466	0.1386	1.0914
0.2123	0.2244	0.1836	0.1688	1.1563
0.2368	0.2503	0.1957	0.1794	1.2100
0.2942	0.3107	0.2217	0.2060	1.3270
0.2026	0.2143	0.1713	0.1567	1.1827
0.0088	0.0093	0.0081	0.0102	1.0864
(108-119.5)		(108-119.5)		(108-119.5)
0.1688		0.1551		1.0883
0.2911		0.2126		1.3692
0.2575		0.2013		1.2792
0.3622		0.2408		1.5042
0.4049		0.2650		1.5279
0.4698		0.2783		1.6881
0.5668		0.3256		1.7408
0.9145		0.4185		2.1852
0.7836		0.4005		1.9566
0.7491		0.3728		2.0094
0.6653		0.3795		1.7531
0.6155		0.3446		1.7861
0.5346		0.3055		1.7499

TABLE 36

Void Fraction as a Function of Superficial Gas Velocity - 2.785 inch Inner Tube

Raw Data from Table 24

Superficial Gas Velocity		Void Fraction		Superficial Gas Velocity by Void Fraction
108-130 u_g ft/sec	130-156 u_g ft/sec	108-130 E_g	130-156 E_g ft/sec	130-156 u_g/E_g ft/sec
0.0172	0.0177	0.0164	0.0150	1.0488
0.0589	0.0606	0.0662	0.0666	0.8897
0.0964	0.0992	0.1150	0.1081	0.8383
0.1504	0.1547	0.1464	0.1326	1.0273
0.1955	0.2009	0.1638	0.1737	1.1935
0.2620	0.2692	0.1874	0.1847	1.3981
0.3313	0.3402	0.2111	0.2167	1.5694
0.3920	0.4026	0.2752	0.2247	1.4244
0.4516	0.4633	0.2701	0.2723	1.6720
0.5075	0.5207	0.2881	0.2818	1.7615
0.5658	0.5806	0.3276	0.2788	1.7271
0.6549	0.6712	0.3240	0.3298	2.0213
0.2833	0.2911	0.2090	0.1972	1.3555
0.2163	0.2223	0.1664	0.1712	1.2999
0.4415	0.4533	0.2593	0.2422	1.7027
0.1219	0.1254	0.1438	0.1256	0.8477
0.0370	0.0381	0.0421	0.0400	0.8789

TABLE 37

Void Fraction as a Function of Superficial Gas Velocity - 3.50 inch Inner Tube

Raw Data from Table 25

Superficial Gas Velocity		Void Fraction		Superficial Gas Velocity by Void Fraction
108-130	130-156	108-130	130-156	130-156
u_g	u_g	E_g	E_g	u_g/E_g
ft/sec	ft/sec		ft/sec	ft/sec
0.0172	0.0177	0.0164	0.0150	1.0488
0.0589	0.0606	0.0662	0.0666	0.8897
0.0964	0.0992	0.1150	0.1081	0.8383
0.1504	0.1547	0.1464	0.1326	1.0273
0.1955	0.2009	0.1638	0.1737	1.1935
0.2620	0.2692	0.1874	0.1847	1.3981
0.3313	0.3402	0.2111	0.2167	1.5694
0.3920	0.4026	0.2752	0.2247	1.4244
0.4516	0.4633	0.2701	0.2723	1.6720
0.5075	0.5207	0.2881	0.2818	1.7615
0.5658	0.5806	0.3276	0.2788	1.7271
0.6549	0.6712	0.3240	0.3298	2.0213
0.2833	0.2911	0.2090	0.1972	1.3555
0.2163	0.2223	0.1664	0.1712	1.2999
0.4415	0.4533	0.2593	0.2422	1.7027
0.1219	0.1254	0.1438	0.1256	0.8477
0.0370	0.0381	0.0421	0.0400	0.8789

Appendix F

NOMENCLATURE

A Parmeter in proposed correlation for Void fraction, dimensionless

A_o Parameter in Equation (32), dimensionless

A_s Parameter for the proposed correlation for slug flow, ft/sec

B_o Parameter of the proposed correlation for void fraction, ft/sec

B_s Parameter of the proposed correlation for slug flow, dimensionless

B_1 1.6 times bubble diameter, d_b, inch

C Constant coefficient in expression for terminal rise velocity, dimensionless.

C_o Parameter in Equation (22), dimensionless

C_1 Parameter in Equation (22), ft/sec.

d_f Density of the fluid (water), lb_m/ft^3

d_g Density of the gas, lb_{m/ft^3}

D Diameter of the pipe or tube, ft.

d_b Bubble diameter, ft.

D_e Equivalent diameter, ft.

D_t Inside diameter of the tube, ft.

D_c Outside diameter of the tube, ft.

E_g Void fraction, dimensionless.

$\bar{E}_g$ Average void fraction along the radial position of pipe, dimensionless.

$\overline{E_g u}$ Average of the product of void fraction and average velocity of the two phases along the radius of the pipe, ft/sec.

E_t Eotvos number.

f Multiplication factor used for correction of air flow rate, dimensionless.

H Distance travelled by a single bubble, inch.

H_f Final height of liquid column, inch.

H_i Initial height of the liquid column, inch.

h, h_1, h_2 Heights of the manometer fluid, cm.

j_{gf} Drift flux, ft/sec.

$\bar{j}_{gf}$ Average drigt flux along the radial position of pipe, ft/sec.

K Constant determined experimentally depending upon geometry, dimensionless.

m_g Viscosity of liquid, lb_m/ft hr.

n Exponent of expression for drift flux.

N_f Dimensionless inverse viscosity.

P Exponent of equation correlating void fraction, E_g and gas velocity v_g

P Pressure at which air flow rate was measured, psig.

P_1 Pressure at the inlet of the larger flowmeter, psia.

P_s Arbitrary referance pressure, psia.

p_a Pressure at the top tap of the column, psia.

p_b Pressure at the bottom tap of the column, psia.

Q Air flow rate indicated by the disk flowmeter, ft^3/min.

r_o Gas injector orifice radius, inch.

r_b bubble Radius, inch.

R^2 Correlation coefficient.

s Surface tension of fluid, lb_f/ft.

s_d Standard deviation.

SS_1 Sum of the squares of the error.

S_A Sum of the squares of mean.

S_T Sum of the squares of treatment.

S_R Sum of the squares of residuals.

t Traverse time required by a single bubble, sec.

T Column operating temperature, $^{\circ}$ F.

T_1 Base temperature of the large flowmeter, 60° F.

T_2 Temperature of air, 70° F.

T_s Arbitrary reference temperature in Equation (52).

$\bar{u}$ Average velocity of the two phases, ft/sec.

u_g Superficial gas velocity, ft/sec.

u_f Superficial velocity of liquid, ft/sec.

$\bar{u}_g$ Average of the superficial gas velocity along the radial position of pipe, ft/sec.

$\bar{u}$ Average of average velocity of the two phases along the radial position of pipe, ft/sec.

v_g absolute velocity of gas, ft/sec.

v_f Absolute velocity of liquid, ft/sec.

v_{gf} Relative velocity between the two phases, ft/sec.

$\bar{v}_g$ Average of the absolute gas velocity along the radial position of the pipe, ft/sec.

v_t Terminal rise velocity, ft/sec.

v_b Bubble rise velocity, ft/sec.

V_1 Flow rate of air across the larger

flowmeter, ft^3/sec.

V_2 Flow rate of air across the smaller flowmeter, ft^3/sec.

REFERENCES

1. Gipson, S.W. and H.W. Swaim. Designed beam Pumping. Proc. 19th Annual Southwestern Petroleum Short Course, Lubbock, Tex., Apr. 1972, p 95

2. Godbey, J.K. and C.A. Dimon. The Automatic Liquid Monitor for Pumping Wells. J. Pet. Tech., 79-83 (1977)

3. Podio, A.L., M.J. Tarillion, and E.T. Roberts. Laboratory Work Improves Circualtions. Oil and Gas J., Aug. 1980, pp 137-146

4. Wallis, G.B. One-dimensional Two-phase Flow. McGraw Hill Book Co. Inc., New York, 1969, p 93,248,255

5. Wallis, G.B. Some Hydrodynamic Aspects of Two-phase Flow and Boiling. Paper No 38, 1st Heat Transfer Conf., ASME, Boulder, Co., 1961

6. Lockett, M.J. and R.D. Kirkpatric. Ideal Bubbly Flow and Actual Flow in Bubble Columns. Trans. Inst. Chem. Engrs., 53, 267-273 (1975)

7. Akita, K. and F. Yoshida. Gas Holdup and Volumetric Mass Transfer Coefficient in Bubble Columns. Ind. Eng. Chem., Process Design and Dev., 12, 76-80 (1973)

8. Haug, H.F. Stability of Sieve Trays with High Overflow Weirs. Chem. Engn. Sc., 31, 295 (1976)

9. Zahradnik, J. and F. Kastanek. Gas Holdup in Uniformly Aeriated Bubble Column Reactors. Chem. Eng. Commun., 3, 413-429 (1979)

10. Mersmann, A. Design and Scaleup of Bubble and Spray Column. Ger. Chem. Eng., 1, 1-11 (1978).

11. Zuber, N. and J. Findlay. Average Volumetric Concentration in Two-phase Flow System. Trans ASME J. Heat Transfer, 87, 453, (1965)

12. Ishii, M. Thermofluid Dynamic Theory of Two-phase Flow. Scientific and Medical Publication of France. Eyrolles, Paris, (1975)

13. Whitaker, S. Introduction to Fluid Mechanics. Prentice-Hall Inc., New York, 1968, pp 189-192

14. Peebles, F.N. and H.J. Garber. Studies in the Motion of Gas Bubbles in the Liquids. Chem. Eng. Prog., 49, 88-97 (1953)

15. Harmathy, T.Z. Velocity of Large drops and Bubbles in Media of Infinite or Restricted Extent. AIChE J., 6, 281 (1960)

16. Shulman, H.L. and L.C. Molstad. Gas Bubble Columns for Gas Liquid Contacting. Ind. Eng. Chem., 42, 1058 (1950)

17. Gaylor, R., N.W. Roberts, and H.R.C. Patt. Liquid-Liquid Extraction IV. Further Study of Hold-up in Packed Columns. Trans Inst. of Chem. Engrs., 31, 57-68 (1953)

18. Miles, G.D., L. Shedlovsky, and J. Ross. Foam Drainage. J. Phys. Chem., 49, 93-107 (1943)

19. Zuber, H. and Hench, J. Steady State and Transient Void Fraction of Bubbling Systems and Their Operating Limits. Report No 62 GL 100, General Electric Co., Schenectady, N.Y., 1962

20. Hikita, H. and H. Kikukawa. Liquid Phase Mixing in Bubble Columns: Effect of Liquid Properties. Chem. Eng. J., 8, 191-197 (1976)

21. Hikita, H., S. Ashai, K. Tanigawa, K. Segawa, and M. Kitao. Gas Holdup in Bubbles Columns. Chem. Eng. J., 20, 59-67 (1980)

22. Godbey, J.K. and C.A. Dimon. The Automatic Liquid Monitor for Pumping Wells. J. Pet. Tech.79-83 (1977).

23. Hughmark, G.A. Hold Up and Pressure Drop with Gas-Liquid Flow in a Vertical Pipe. Ph.D Dissertation, Louisiana State U., Baton Rouge, LA (1959)

24. Mashelkar, R.A. Bubble Columns. Brit. Chem. Eng., 15, 1297-1304 (1970)

25. Zahradnik, J. Intensification of Mass Transfer in Seive Plate Bubble Columns. Coll. Czeck. Chem. Commun., 44, 348 (1979)

26. Kawagoe, K., T. Inove, K. Nakao, and T. Otake. Flow Patterns and Gas Holdup Conditions in Gas-Sprayed Contactors. Int. Chem. Eng., 16, No 1, 176-183 (1976)

27. Bhaga, D. and M.E. Weber. Holdup in Vertical Two and Three Phase Flow; Part I; Theoretical Analysis and Part II; Experimental Investigation. Can. J. Chem. Eng., 50, 323-336 (1972)

28. Griffith, P. The Prediction of Low Quality Boiling Voids. A.S.M.E. Paper No 63-HT-20., Nat. Heat Transfer Confc., Boston, Mass., 1963

29. Wallis, G.B. General Correlations for the Terminal Rise Velocity of Cylinderical Bubbles in Vertical Tubes. Report No 62G1130, General Engineering Laboratory, General Electric Company, Schenectady, N.Y., August 1962.

30. White, E.T. and R.H. Beardmore. Velocity of Rise of Single Cylinderical Air Bubbles Through Liquids Contained in Vertical Tubes. Eng. Sci., 17, 351-361 (1962)

31. Dumitrescu, D.T. Stromung an einer Luftblase im senkrechten Rohr. angew Math. Mech., 23, 139 (1943)

32. Nicklin, D.J., J.O. Wilkes, and J.F. Davidson. Two-phase Flow in Vertical Tubes. Trans. I. Che. Engrs., 40, 61-68 (1962)

33. Birkoff, G. and D. Carter. Rising Plane Bubbles. J. Rational Mech and Anal., 6, No 6, 769-780 (1957)

34. Davis, R.M. and G.I. Taylor. Proc. of Royal Doc.(London) 200 series A, 375-390 (1950)

35. Christeansen, H. Power to Void Transfer Functions. Ph.D Thesis, Nuclear Eng. Dept., M.I.T., (Sept. 1961)

36. Griffith, P. and G.B. Wallis. Two-phase Slug Flow. J. Heat Trans. ASME SeriesC, 83, 7-21 (1961)

37. Radovich, N.A. and R. Moissis. The Transition from Two Phase Bubble Flow to Slug Flow. Report No 7-7673-22, Dept. of Mech. Eng., MIT, 1962

38. Taitel, Y. and A.E. Dukler. Flow Regime Transition for Vertical Upward Gas-Liquid Flow: A Preliminary Approach through Physical Modeling. AIChE 70th Annual Meeting, New York, 1977

39. Taitel, Y., D. Bornea, and A.E. Dukler. Modeling Flow Pattern Transition for Steady Upward Gas-Liquid Flow in Vertical Tubes. AIChE J., 26, 345-354 (1980)

40. Edger, C.B. Jr. AEC Report No NYO-3114-14 by Wallis, G.B. 19-21 (1966) 29-34 (1982)

41. Kutateladze, S.S. and M.A. Sturikovich. Hydraulics of Gas-Liquid Systems. Moscow, Wright Field trans. F-TS-9414/V (1958) As reported by Wallis (5).

42. Tarrillion, M.J. An Experimental Investigation of Gradient Correction Factor: Correction for Liquid Columns Containing Gas Bubbles. M.S. Thesis, University of Texas, Austin, TX., (1978) pp 48

43. Handout, ChE 331 and ChE 332, Department of Chem. Engr. U. of North Dakota, Surface Tension of a binary Solution (Drop Number method) and Use of the Westphal Balance

44. Betha, R.M., B.S. Duran, and T.L. Boullion. Statistical Method for Engineers and Scientists. Marcel Dekker Inc., New York, 1975, p 320,527